SOME ELECTRICAL AND OPTICAL

PROPERTIES OF CADMIUM SULPHIDE

BY

Leonard Jeffrey Fass, B.Sc.(Eng), A.C.G.I.

A Thesis for the degree of

Doctor of Philosophy

Electrical Engineering Department,

Imperial College,

University of London,

February 1969.

ABSTRACT

An apparatus for the growth of cadmium sulphide single crystal platelets by the flow technique was constructed. The platelets so grown were examined by various physical techniques; X-ray photography, electron diffraction microscopy, optical absorption and photoluminescence.

Devices were constructed with various contact materials on the two large area faces of the platelets. The contact materials used were, cuprous sulphide, gold, silicon monoxide and cuprous iodide, which were non-ohmic, and indium and gallium, which appeared to be ohmic.

The radiation wetting technique using atomic hydrogen was adapted for the simultaneous melting of indium and the attachment of gold wire leads directly to the platelet surface or to a specific contact. Heat treatment of the devices was performed in the radiation wetting apparatus.

Devices with one ohmic and one non-ohmic contact behave as diodes, the easy current direction being with positive bias to the non-ohmic contact.

Hole injection probably by a filamentary mechanism into cadmium sulphide from cuprous sulphide was indicated by the observation of negative resistance in the forward characteristic of devices with a cuprous sulphide anode. Volume oscillations below $100°K$ observed in devices with

a cuprous sulphide anode appear to be due to carrier
recombination and provide further evidence of minority
carrier injection in this system.

ACKNOWLEDGEMENTS

INDEX

MISCELLANEOUS

LIST OF SYMBOLS USED

E_G — Energy gap between valence and conduction bands

E_C — Energy of bottom of conduction band

E_V — Energy of top of valence band

E_F — Energy of Fermi-level

E_R — Energy of recombination centre level

ϵ — dielectric constant

ϕ — electronic work function

χ — electron affinity

N_A — density of acceptors

N_D — density of donors

N_R — recombination centre density

N_R^o — neutral recombination centre density

N_R^- — negatively charged recombination centre density

n — injected free electron density

n_o — equilibrium electron density

p — injected free hole density

p_o — equilibrium hole density

V_B — double injection breakdown voltage

V_M — minimum voltage after double injection breakdown

σ_n^o — capture cross-section for electrons of a neutral centre

σ_p^- — capture cross-section for holes of a negatively charged centre

t_n — electron transit time

t_p – hole transit time

τ_n – electron lifetime

τ_p – hole lifetime

μ_n – electron mobility

μ_p – hole mobility

D_n – diffusion constant for electrons

D_p – diffusion constant for holes

J – current density

J_n – electronic current density

J_p – hole current density

E – electric field

e – electronic charge

k – Boltzmann's constant

C – dissipation coefficient/unit length

R – resistance/unit length

d – device thickness

n' – electron perturbation

p' – hole perturbation

E' – field perturbation

v_p – velocity of perturbation

f – frequency

T – absolute temperature

T_o – ambient temperature

CHAPTER I

INTRODUCTION

1.1 II - VI COMPOUNDS

Cadmium sulphide belongs to a group of compounds known as the "II - VI" compounds. Although this could mean compounds formed from any of the elements of groups II and VI of the periodic table it usually refers to the oxides, sulphides, selenides and tellurides of zinc cadmium and mercury. These compounds form a series having related physical and chemical properties.

The series is bounded at one end by zinc sulphide with a band gap of 3.7 eV which is an insulator and at the other end by mercury selenide with a band gap of -.07 eV which is a semimetal. Cadmium sulphide, which has a band gap of 2.4 eV at room temperature, can be prepared with properties both of a semi-conductor and a semi-insulator with a resistivity variation between 10^{-2} and 10^{13} ohm-cm.

A wide variety of applications have been found for the II - VI compounds. Historically, interest was first centred on the photoluminescence derived from deep luminescence centres in zinc sulphide and photo-conductivity in cadmium sulphide. The development of techniques for the growth of all the II - VI compounds in a high purity form has led to a better understanding

of the earlier investigated properties and also to the investigation of other effects such as electroluminescence, piezoelectric electronphonon coupling, thermomagnetic cooling and the stimulated emission of radiation.

The properties of the II - VI compounds such as band gap, impurity ionization energies and carrier mobilities, are related to more fundamental parameters such as ion size, bond distance, polarizability and the electronegativity difference (ionicity) of the constituents. It is from a consideration of some of these parameters that the properties of cadmium sulphide can be related to those of other semiconductors and physical explanations offered for results obtained in this thesis.

1.2. SPECIFIC PHYSICAL PROPERTIES OF CADMIUM SULPHIDE
1.2.1. CRYSTAL STRUCTURE

Cadmium sulphide crystallizes in two modifications. The most common is the hexagonal (wurtzite) structure with lattice constants $a = 4.136A^{\circ}$ and $c = 6.713A^{\circ}$ at room temperature. When grown below $250^{\circ}C$ the cubic (zinc blende) structure with lattice constant $a_o = 5.82A^{\circ}$ occurs.

The lattice parameters of the II - VI compounds have shown a large scatter in the measured values which in many cases is greater than the precision of measure-

ments, due to the distortion of the lattice by the presence of impurities and imperfections. WEBER (1961) showed how the addition of various impurities such as chlorine copper and gallium to cadmium sulphide of wurtzite structure could slightly alter the cell dimensions. In general the lattice constants are decreased by the addition of impurities.

The two crystal modifications for cadmium sulphide are shown in Fig. 1.1. In the wurtzite structure half the tetrahedral sites of the hexagonal close packed cadmium lattice are occupied by sulphur atoms, whereas in the zinc blende structure half the tetrahedral sites of the cubic close packed cadmium lattice are occupied by sulphur atoms. An important aspect of these two structures is that they lack a centre of symmetry or inversion, with the result that opposed crystal faces and directions may have different physical and chemical properties. A consequence of this is that wurtzite and zinc blende crystals are piezoelectric. VON HIPPEL (1952) considered that the group II and group VI ions having opposite polarity formed a network of permanent dipole moments. Distortion of the lattice disturbs the balance of these moments and creates a potential difference the sign of which depends on whether the applied stress is compressive or tensile. In the unstressed wurtzite
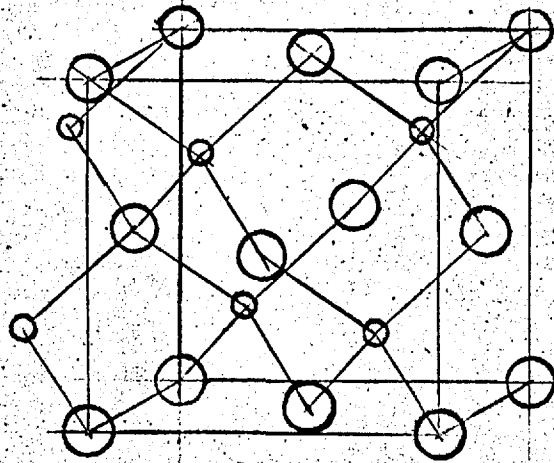
Zinc-blende structure
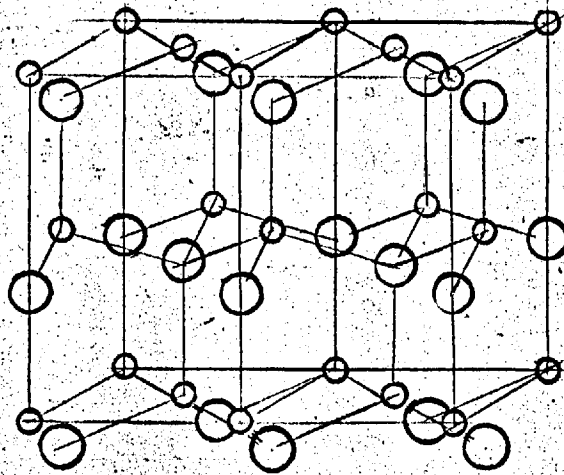
Wurtzite structure

Fig. 1.1

lattice these moments do not completely balance and create a single polar axis in the (0001) direction. Hence wurtzite cadmium sulphide is also pyroelectric and developes potential differences on heating and cooling.

The faces ending in cadmium or sulphur atoms can be shown to be different by their dissimilar etching characteristics (WAREKOIS et al 1962).

1.2.2. CHEMICAL BONDING

There are three main varieties of chemical bonding ionic, covalent and metallic. The II - VI compounds cannot be described completely by any of the above types. SEITZ (1940) originally classified the II - VI compounds as ionic solids. In cadmium sulphide for example, this would involve complete transfer of $5s^2$ electrons from cadmium to the 3p orbital of sulphur forming the ions with stable closed shell configurations $Cd^{+2}(4s^2 4p^6 4d^{10})$ and $S^{-2}(3s^2 3p^6)$. SHERMAN (1932) observed that calculations of the crystal energies of cadmium sulphide and selenide indicated that the binding is not completely ionic.

The distances between the group II and group VI atoms calculated from conventional ionic radii are significantly larger than those observed. For the zinc-blende modification of cadmium sulphide the observed cadmium - sulphur distance is $2.52A^o$ (MILLIGAN 1934)

whereas the calculated distance assuming ionic bonding is 2.66A^o and assuming covalent bonding is 2.52A^o.

The tetrahedral co-ordination observed in cadmium sulphide indicates covalent; treatment of directed valence bonds shows that four hybrid sp^3 orbitals with maximum bond forming power are formed with the bond directions making tetrahedral angles with one another.

Consideration of the periodic table indicates that ionic bonding occurs between elements of the extreme left and extreme right hand portions whereas covalent bonds are formed between elements near the centre. The II - VI compounds are often considered to have an inter- mediate type of bonding. The bonding is treated as essentially covalent and a fraction is assigned to des- cribe the partial ionic character of vice versa. WEBER (1961) has ascribed an ionic character to the bonding of cadmium sulphide with a covalent contribution of 15±15%. He determined the electron distribution between the atoms by Fourier analysis of X-ray diffraction structure factors. Since Bragg scattering does not occur for sufficiently small values of $\sin \frac{\theta}{\lambda}$ (where θ is the Bragg angle and λ is the X-ray wavelength) the accuracy of the above methos is doubtful due to the inability to measure the electron distribution at large distances from the nucleus (BIJVOET and LONSDALE 1953). MOOSER

and PEARSON (1961) have pointed out that the whole concept of assigning a partial character to the bonding may be misleading.

It seems likely that the bonding will have a maximum ionic character in zinc sulphide and oxide and a minimum in mercury selenide and telluride in accordance with the electronegativity difference between the constituents (PAULING 1960).

When high pressures (of the order of 30 atmospheres) are applied to cadmium sulphide the bonding appears to become completely ionic (KABALKINA and TROITSKAYA 1964). The crystal structure changes from a wurtzite or zinc blende to a sodium chloride type of structure. This is a transformation from a tetrahedral to an octahedral co-ordination. On removal of the pressure a zinc blende structure is always obtained.

It is the mixed covalent - heterovalent bonds with various degrees of ionicity which gives the II - VI compounds their characteristic properties.

1.2.3. QUALITATIVE TRENDS IN SEMICONDUCTING PROPERTIES.

The semiconducting properties of cadmium sulphide can be predicted in a qualitative manner by consideration of trends observed in other semiconductors. For example, consideration of the group IV series of semiconductors grey tin, germanium, silicon and carbon (diamond) shows

that decreasing atomic size and lattice constant lends
to increasing band gap and crystal cohesion energy
(melting point), see table 1.1.

Substance	A° Atomic Size	A° Lattice constant	eV Energy gap	$^\circ C$ Melting point
— Sn	1.40	3.567	.08	232
Ge	1.22	5.431	.68	947
Si	1.17	5.567	1.09	1410
C	.77	6.491	5.2	3500+

Table 1.1

Increasing ionicity (electronegativity difference)
also leads to increasing band gap. This is demonstrated
in the isoelectronic series germanium, gallium arsenide,
zinc selenide and cuprous bromide, see table 1.2.

Substance	Electronegativity difference	Energy gap eV
CuBr	1.0	2.9
ZnSe	.8	2.6
GaAs	.6	1.4
Ge	0	.68

Table 1.2

The band gaps of the II – VI compounds are related
to the various degrees of ionic character in a mixed
covalent – heterovalent bond, see table 1.3.

Substance	Electronegativity difference	Energy gap eV
ZnS	1.0	3.7
ZnSe	.8	2.6
CdS	1.0	2.4
CdSe	.8	1.7

Table 1.3

The mobility of carriers is an increasing function of the width of the allowed bands in which the carriers move. The width of the allowed bands increase with increasing covalency of the bonds and polarizability of the atoms. Cadmium sulphide, which is more ionic (less covalent) than cadmium selenide, has an electron mobility, at room temperature, about half that of cadmium selenide with the same scattering mechanisms occurring.

The increase in polarizability of the III - V compounds such as indium antimonide over that of the group IV compounds outweighs any decrease in covalency and leads to very high measured values of mobility. The reverse is true for the II - VI compounds.

In a binary compound consisting of a metal and a non metal it is probable that the conduction band is influenced by the metal and the valence band by the non metal. The smaller the size of the atom the smaller the band it influences and hence the mobility. In zinc telluride, for example, the zinc atom has a tetrahedral

radius of $1.31A^O$ and the tellurium atom one of $1.32A^O$.
The ratio of electron to hole mobility at room tempera-
ture is of the order of 3 (TUBOTA 1963). In cadmium
sulphide there is a large difference between the atomic
sizes, the cadmium atom having a tetrahedral radius of
$1.48A^O$ and the sulphur atom one of $1.04A^O$. The ratio
of electron to hole mobility at room temperature is of
the order of 20 (SPEAR and MORT 1963).

The dielectric constant of a material increase
with the covalency of the bonding and the averaged
polarizability of the atoms. In the II - VI compounds
the dielectric constant increases from sulphide to
telluride, that is with increasing covalency. The
coulombic binding force of a carrier to an impurity
centre in the band gap decreases with increasing dielec-
tric constant. The higher the dielectric constant the
shallower is the centre, that is the closer it is to a
band edge, see table 1.4.

Substance	Electronegativity difference	Dielectric constant $Ks11$	Donor Level Range eV
CdS	1.0	9.02	.024-.032
CdSe	.8	10.20	.014-.03
CdTe	.6	10.60	.011-.022

Table 1.4

The impurity levels associated with broad bands are
shallower than those associated with narrow bands. The

valence band corresponds to an atom shell which is closer to the nucleus and less polarizable than the shell which is associated with the conduction band. The valence band is narrower in energy range than the conduction band in most semiconductors and donor levels are shallower than acceptor levels in the same crystal. In cadmium sulphide donor levels are not much more than .03eV below the conduction band edge, whereas acceptor levels can be more than 1.0eV below.

The word acceptor is used for cadmium sulphide to describe impurities which from consideration of valency would normally produce p-type conduction. It is doubtful whether p-type conduction can be achieved in cadmium sulphide by impurity doping although claims have been made to the contrary (WOODS and CHAMPION 1959). The reason that cadmium sulphide cannot be made p-type is the mechanism of auto-compensation, which is a common phenomenon in wide band gap semiconductors (KRÖGER and VINK 1954, MANDEL 1964). Hole conduction in cadmium sulphide will occur if they are injected through external contacts (KEATING 1963, SMITH 1956) or produced by external radiation.

1.2.4. SELF COMPENSATION AND IMPURITY DOPING

At the high preparation temperature of cadmium sulphide (of the order of $1000^{\circ}C$) the crystal so formed will, by thermodynamic necessity, contain Schottky

defects in fairly high concentrations. These are cadmium and sulphur vacancies. The number of these defects at any temperature varies inversely with the crystal cohesion energy. A fraction of them will be frozen when the crystal is cooled to room temperature and the concentration will depend on the speed of quenching. The sulphur vacancies act as donors and the cadmium vacancies as acceptors. When the crystals are grown in an inert atmosphere equal numbers tend to occur and compensate each other and the crystal is insulating because the number of thermal carriers is small. Equal numbers of vacancies occur because energy is gained by donor electrons recombining with acceptor holes and by oppositely charged vacancies forming pairs on neighbouring lattice sites.

The heating of cadmium sulphide in the vapour of one of its constituents will cause an imbalance in the vacancy concentrations. Cadmium sulphide heated in cadmium vapour becomes n-type because of the increase of sulphur vacancies. Cadmium sulphide heated in sulphur vapour does not become p-type but only more insulating.

When cadmium sulphide is heated in cadmium vapour a sulphur atom will migrate to the surface leaving behind a vacancy and combing with a cadmium atom thereby gaining energy (going to a lower potential energy state) according to the equation

$$Cd_g + S_g = CdS_s \quad \ldots\ldots 1.1$$
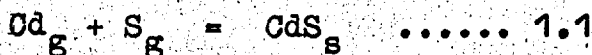
When cadmium sulphide is heated in sulphur vapour
a cadmium atom is freed from the lattice to combine with
a sulphur atom on the surface according to the equation

$$Cd_g + \tfrac{1}{2}S_{2g} = CdS_s \quad \ldots\ldots 1.2$$
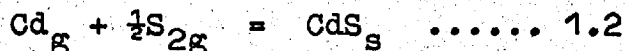
The energy gained is now less, due to the dissocia-
tion energy of sulphur. Cadmium vacancy formation is
therefore energetically less likely than sulphur vacancy
formation.

The dissociation energies decrease as atomic weight
increases in the series S_2, Se_2, Te_2. The formation
of cadmium vacancies in cadmium telluride by heating in
tellurium vapour is more probable than the formation of
cadmium vacancies in cadmium sulphide by heating in
sulphur vapour.

The extremely large conductivity variations ob-
tained in "pure" cadmium sulphide are due to the form-
ation of sulphur vacancies in various concentrations,
produced for example by control of the cadmium vapour
pressure during growth or after treatment.

Cadmium sulphide can be doped n-type by addition
of impurities which are atoms in groups III or VII of
the periodic table. The group III atoms substitute
for cadmium and the group VII atoms for sulphur.

The addition of group 1 or group V impurities does
not dope cadmium sulphide p-type due to the simultaneous
formation of sulphur vacancies which compensate the

material (KROGER and VINK 1954).

The criterion for compensation to occur is that if the energy gained by compensation is greater than the energy needed to form a vacancy then compensation will proceed. The energy gained by compensation is the recombination energy of the carriers attached to the impurity centre with those attached to the vacancy.

The energy needed to form a vacancy increases with the crystal cohesion energy. Crystal cohesion energy decreases with ionicity and atomic size. Compensation is greatest in soft ionic materials with large energy differences between the levels due to impurities and those due to the formation of the vacancy. A wide band gap material such as zinc sulphide with the same degree of ionicity as a smaller band gap material such as cadmium sulphide will be more compensation prone.

The fact that sulphur vacancies occupy shallow levels and cadmium vacancies occupy deep levels leads to small energy gain by compensation of n-type impurities and large energy gain for p-type impurities in cadmium sulphide.

If cadmium sulphide was available as both p and n-type material then p-n homojunctions could be prepared. An applied field would cause minority carrier injection leading to recombination and electroluminescence or even laser action due to the recombination radiation.

Cadmium sulphide is a direct band gap material the extrema of the conduction and the valence bands probably occurring at $K = (0,0,0)$ in momentum space. The existence of the direct gap has been shown by the analysis of the structure of the exciton spectrum at liquid helium temperatures (HOPFIELD and THOMAS 1959, THOMAS and HOPFIELD 1961) and by near threshhold absorbtion (THOMAS et al) showing the existence of longitudinal optical phonon direct exciton creation.

The existence of a direct band gap with a transition giving emission in the blue green region of the optical spectrum makes cadmium sulphide a highly desirable material for laser applications. Laser action has been observed at room temperature and below under high energy electron beam excitation (HURWITZ 1966, NICOLL 1967, BASOV et al 1964). The emitted light is polarized along the C-axis. Laser action has also been observed with optical pumping from a ruby laser (BASOV et al 1966) when a two photon excitation process occurs. No laser action has been reported due to minority carrier injection, as observed for example in gallium arsenide. For this reason and also for the preparation of photovoltaic devices much effort has been made in attempting to prepare p-type cadmium sulphide.

Several investigators (WOODS and CHAMPION 1959, REYNOLDS et al 1955, AVEN and WOODBURY 1962, BUBE et al

1962) claimed to have prepared p-type cadmium sulphide by heavily doping with copper (1 - 2%). The conduction mechanism could be impurity conduction, impurity band conduction, or conduction along filaments of cuprous sulphide which is a p-type semiconductor. The latter mechanism seems the most probable although WOODS and CHAMPION (1959) claimed that X-ray and thermoelectric power measurements did not support this theory. The observed values of hole concentration were at least three orders of magnitude less than the concentration of copper atoms, suggesting compensation or precipitation had occurred.

That the mechanism was almost certainly due to filamentary conduction was demonstrated by other investigators (VITRIKHOVSKII and KURIK 1966, STURNER and BLEIL 1964, DREBEEN 1964). These filaments could clearly be seen by optical microscopy which was not performed by the earlier investigators. STURNER and BLEIL (1964) observed that the limiting concentration that could be incorporated before precipitation occurred was 2×10^{-2}%. The precipitated filaments were observed to line up parallel to the C-axis producing a small degree of lattice strain which prevents them from forming too close to one another. The small value of misfit vector (STURNER and BLEIL 1964) probably accounts for the

difficulty of observing the precipitation by X-radiation (WOODS and CHAMPION 1959). SINGER and FAETH (1967) showed that heavy copper penetration (up to 60%) into cadmium sulphide caused by immersion into a cuprous chloride solution resulted in the precipitation of cuprous sulphide in single crystal form. The cuprous sulphide was exactly $Cu_{2.00}S$ (SINGER 1968) and of the chalcocite (orthorhombic) structure. The lattice constants of the chalcocite and wurtzite structures are:

a_o of CdS $\quad$ 4.136A^o $\quad$ a of Cu_2S $\quad$ 11.88A^o

a_o of CdS $\quad$ 4.136A^o $\quad$ b of Cu_2S $\quad$ 27.32A^o

c_o of CdS $\quad$ 6.713A^o $\quad$ c of Cu_2S $\quad$ 13.49A^o

The a axes are 4% from a factor of 3 apart and the c axes 0.4% from a factor of 2 apart which permits the two crystal structures to line up along their principle axes.

Thermoelectric power measurements (VITRIKHOVSKII and KURIK 1966) indicated a degenerate hole concentration typical of cuprous sulphide. Since the ionisation energy of copper acceptors in cadmium sulphide is of the order 1eV (BUBE 1960) this could not be the cause of the observed hole gas. Furthermore a degenerate valence band should cause a shift in the fundamental absorbtion edge which does not occur (VITRIKHOVSKII and KURIK 1966).

CHERNOW et al (1966) claimed to have grown, from the vapour phase in argon, platelets of high resistivity p-type cadmium sulphide. The p-type character was demonstrated by the results of pulsed light photovoltage, persistent internal polarization and thermoelectric power measurements. Only crystals which were given electrodes of gold, silver or platinum exhibited this behaviour. The crystals were immediately made n-type when indium electrodes were attached, which is likely to prevent the fabrication of a useful device.

Except for the above case all as grown undoped cadmium sulphide crystals are n-type, the conduction being due to sulphur vacancies. Low resistivity (of the order of 1ohm - cm) crystals often grow when a sealed tube method of growth is used (PIPER and POLICH 1961). Crystals grown by a dynamic vapour transport method (FRERICHS 1947) are usually high resistivity (of the order of 10^{10}ohm - cm), due to a high degree of self compensation. Most of the measurements discussed in this thesis are on crystals grown by a dynamic method with no intentional impurities added. These crystals are high resistive but current flow is obtained at low voltages by the injection of charge through external contacts leading to non-equilibrium current flow.

1.3 SPACE CHARGE LIMITED CURRENT

Conduction in a solid is normally due to the movement of mobile charge carries already present in the bulk of the solid. In metals this takes the form of a drift current (electronic)

$$J_{drift} = \mu e n E \quad \ldots\ldots 1.3$$

with a linear relationship between the current and the applied field.

In a semiconductor the carriers are less mobile than in metals and, hence, a non uniform distribution of current carriers can occur, leading to diffusion down the concentration gradient characterised by diff-usion currents of the form

$$J_{diff} = e D_n dn/dx \quad \ldots\ldots 1.4$$

Since metals and semiconductors contain mobile charge no excess charge can accumulate.

High currents can be passed through a semi-insulator such as high resistivity compensated cadmium sulphide if the carrier concentration in the bulk can be increased by external means. Generation of electron hole pairs by external radiation such as light, electrons, X-rays and gamma-rays is one method. (The high sensistivity of

cadmium sulphide in various forms to these various stimuli has led to its use in various forms of detectors.) The other method is to inject carriers through externally applied contacts.

If the dielectric relaxation time is very much greater than the transit time of the carrier then significant currents can flow. These currents will be greatly reduced if carrier trapping centres are present as is the case with cadmium sulphide. The main barrier to further current flow is the space charge which builds up to oppose further injection.

MOTT and GURNEY (1940) performed a simple analysis for drift controlled single carrier space charge limited current in a trap free insulator. They found the current to be proportional to the square of the applied voltage

$$J_{SCL} = 9\epsilon\mu V^2/8d^3 \quad \ldots\ldots 1.5$$

a solid state analogue of the Childs Law for the vacuum triode, where the current is proportional to the three-halves power of the voltage. In general the expression for the space charge limited current in a solid is complicated by the presence of diffusion currents (WRIGHT 1960) and trapping effects (LAMPERT 1956, ROSE 1955). The simplified analysis of LAMPERT (1956), leads to a three regime current-voltage characteristic. Initially the current is ohmic due to the thermal carriers already

present in the material. The ohmic characteristic is replaced by a steeply rising characteristic (traps filled limit) as the injected density increases and fills the traps. When the traps are filled the square law characteristic of MOTT and GURNEY (1940) applies.

The requirements for observing space charge limited currents are:-

1) The semi-insulator must be relatively free from traps.

2) One or both electrodes must provide a large reservoir of carriers with no barrier to the appropriate conduction band (ohmic contact).

3) The anode-cathode separation should be small.

These conditions mean that a carrier has a high probability of transit across the crystal after having been injected at one electrode.

The discovery by SMITH and ROSE (1953) that indium and gallium make ohmic contact to cadmium sulphide and the use of thin crystal platelets led to the first measurements of space charge limited currents in solids. SMITH and ROSE (1955) observed high transient currents which could only be attributed to space charge effects. WRIGHT (1958) observed a square law dependence of current on voltage in a cadmium sulphide crystal having one ohmic and one blocking (non-injecting) contact. It is difficult to observe the square law regime under steady

state direct current conditions as breakdown occurs at the required currents. RUPPEL (1958) who observed a square law regime in zinc sulphide suggested that breakdown was less likely to occur before the square law regime in zinc sulphide due to the higher concentration of shallow traps.

The dependence of space charge limited current on electron traps (ROSE 1955, LAMPERT 1956) has led to its use in determining electron trapping parameters in wide band gap semiconductors, such as cadmium sulphide (SMITH 1959, BUBE 1962, MARLOR and WOODS 1965, BUGET and WRIGHT 1965, TRODDEN 1967). This technique is commonly used in conjunction with other techniques such as photoconductive decay, Hall effect and thermally stimulated current measurements (BUBE 1962).

The results of early investigators (WRIGHT 1958, 1959) applying the theory of LAMPERT (1956) led to extraordinarily low trap distributions of the order of $10^{12}/cm^3$. MARLOR and WOODS (1963) suggested that this is because the steeply rising portion of the current voltage characteristic is due to trap emptying rather than trap filling. Double injection, that is, the simultaneous injection of electrons and holes through two external contacts was suggested by BUBE (1962) as a possible cause of the steeply rising portion of the characteristic.

1.4   DOUBLE INJECTION

Single carrier injection leads to space charge limited current flow whereas double injection leads to space charge compensated current flow. The injected holes compensate the space charge due to the electrons permitting higher currents to pass. Often the recombination of the holes and electrons can lead to the emission of radiation. Double injection has been used to explain electroluminescence observed in cadmium sulphide (SMITH 1957, KOMIYA et al 1962, KEATING 1963, LITTON and REYNOLDS 1964, RUSHBY and WOODS 1966).

HALL (1952) was the first to consider double injection in the design of power rectifiers and transistors of germanium. Since then the phenomenon has been investigated in a wide variety of semiconductors and insulators. The form of the current voltage characteristics depends greatly on the trapping parameters, carrier mobilities and diffusion lengths, and the physical dimensions of the materials used. In consequence a great variety of models have been developed to explain the various observed characteristics. ROSE (1964) comparatively reviewed several of these models.

Many of the models use the same three initial starting equations.

1) The current flow equation which, in general, contains terms for both drift and diffusion

currents. Most theories in order to simplify the mathematics only consider one type of current flow although this can lead to error (BARON 1965).

2) The continuity equation which shows how the carriers are concerved in space and time.

3) Poisson's equation relating the electric field to the net space charge and which, in general, includes terms due to the charges on traps and recombination centres.

Often the onset of a negative resistance regime in the current voltage characteristic is evidence of double injection and is predicted from the analysis of various models (STAFEEV 1959, LAMPERT 1962, ASHLEY and MILNES 1964). The negative resistance is attributed to the increase of hole lifetime with injection level due to the filling of hole traps.

DUMKE (1964) suggested an alternative mechanism for the observed negative resistance in gallium arsenide p-i-n diodes. The space charge limited current injected at the cathode recombines radiatively with holes at the anode. The generated light creates electron hole pairs which fill up photoconductivity centres causing an increase in the electronic current. If the quantum efficiency is a superlinear function of current then a negative resistance will occur.

It is relatively easy to make efficient injecting contacts to the semiconductors like silicon and germanium. These semiconductors can be made semi-insulating by doping with a deep acceptor like gold and compensating with a shallow donor. Double injection has been observed (TYLER 1954, LEBEDEV et al 1957, WAGENER and MILNES 1965) and agrees well with theory (LAMPERT 1962, ASHLEY and MILNES 1964). There is no efficient hole injecting contact to cadmium sulphide and in consequence the observed cases of double injection are difficult to reconcile with one particular theory (SMITH 1957, KEATING 1963). The current may be contact controlled (STOCKMANN 1963). If the contact supplies less current than can be carried away in the crystal then the current is contact limited. At high fields the contact resistance may decrease strongly with increasing field due to contact breakdown caused by field or Schottky emission.

Cadmium sulphide has shallow electron traps and deep hole traps. A device fabricated with a poor hole injecting contact will only permit a few holes to be injected under an applied field and the holes will be captured by, and stored for a long time in, the hole traps. The trapped holes will reduce the barrier to electron flow and the electron current increases as in a photoconductor. Some of the electrons are accelerated into the anode causing more holes to mount the contact

barrier after collision. The process is illustrated in fig. 1.2. for a contact material having a band gap smaller than cadmium sulphide. STEELE et al (1962) have theoretically considered double injection produced by impact ionization at the contact.

BARNETT (1966) observed that double injection in semi-insulating silicon preferentially occurs along a filament where the impurity doping conditions are most favourable. Filamentary breakdown could be the mechanism in cadmium sulphide. SMITH (1957), for example, observed streams of light in his crystals which could be deviated by a magnetic field.

Hysteresis and relaxation oscillations of the current voltage characteristic are also indications of double injection. The hysteresis is due to the finite trapping time of holes and the oscillations are due to the interaction of the negative resistance and the external circuit elements.

1.5. ELECTRICAL CONTACTS TO CADMIUM SULPHIDE

The greater part of this thesis is concerned with attempts to prepare hole injecting contacts to thin platelets of cadmium sulphide and to measure their properties. Since p-type cadmium sulphide is unavailable, only heterojunction devices can be studied.
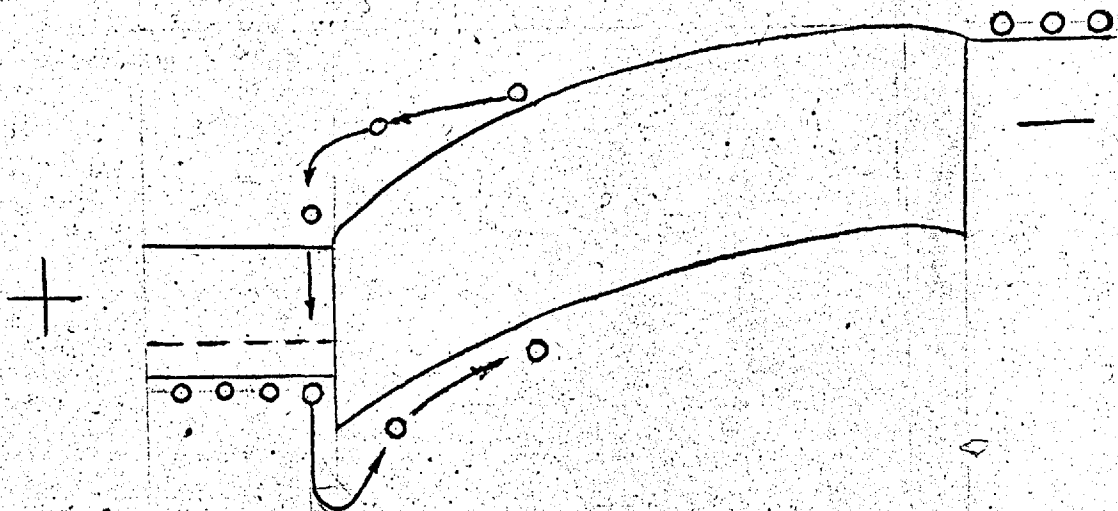
Fig. 1.2

Ionization of holes in anode
by energetic electrons

1.5.1. OHMIC CONTACTS

Ohmic contacts to a semiconductor are characterized by a low resistance so that any applied potential appears across the bulk of the semiconductor rather than at the contacts. There should be no barrier to carrier flow at the junction and this requires the use of a contact material having a higher work function than the semi-conductor for p-type material, and a lower work function than the semiconductor for n-type material. The two cases for a metal-semiconductor contact are shown in fig. 1.3.

Ohmic contacts can often be prepared when the contact material acts as an impurity in the semiconductor causing impurity conductivity of the same sign as that of the semiconductor.

Often the presence of surface states can lead to a barrier which can be overcome by "forming", that is, damaging mechanically or electrically the surface area involved in the contact, for example, by the use of a high current capacitor discharge (SIHVONEN and BOYD 1958).

Indium and gallium were the first substances to be used to give ohmic contact to cadmium sulphide (SMITH and ROSE 1953). The ohmic properties are probably due to a combination of the lower work functions of indium and gallium than cadmium sulphide and of diffusion of
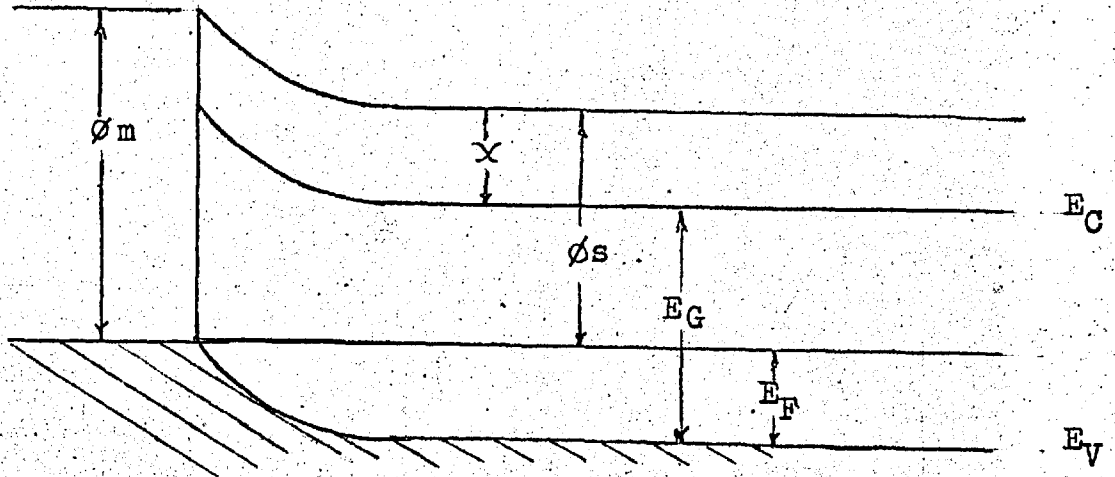
High work function metal to p-type semiconductor
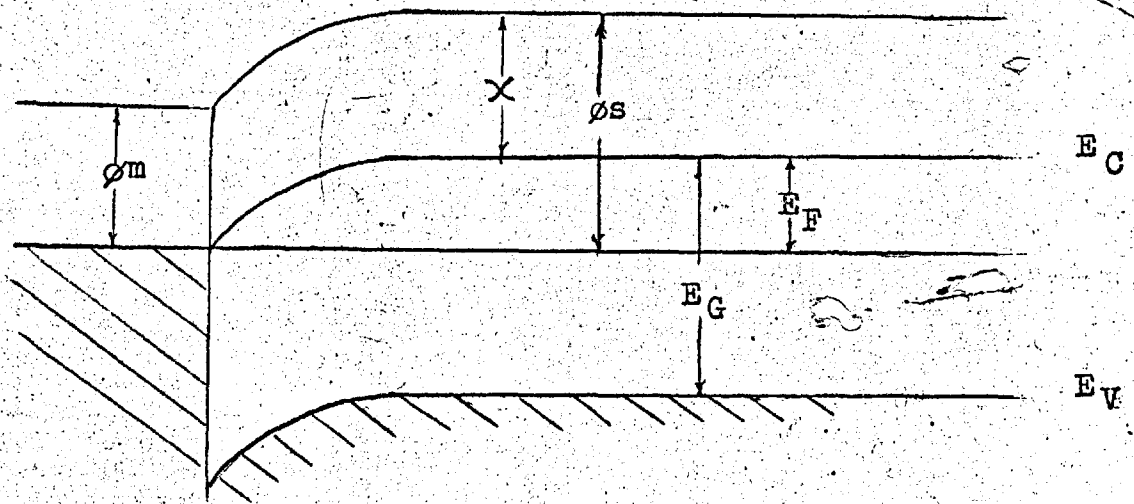
Low work function metal to n-type semiconductor

Fig. 1.3

Ohmic metal-semiconductor junctions

indium and gallium, which are n-type impurities, into the cadmium sulphide surface layers.

The work function of cadmium sulphide is not known with certainty although READ (1968) is measuring it on platelet crystals. High work function materials such as copper, gold, silver and platinum give blocking contacts. KROGER (1956) suggested that the blocking may be attributed to the fact that they are p-type impurities in cadmium sulphide.

Contacts may be prepared using melted or evaporated indium and gallium on the surface of cadmium sulphide. Several investigators required the use of electron or ion bombardment prior to evaporation in order to get good ohmic contacts (FASSBENDER 1956, KROGER et al 1956, BUTTLER and MUSCHEID 1954, MARLOR and WOODS 1963). The effect of bombardment is enhanced by a reducing atmosphere (FASSBENDER 1956) suggesting the formation of sulphur vacancies resulting in a low resistivity surface layer. It appears that many metals make ohmic contact to a bombarded cadmium sulphide surface (BUTTLER and MUSCHEID 1954).

Contacts prepared in the above ways often lose their ohmic nature or else diffuse into the bulk at elevated temperatures. BÖER and HALL (1966) have suggested a multilayer technique with improved high

temperature characteristics. The technique involves
the consecutive evaporation of a preparative layer,
an active metal and a covering metal. The preparative
layer desorbs undesired surface layers and also renders
them chemically inactive making them suitable for the
active metal. The covering metal prevents corrosion
from the atmosphere.

Only ohmic contacts which can supply electrons
have been prepared to date. In this thesis melted
indium and gallium have been used as electron injecting
contacts.

1.5.2. NON-OHMIC CONTACTS

Non-ohmic contacts, which are often called inject-
ing or blocking contacts, are high resistive, rectifying
and noisy (GREINER et al 1957) usually occurring between
materials with large differences in their work functions.
Fig. 1.4. shows injecting contacts to both p and n-type
semiconductors.

Many metals make non-ohmic contact to cadmium
sulphide. GOODMAN (1963) investigated the behaviour of
evaporated gold, silver, copper, palladium, aluminium
and platinum. He obtained a value of 4 volts for the
electron affinity of cadmium sulphide.

When a cadmium sulphide crystal is fabricated with
one ohmic and one blocking contact then the resulting
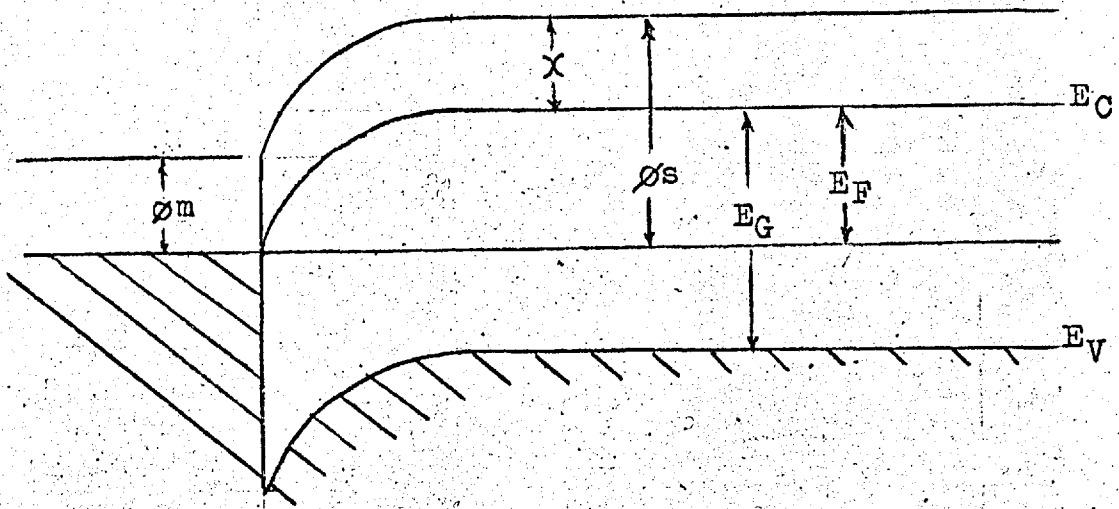
Low work function metal to p-type semiconductor
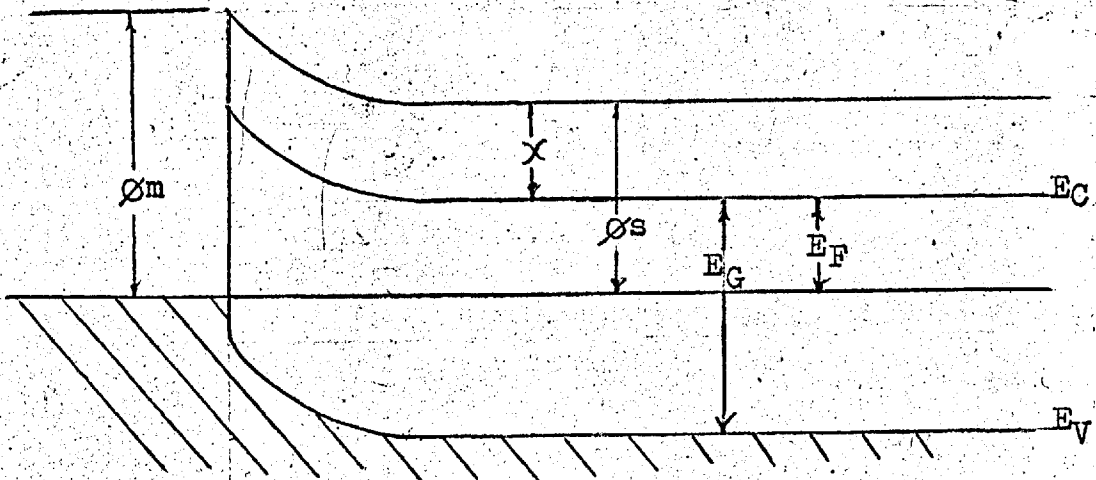
High work function metal to n-type semiconductor

Fig. 1.4

Injecting metal semiconductor junctions

device acts as an efficient rectifier. Rectification ratios as high as 10^6 are obtained (SMITH 1955, REYNOLDS et al 1956, KEATING 1963). These rectifiers suffer from low values of reverse breakdown voltage.

1.5.3. HOLE INJECTING CONTACTS TO CADMIUM SULPHIDE

No efficient hole injecting contact to cadmium sulphide has yet been prepared. The barrier to injection is often large (of the order of 1eV) and the mechanism of intro- duction of holes is usually more complicated than simple injection over the barrier.

SMITH (1957) claimed to have achieved hole inject- ion from gallium electrodes at 77°K on the grounds that he observed recombination radiation. Gallium is normally an ohmic contact for electrons and blocking for holes so that it is difficult to visualize how the holes are injected. The mechanism may be tunnel or avalanche injection.

Tunnel injection normally takes place through a thin insulating layer (of the order of $100A^{\circ}$) and is an efficient method of carrier injection because the thin insulator reduces majority carrier (electron) extraction, see fig. 1.5. The thin insulating layer could be produced by the diffusion of the contact into the bulk, such as copper for example, which makes the cadmium sulphide high resistive. Several investigators

extraction

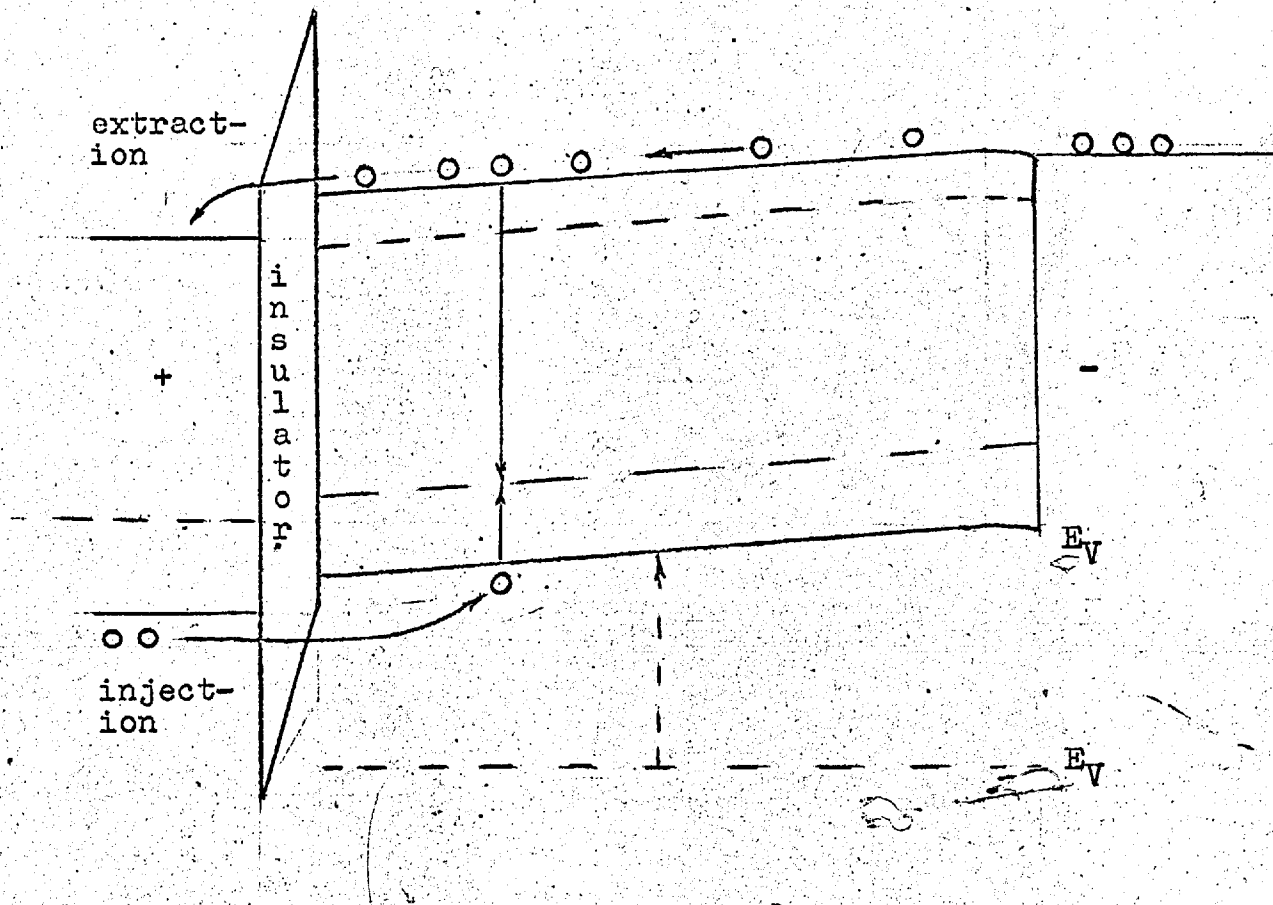injection

insulator

+

−

E_V

E_V

Fig. 1.5

Tunnel injection through a thin insulating layer

have prepared devices with a thin evaporated insulating
film between an injecting contact and low resistivity
cadmium sulphide (FISCHER and MOSS 1963, JAKLEVIC et al
1963, O'SULLIVAN and MALARKEY 1965). The insulators
used include calcium fluoride, magnesium oxide, alum-
inium oxide, silicon oxides, zinc fluoride and sodium
silicate. The injecting contacts used include gold,
silver and cuprous iodide which is a wide band gap (3eV)
p-type semiconductor. The passage of high currents
(of the order of $20,000A/cm^2$) through a layered device
of gold, chromium silicon monoxide and chlorine doped
cadmium sulphide resulted in the line narrowing of the
recombination radiation although no laser action was
observed (O'SULLIVAN and MALARKEY 1965). The efficiency
of these devices is reduced by the presence of inter-
facial surface states and because the tunnelling barrier
to the injection of holes is generally more than the
barrier to the extraction of electrons.

Heterojunctions involving cadmium sulphide and
p-type semiconductors are another means of obtaining
hole injection. SAL'KOV (1965) prepared heterojunctions
by growing a cadmium sulphide crystal on a p-type
silicon carbide crystal. Negative resistance and the
emission of radiation were observed under forward bias
indicating double injection had occurred. The radiation
saturated at high currents probably due to the presence

of surface states. AVEN and GARWACKI (1963) observed
negative resistance and the emission of radiation from
heterojunctions prepared by the epitaxial deposition
of cadmium sulphide on to the (III) zinc face of a
p-type copper doped zinc telluride crystal.

Cuprous sulphide is a highly degenerate p-type
semiconductor (WOODS and CHAMPION 1959) and has been
of interest as a contact material in the production of
cadmium sulphide and gallium arsenide photovoltaic cells.
The majority of cadmium sulphide photovoltaic devices
are dependent on copper as an impurity for efficient
performance. The action appears to be associated with
the interface between the copper sulphide and cadmium
sulphide (CUSANO 1963) rather than the formation of
p-n homojunction by copper doping (WOODS and CHAMPION
1959).

KEATING (1963) observed an S-type negative resist-
ance and the emission of long wavelength radiation at
room temperature in devices consisting of cadmium
sulphide platelets having an evaporated cuprous sulphide
contact. He attributed the results to hole injection
through a p-n heterojunction with recombination at a
deep level although the explanation of DUMKE (1964)
would give the same result. All of the emission was
concentrated at the anode and was of low efficiency.

The low efficiency is probably due to a combination
of surface states, "killer" centres in the band gap
due to transition element impurities, and to the fact
that cuprous sulphide has a smaller band gap than cad-
mium sulphide, causing inefficient injection (FISCHER
1961).

The band gap of cuprous sulphide has been recently
measured by several investigators (SPAKOWSKI 1965,
MARSHAL and MITRA 1965, SOROKIN et al 1966, ABDULLAEV
et al 1968). The values obtained vary considerably
as can be seen in table 1.5. No comment has been given
by any investigator on the different values obtained.

Table 1.5

Author	Band Gap eV
SPAKOWSKI	.90
MARSHAL and MITRA	1.20
SOROKIN et al	1.84
ABDULLAEV et al	1.80

The composition of the cuprous sulphide was pro-
bably different in at least three of the above cases.
Copper sulphide occurs in many forms, for example, Cu_2S,
$Cu_{1.96}S$, $Cu_{9-x}S_5$, showing variations in its copper con-
tent. It is the copper deficiency which gives cuprous
sulphide its p-type behaviour. The crystal structure
of the copper chalcogenides is very strongly dependent

on stochiometry (JUNOD 1959) and could account for the
variations in band gap. The modifications of crystal
structure for cuprous sulphide include, tetragonal
cubic, hexagonal and orthorhombic forms. (ASTM index).

1.6. CURRENT INSTABILITIES IN D-C FIELDS

Many oscillations observed in bulk semiconductors
are due to the formation of high field domains which
travel through the sample. The domains are associated
with a negative differential conductivity (RIDLEY 1965).
There are several mechanisms which are responsible for
domain formation and they are characterized by the
domain velocity. The Gunn effect, first observed in
gallium arsenide (GUNN 1964) and which is due to a
redistribution of carriers over energy bands with
different effective masses, leads to a domain velocity
of the order of 10^7cm/sec. Acoustic amplification,
first observed in cadmium sulphide (HUTSON 1961) and
which is due to energy transfer from the electric field
to the acoustic field when the carrier velocity exceeds
the velocity of sound in the material, leads to a domain
velocity of $10^5 - 10^6$cm/sec. Low frequency oscillations
with domain velocities of the order of 1cm/sec. are
usually associated with field dependent trapping and
trap emptying and have been observed in cadmium
sulphide (BOER and WILHELM 1964), in gold doped

germanium (RIDLEY and PRATT 1964), in manganese doped zinc sulphide (FISCHLER-HAZLONI and WILLIAMS 1965) and in gallium arsenide (BARRAUD 1963, NORTHROP et al 1964, SMITH 1965).

The occurrence of oscillations in the positive resistance regime of the current voltage characteristic of a semiconductor having deep impurity levels was predicted by KONSTANTINOV and PEREL (1965). The oscillations are due to the formation of recombination waves and depend on the presence of both types of current carrier. Normally any increase in free carrier density decays exponentially with time. If a constant field is applied to a semiconductor containing two types of carrier with different lifetimes then any fluctuations in the free carrier density will move under the influence of the drift field and will not necessarily decay with time. If the drift velocity exceeds a certain critical value the fluctuation can capture more carriers than are lost by decay and a recombination wave travels at a constant amplitude representing a free oscillation. Cadmium sulphide with very different lifetimes for electrons and holes could exhibit such oscillations.

HOLONYAK and BEVACQUA (1963) observed oscillations which occurred in semiconductors such as silicon compensated with deep levels. The oscillations were in a

positive resistance regime of the characteristic and were thought to be associated with the simultaneous injection of both types of carrier and the charge condition of the traps. MOORE et al (1967) suggested that the oscillation is related to the finite time of recombination whereby the space charge barrier to electron flow successively collapses and reforms. This type of oscillation is not due to domain motion but to domain build up and decay. The oscillation period will be a function of the recombination time and in materials such as cadmium sulphide will depend mainly on the electron lifetime. The oscillations reported in this thesis appear to be of the space-charge recombination type.

YASUKAWA et al (1966) have observed similar oscillations in cadmium sulphide crystals under simultaneous illumination with visible and infra-red radiation. The presence of free holes appeared essential for the formation of these oscillations since they did not occur above a limiting infra-red wavelength.

Although piezoelectric oscillations are often observed in cadmium sulphide crystals they are not likely to occur in the devices used in the present work due to the high resistivity (of the order of 10^{10} ohm-cm) and the short device length (of the order of 3×10^{-3} cm) which leads to extremely small values of round trip gain (HAYDL 1967).

CHAPTER II

2. GROWTH OF CRYSTALS

2.1. INTRODUCTION

In the study of the electrical and optical properties of cadmium sulphide it is desirable to use highly perfect single crystals. The presence of grain boundaries and surface imperfections would lead to inaccurate measurements. Single crystals of cadmium sulphide have been grown by a variety of methods:

1) Growth from solution (ALLEN and CRENSHAW 1912)

2) Growth by sublimation (FRERICHS 1947)

3) Growth from the melt (MEDCALF and FAHRIG 1958)

4) Hydrothermal growth (NIELSEN and KOLB 1963)

The relative ease of growth from the vapour phase has led to the growth of the majority of cadmium sulphide crystals by a sublimation technique. The use of the melt technique, which should produce good quality crystals, has been hampered by the lack of a suitable container material for use at the melting point of cadmium sulphide of $1475^{\circ}C$, at a minimum pressure of 3.8 atmospheres. Solution growth and hydrothermal growth techniques have not yet been developed to produce good quality crystals.

The crystals used for the measurements reported

in this thesis were all grown from the vapour phase.

2.2. THE EVAPORATION OF CADMIUM SULPHIDE

Cadmium sulphide does not melt at atmospheric
pressure but sublimes at temperatures greater than
1000°C. No evidence for sublimation as the molecular
species (CdS) has been found (GOLDFINGER and JEUNEHOMME
1963). Cadmium sulphide sublimes according to the
reaction:

$$CdS = Cdg + \tfrac{1}{2}S_2g \quad (POGORELYI\ 1948) \quad .....2.1$$
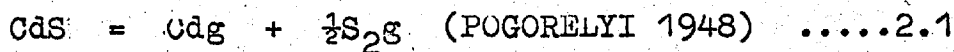
IBUKI (1959), however, assumed that sublimation
occurred with little or no dissociation.

It appears that the following steps precede
evaporation:

1) Formation of Cd and S atoms on the surface

2) Diffusion of Cd and S atoms on the surface

3) Recombination of S atoms to form S_2 molecules

4) Evaporation of Cd and S_2 from the surface

The control of vapour pressure is important for the
growth of highly perfect crystals. The saturated vapour
pressure of cadmium sulphide has been measured by various
investigators (VESELOVSKII 1942, POGORELYI 1948, HSIAO
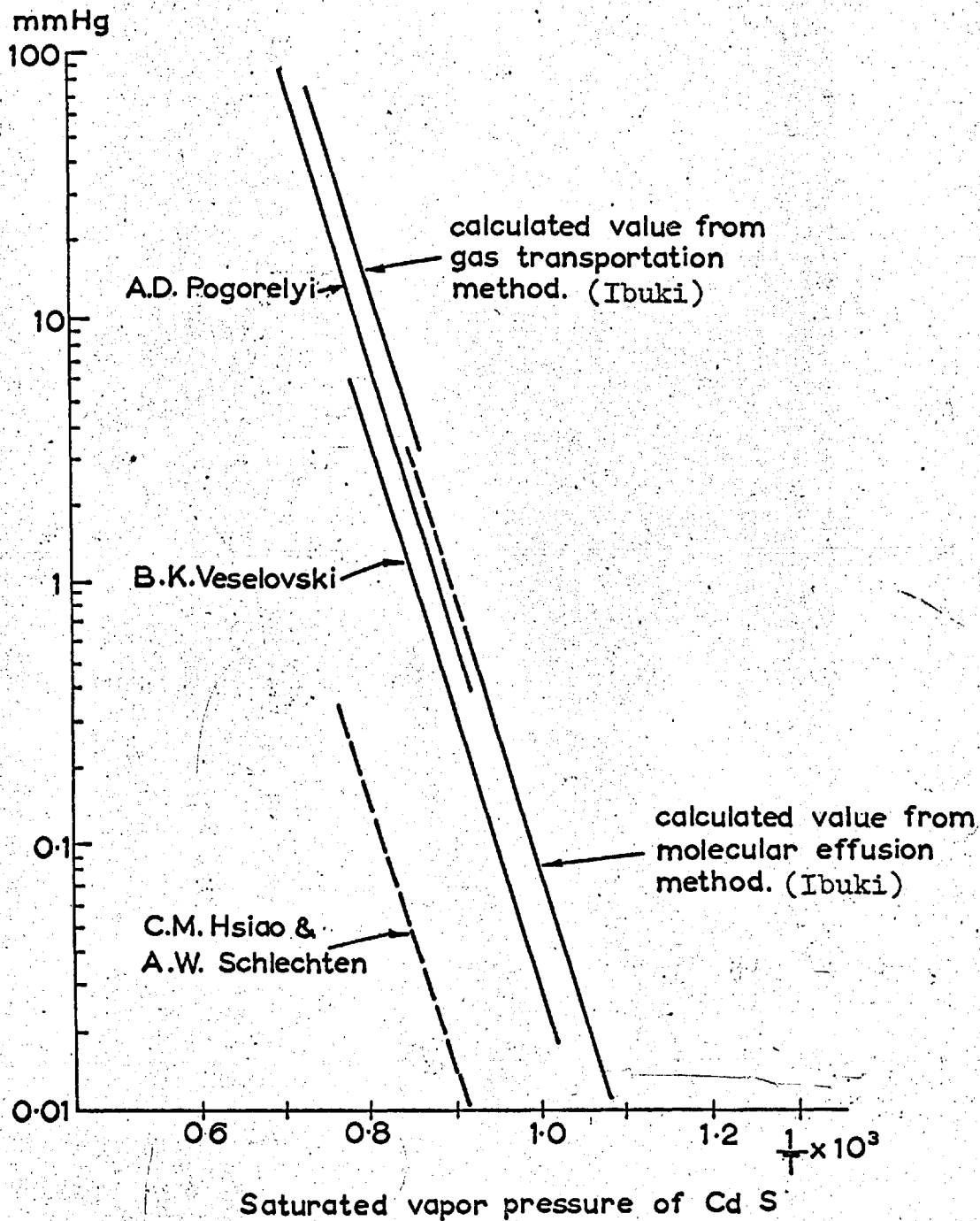and SCHLECHTEN 1952, IBUKI 1959) and their results are
shown in fig. 2.1.

Fig. 2.1.

The evaporation rate is a function of the temperature, the surface area and surface reactions such as dissociation or association. The evaporation rate could be controlled most accurately by evaporating from one face of a single crystal. The evaporation rate is not the same for different faces. When a large amount of charge transfer is required it is not practical to use a single crystal and sintered powder charges or polycrystalline lumps are used in crystal growth.

2.3. GROWTH FROM THE VAPOUR PHASE

Vapour phase growth involves the evaporation transport and solidification of cadmium sulphide. The many techniques that have been used are modifications of two basic methods:

1) Dynamic System - open tube methods using a carrier gas.

2) Static System - sealed tube methods.

Dynamic systems use a carrier gas to carry vapour from the initial charge to a cooler part of the growth tube where the vapour becomes supersaturated and crystallization occurs, usually on the walls of the growth tube. Static systems rely on sublimation and diffusion in an evacuated tube placed in a temperature gradient.

Crystal growth in sealed tubes suffers from the

disadvantage that impurities evolved during growth remain in the system. Due to the slower rate of charge transport, crystals take longer to grow in sealed tubes (of the order of days) than in open tubes (of the order of hours). The growth rate in sealed tubes may be increased and the growth temperature lowered by the incorporation of a halogen in the starting material (NITSCHE 1960). Causing the formation of volatile halides. The halogen finally appears as an irremovable impurity in the crystal (BEUN et al 1962).

Sealed tube methods have been developed, to produce large single crystal boules, from the original method of PIPER and POLICH (1961). Nucleation occurs in the sharp tip of the growth tube as it is slowly moved through a steep temperature gradient. These methods, which can produce large quantities of crystals with consistent properties, are very suitable for industrial production.

Open tube methods generally produce a great variety of crystal modifications depending on the conditions of temperature and flow rate. The modifications include ribbons, neddles, platelets and chunky crystals.

In the study of injected charge carriers and related phenomena it is desirable to use thin single crystals (less than 50 microns thick) so that bulk effects do not predominate. Thin slices cut from boules suffer

surface damage and have too low a resistivity, so that it is desirable to use as grown thin single crystal platelets.

The bulk of the crystals used in this study were prepared by a flow technique and were of the form of thin platelets. Some crystals were grown by the halogen transport technique using iodine but were found to be heavily contaminated by iodine.

2.4. THE FLOW TECHNIQUE

LORENZ (1891) in his study of synthetic minerals was the first to prepare synthetic single crystal cadmium sulphide. FRERICHS (1947) modified the method of LORENZ (1891) to produce ribbon like single crystals. Hydrogen gas was passed over heated cadmium and carried the cadmium vapour to a zone of the growth tube where it met a stream of hydrogen sulphide, to react, and form cadmium sulphide which crystallized out in a cooler portion of the tube. KROGER et al (1954) prepared single crystals by the FRERICHS (1947) technique but with an initial charge of cadmium sulphide. SCHOSSBERGER (1955) modified the FRERICHS (1947) technique to give more control over the evaporation rate of cadmium. KREM-HELLER (1955), STANLEY (1956) and IBUKI (1959) used a stream of nitrogen or argon to transport the vapour from an initial charge of cadmium sulphide. FOCHS and

LUNN (1963) used argon as a carrier gas and a two zone furnace to control the position of nucleation. They studied nucleation on silicon fibres and quartz single crystals. GREEN and GEESNER (1967) grew crystals of different optical properties in a multi-zone furnace using mixed carrier gases such as hydrogen sulphide and argon, and oxygen and argon. SASAKI (1968) used a selfpurification technique where cadmium sulphide vappur was passed over successive charges of cadmium sulphide.

2.5. METHOD USED TO GROW CADMIUM SULPHIDE PLATELETS.

The method used is based on that of FOCHS and LUNN (1963). This technique involves the use of a U-shaped growth tube made of silica instead of the more conventional straight flow tube as used for example in the work of FRERICHS (1947). The U-tube is non-symmetrical having one narrow and one wide arm. A stream of high purity argon entering along the narrow arm carries vapour from a charge of cadmium sulphide in the hot zone of the furnace to cooler regions where crystallization takes place on the walls of the silica tube under suitable conditions of supersaturation.

2.6. EXPERIMENTAL DETAILS

2.6.1. FURNACE CONSTRUCTION

The factors affecting the furnace design are:
1) Temperature of the vapourization zone.

2)   Temperature of the growing zone.

3)   Temperature gradient in the growing zone.

4)   Overall temperature stability.

FOCHS (1960) used a two winding furnace to obtain the correct conditions. In the present study a single graded winding was used.

Two furnaces have been constructed. The first consisted of a single ended mullite tube with a KANTHAL AI winding (upper limit 1375°C). The second was constructed from an open ended high purity alumina tube with a KANTHAL AI main winding and supplementary end windings. High purity alumina cement was used to imbed the windings. The furnace element was mounted on shaped firebrick supports and surrounded by micafil which acted as an insulator. The micafil was contained by sindanyo panels in a steel framework. The whole furnace was mounted on bearings which allowed it to be rotated from a horizontal to a vertical position.

The temperature of the furnace was controlled using an ETHER 991 anticipatory controller activated by a platinum/platinum - 13% rhodium thermocouple embedded in the furnace winding near the hot zone. A bistable multivibrator was placed in series with the thermocouple to give a small alternating voltage of frequency 1.5 seconds and amplitude 1mV superimposed on the thermo-

couple voltage. The oscillation caused the galvonometer
needle of the controller to vibrate slightly which
increased the anticipation of the system and overcame
any tendency of the needle to stick. The current switched
was inductive and of the order of 5 amps. To prevent
any damage, to the controller relay, a high current
relay was placed in series. A 4 microfarad oil filled
capacitor was placed across the high current relay to
prevent sparking. A cut out switch placed across the
ammeter prevented the suspension being subjected to
repeated oscillations. The circuit diagram for the con-
trol system is shown in fig. 2.2.

The temperature profiles of the two furnaces under
the usual operating conditions are shown in fig. 2.3.

2.6.2. GROWTH TUBE CONSTRUCTION

Several silica growth tubes have been used in this
study. They were typically 75cm in length with a narrow
arm of 5mm bore and a wide arm of 30-35mm bore. The
wide arm terminated in a B-34 silica socket. The B-34
cone which fitted into the socket was furnished with an
optically flat glass plate to permit observation of the
crystal growth. The exhaust line for the carrier gas
was connected to the side of the cone. A typical
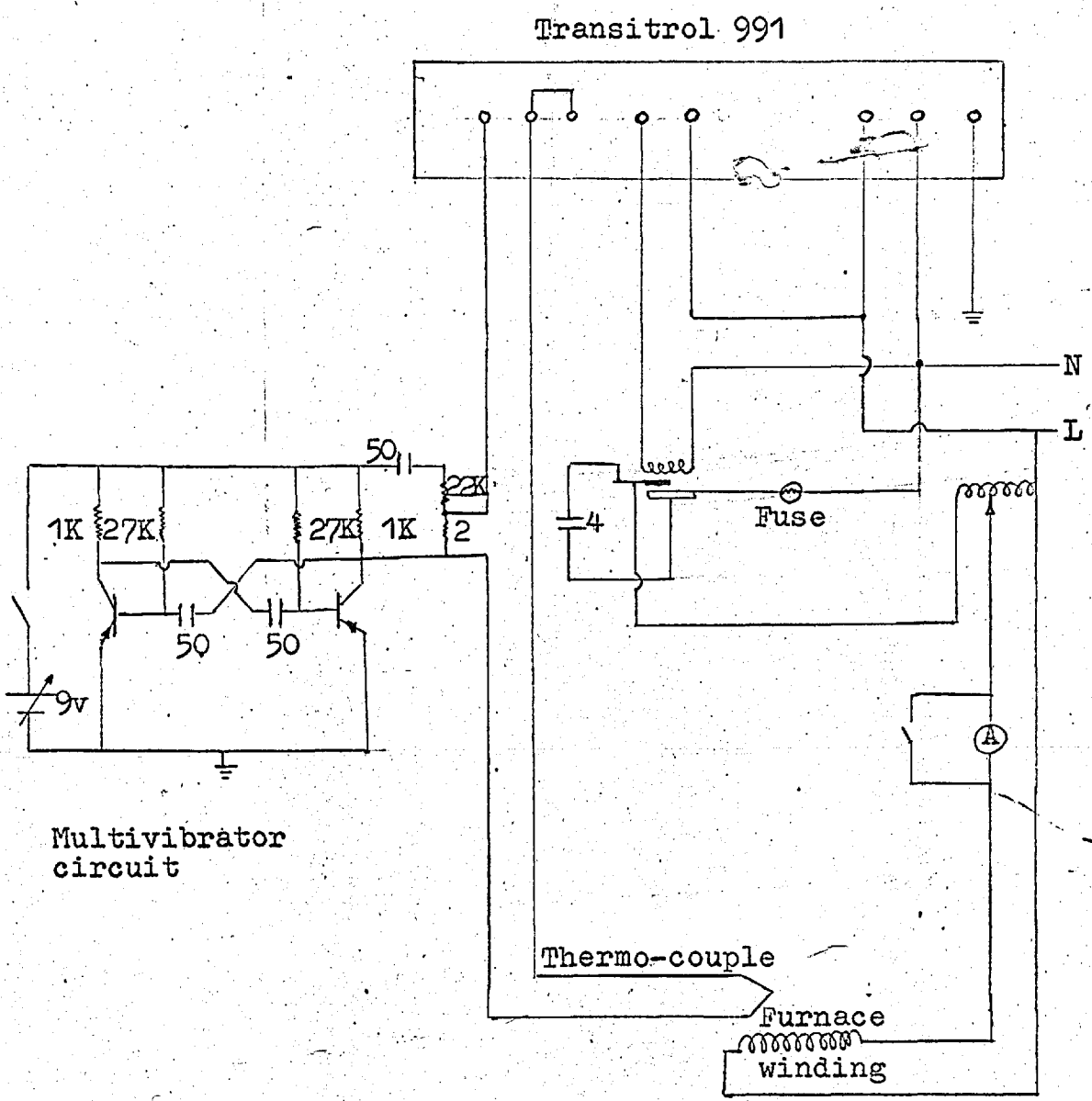growth tube is shown in fig. 2.4.

Transitrol 991

Multivibrator
circuit

Thermo-couple

Furnace
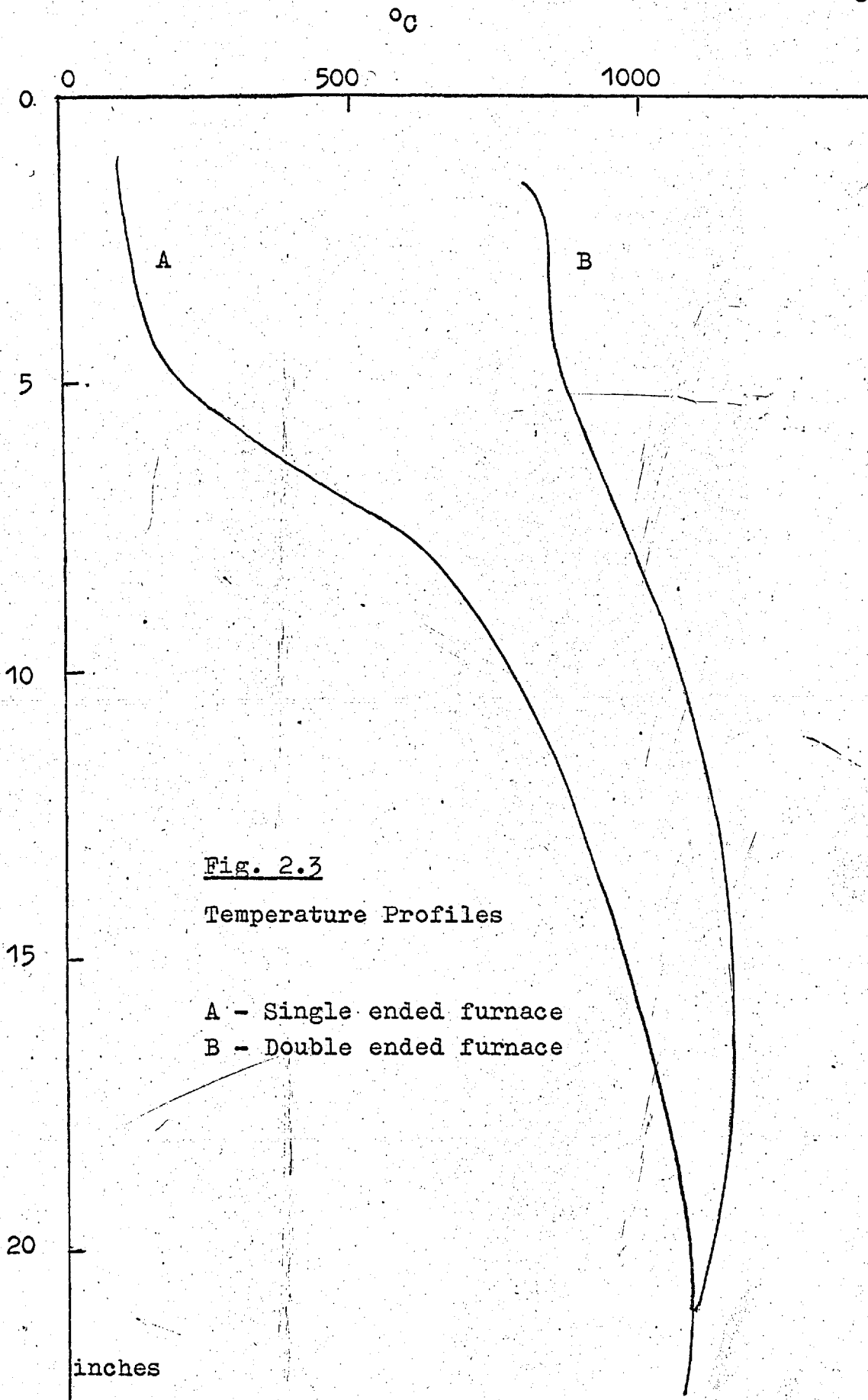winding

Fuse

N

L

Fig. 2.2

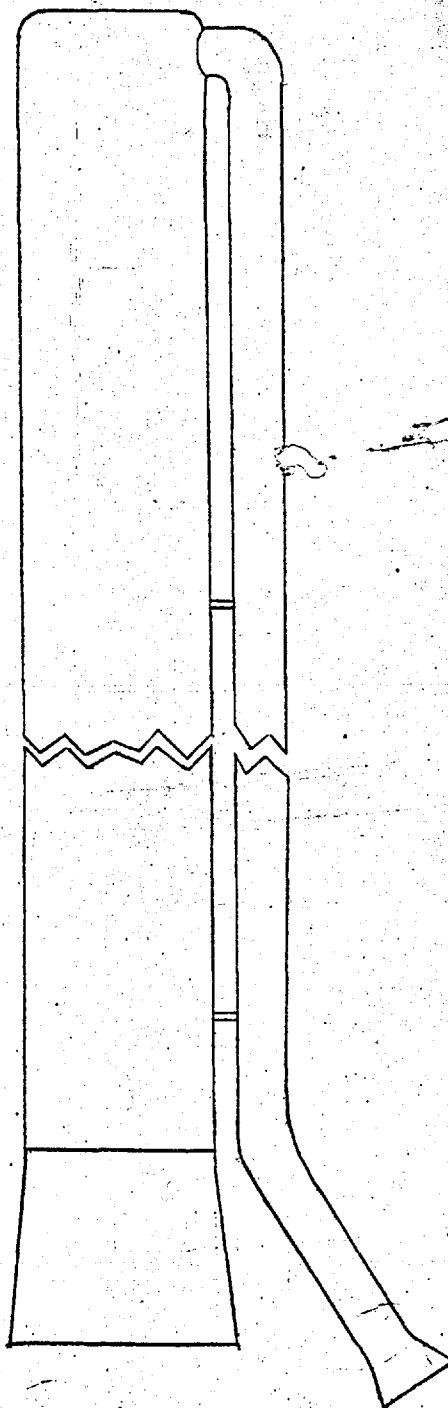Furnace Control Circuit

Fig. 2.3

Temperature Profiles

A – Single ended furnace
B – Double ended furnace

Fig. 2.4

Silica growth tube

2.6.3. GROWTH TUBE PREPARATION

The silica growth tube was thoroughly cleaned before each crystal growing run to reduce the possibility of contamination of the crystals. The following procedure was used:

1) The tube was initially soaked in a 2% solution of RBS concentrate to remove any organic matter on the surface.

2) The concentrate was removed, by thoroughly washing with deionized water, to prevent it drying onto and contaminating the surface.

3) The tube was then filled with a special polishing etch of composition 5% hydrofluoric acid: 35% nitric acid: 60% deionized water for half an hour.

4) The tube was emptied, washed with deionized water and dried.

After the tube had been cleaned it was flamed to white heat in the flame from an oxy-hydrogen torch. The heating procedure performed two important functions:

1) It removed volatile impurities from the surface of the silica tube.

2) It locally melted the silica, which reduced the number of nucleation sites on the wall of the tube and also prolonged the life of the tube by avoiding devitrification. The result of reducing

the number of nucleation sites was that fewer
but better quality crystals grew spaced widely
apart.

2.6.4. CHARGE PREPARATION

The initial charge of cadmium sulphide was either
"pure" cadmium sulphide powder obtained from Levy West
Laboratories or "pure" polycrystalline lumps obtained
from B.D.H. as OPTRAN material. No pretreatment was
applied to the polycrystalline lumps before growth. The
powder, however, was sintered into a solid charge immed-
iately before the crystal growing run. The sintering
was carried out in a silica boat, in a stream of high
purity argon, at a temperature of $1150^{o}C$, for a period
of 10 minutes, in a separate sintering furnace. Volatile
impurities such as excess sulphur, sulphur dioxide and
water were driven off in the gas stream. The very fast
flow rate (10 litres/minute) led to the appearance of
very fast growing dendritic ribbon and needle crystals
of cadmium sulphide on the walls of the sintering tube.
Crystals also grew on the surface of the charge similar
to those observed by CZYZACK et al (1952) in their static
growth technique.

The use of an initial charge of cadmium sulphide,
rather than separate charges of cadmium metal and sulphur

or cadmium metal and hydrogen sulphide gas, leads to a smaller number of variables to control; the variation in the evaporation of cadmium being one of the most difficult.

2.6.5. GROWTH TECHNIQUE

The growth tube was placed in the furnace immediately after being cleaned and flamed. The tube was positioned such that the U-bend was in the hottest portion of the furnace between 1050 and 1150°C.

The initial charge which was either the sintered pellet or several large polycrystalline lumps was placed in the cold end of the tube which protuded from the mouth of the furnace. The end cap was placed in position and high purity argon (5N) was passed through the system, for several hours, at the rate to be used for growth (of the order of .25 litres/minute). This removed oxygen from the growth tube and allowed the system to come to thermal equilibrium. Water vapour was removed from the argon by passage through a molecular sieve surrounded by solid carbon dioxide. The exit for the argon was either a bubbler filled with heavy oil or a butterfly valve. The second method was less likely to cause pressure variations along the growth tube.

When steady conditions had been attained, the furnace was tilted to a near vertical position, as in fig. 2.5.,

Fig. 2.5

Rotation of furnace
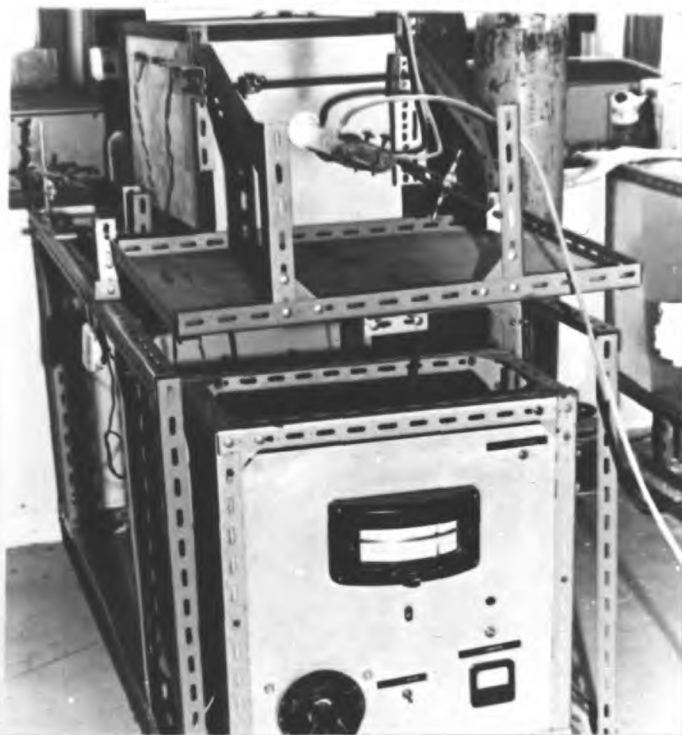
a) Horizontal
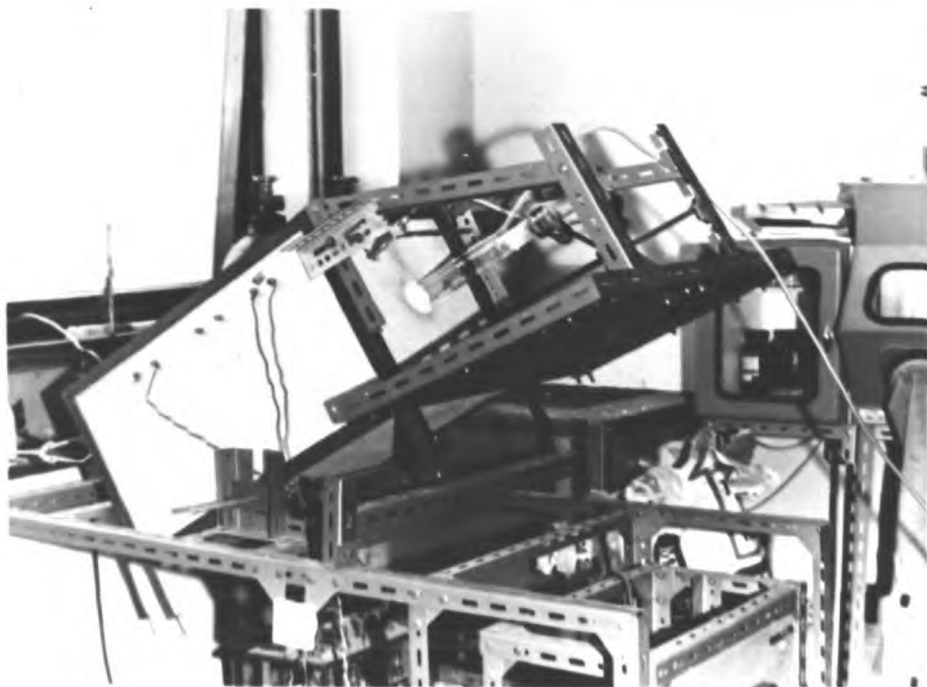
b) Tilted

causing the charge of cadmium sulphide to slide down to the hot zone of the furnace. The furnace was then returned to the horizontal position.

At the end of the crystal growing run, which typically lasted between one and two hours, the whole growth tube was removed from the furnace. It was not necessary to disconnect the argon supply to perform this operation because a U-shaped tube was used. The U-shaped tube also had the advantage that the temperature stability was increased, by preheating of the argon before it passed over the charge. All the crystal growing runs were air quenched in the above manner to prevent the incorporation of impurities from the residual charge and the thermal etching of the grown crystals, which occurs when slow cooling is used. The quenching procedure was likely to produce Frenkel defects (GREENE and GEESNER 1967), which are intestitial sulphur and cadmium atoms together with the corresponding vacancy.

On examination of the tube it could be seen that crystal growth occurred in a temperature range 800 to 1050°C in an average temperature gradient of the order of 15°C/cm. Several types of crystals grew; chunky crystals which grew nearest the charge, plate shape crystals, needles, ribbons, rods, and whiskers.

Specific interest was taken in the growth of the

platelet type of single crystals, since they have a
convenient shape for electrical and optical measure-
ments, which grew in a region between 850 and 950°C.
The platelets either grew directly on and perpendicular
to the walls of the silica tube or else from the side
of a needle as a "flag" crystal. The platelets had
typical dimensions of 1cm x0.5cm x 30 microns. Crystals
of thickness less than 1 micron could be obtained if
a run was terminated after about thirty minutes. The
thin crystals exhibited vivid interference colours.

In order to obtain platelets free from surface
striations it was necessary to keep the vapour pressure
and hence the temperature constant in the growing region
during their formation. If a run was left on for a
long period after the crystals had grown then the plate-
lets started to thicken up and allow other crystals to
grow out of their flat faces.

When the growth tube had cooled, the crystals
could be removed by gently tapping the side of tube
causing the crystals to drop out onto tissue paper.
The thicker crystals were handled by means of vacuum
tweezers whereas the thinner ones could be picked up
with tissue paper moistened with acetone, which allowed
them to drop off when the acetone had evaporated.

2.6.6. VARIATIONS OF THE GROWTH TECHNIQUE

In order to simplify the method of extraction several variations of the growth technique have been attempted.

Initially, silica fibres and quartz crystals were used as nucleation sites following a procedure similar to that used by FOCHS and LUNN (1963) in their investigation of the mechanics of the growth process.

The fibres which were about 25 microns in diameter were stretched between two pillars of 1mm. in diameter, shown diagrammatically in fig. 2.6a. The fibre and the cradle were flamed to white heat before the start of the run. The cadmium sulphide charge was placed in the cradle, the position of which could be controlled from outside the growth tube by the long silica rod, which fitted closely through a tube sealed into the end cap as in fig. 2.6b.

At the start of the run the cradle was kept in the cold zone of the growth tube. When thermal equilibrium was reached it was pushed into the growth tube so that the fibre was at the hottest part of the furnace, at a temperature above the condensation temperature of cadmium sulphide. The whole furnace was then tilted and the charge transfered from the cradle to the hot zone. The fibre was pulled back into the growing region
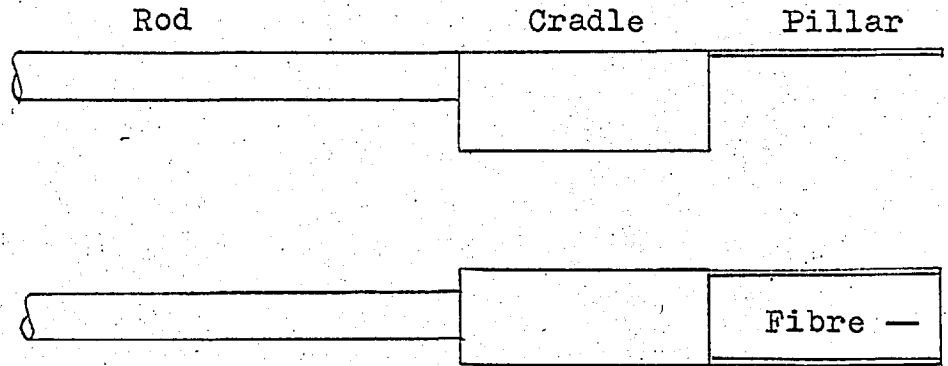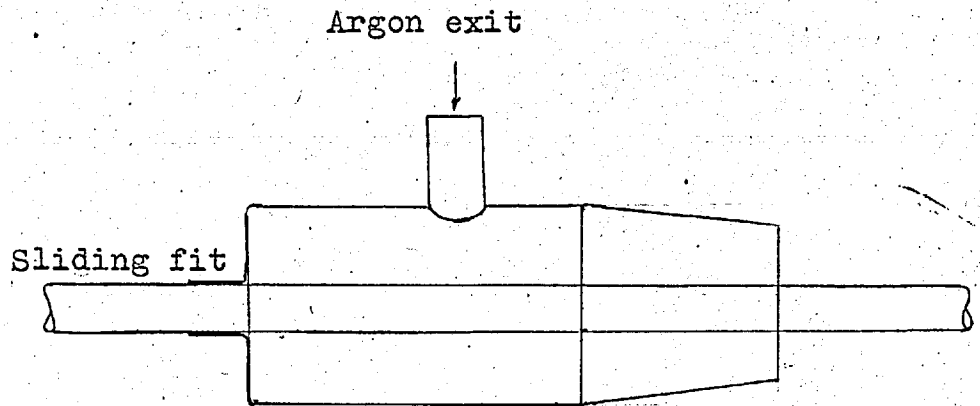
Rod   Cradle   Pillar

Fibre —

Fig. 2.6(a)

Argon exit

Sliding fit

B - 34 cone

Fig. 2.6(b)

Charge Positioning System

after a few minutes had elapsed to allow the flow to become stabilized.

A similar procedure was used for growth on quartz crystals. The quartz crystal was suspended on one of the silica pillars by means of a hole, ultrasonically drilled, through one of its faces.

The crystals which grew on the fibres or the quartz crystals were never as perfect or as large as those which grew on the walls of the silica tube itself. The reason is probably due to the lack of suitable nucleation sites, (such as steps on the surface) in the case of the fibres, and to too many close together on the surface of the quartz block.

To facilitate the removal of plate crystals which grew on the surface of the silica tubing, a series of double tube systems were used with an inner "liner" tube on which the crystals could grow. Several versions of these are shown in fig. 2.7.

2.7. EXAMINATION OF PLATELET CRYSTALS.

Platelets were selected from each run which were of a reasonable area (at least .5cm x .5cm) and of good perfection as in fig. 2.8. Platelets which exhibited surface striations as in fig. 2.9. were not used.

All the platelet crystals had the c-axis (0001 axis) in their large area face. Most of the crystals contained

Argon entry ⟶

crystals   liner tube

charge

crystals

detachable for ease of access
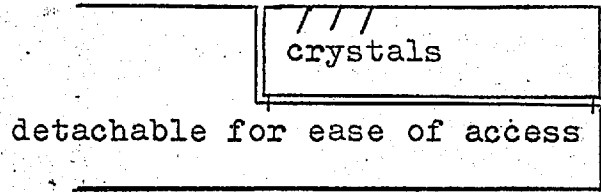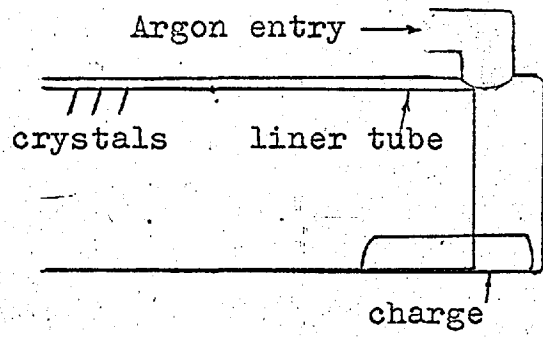
Split liner
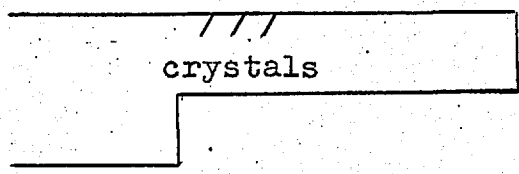
crystals

Half liner

Fig. 2.7

Liner   Tubes

Fig. 2.8

Flat platelet crystals

Fig. 2.9

Striated crystals

the 1120 plane as their large area face although 1230
and 1010 planes were also observed. Fig. 2.10.. shows
the transmission Laue X-radiographs of the 1120 and
1230 planes. The diffraction pattern of 1120 plane is
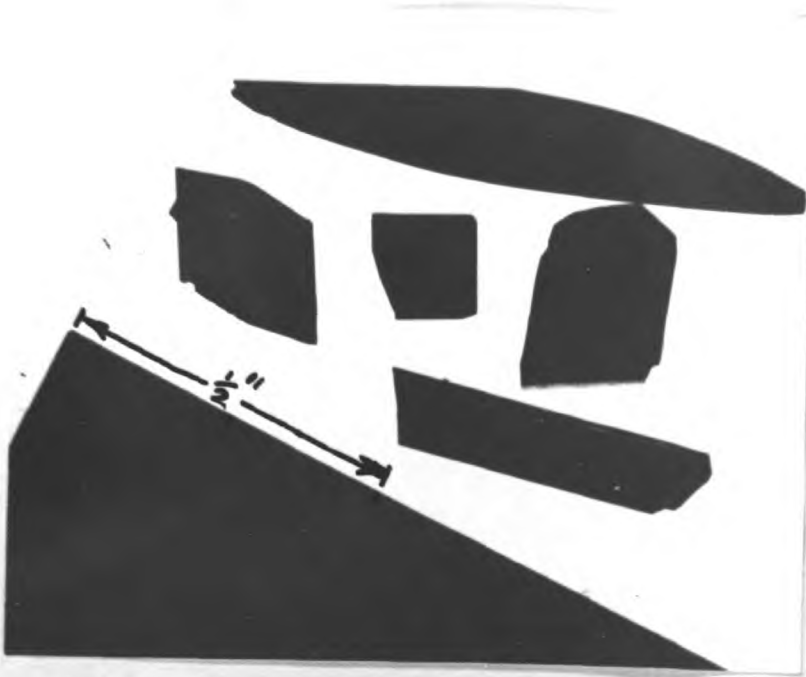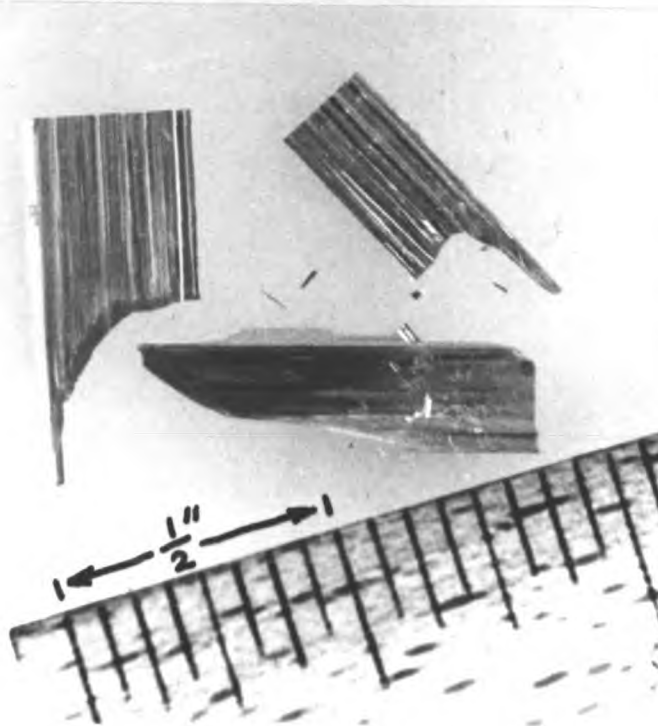symmetrical and could be used to identify other planes
by the angle needed to move on the goniometer to obtain
the 1120 pattern.

Very thin crystals (less than 1 micron thick),
obtained when the crystal growing run was stopped after
only a short time, were very amenable to study by trans-
mission electron microscopy as there was no need for
chemical thinning. A JEM - 7 electron microscope was
used for this investigation.

The very thin crystals were highly perfect showing
very few observable defects. The thicker crystals used
in later measurements will not have been so perfect as
more defects occur as growth progresses. Observation of
the thinner crystals, however, gave some indications of
possible growth mechanisms.

The electron diffraction pattern of a 1010 orienta-
tion is shown in fig. 2.11. The pattern shows a high
degree of crystallinity as did all those examined in
this manner.

Observation of the growing edge of some of the
crystals showed some unusual structures. Fig. 2.12.

Fig. 2.10

Transmission Laue X-ray photographs
of platelet crystals
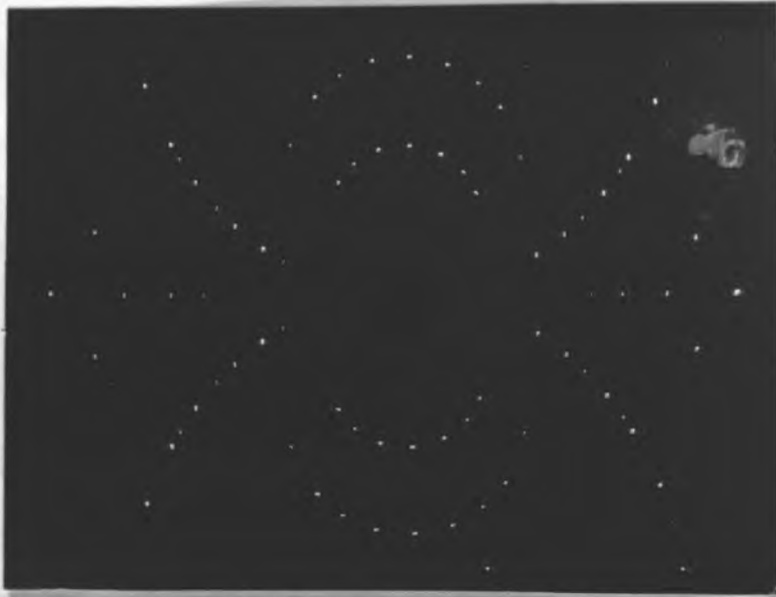
a) 11$\bar{2}$0 orientation

b) 1$\bar{2}$30 orientation

Fig. 2.11

Electron diffraction pattern

10$\overline{1}$0 orientation
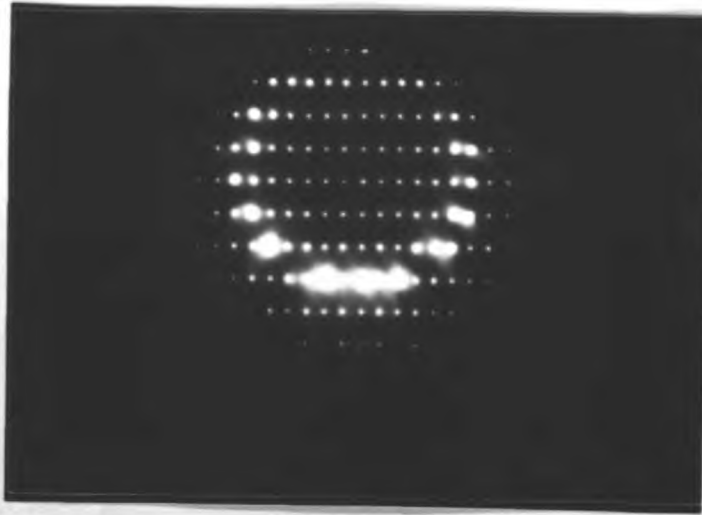
Fig. 2.12

Hair structures on growing edge

exhibits what appear to be hair like structures on the growing edge of a crystal parallel to the direction of crystal growth. They appear to merge directly into the crystal bulk. An ordered crystal is unlikely to grow in this manner. The whisker growths are probably an effect of constitutional supercooling as the growth tube was removed from the furnace.

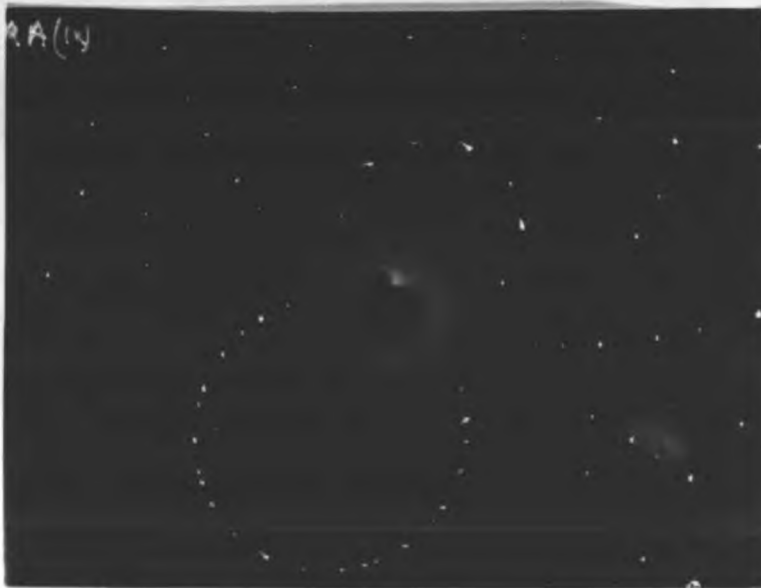Small globules were seen on the growing edge of another crystal and are shown in fig. 2.13. These are similar to those observed in the SLV (Solid Liquid Vapour) type of growth, where a small impurity acts as a condensation site for the vapour and pushes out solid behind it. The existence of a liquid phase involved in the growth mechanism is possible because it is difficult to conceive how an ordered structure can be obtained by a direct vapour - solid transformation.

The crystals could be cleaved very easily parallel and perpendicular to the c - axis which is very useful if they are to be used as a laser device. A parallel sided section cleaved out of a thin crystal is shown in fig. 2.14. This crystal also exhibits interference contours caused by the buckling of the crystal under the electron beam.

Very few dislocations were observed and these were probably introduced by handling after growth. Several

Fig. 2.13

Globules on growing edge
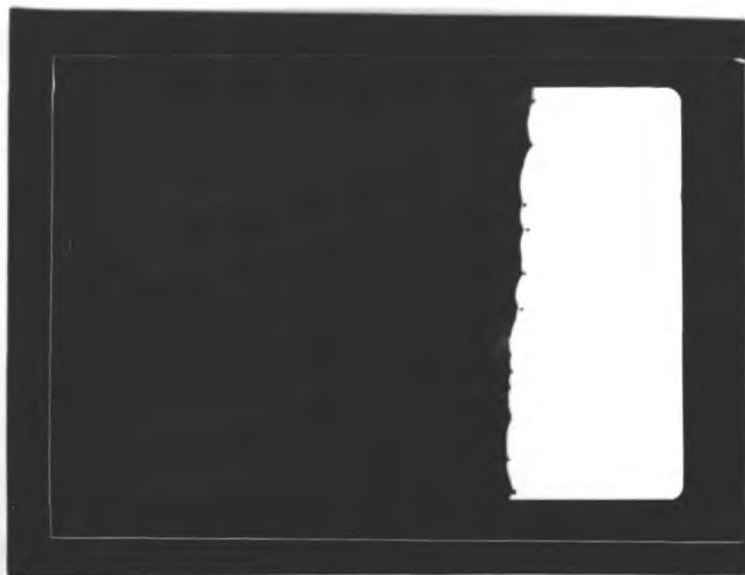
Fig. 2.14

Cleavage
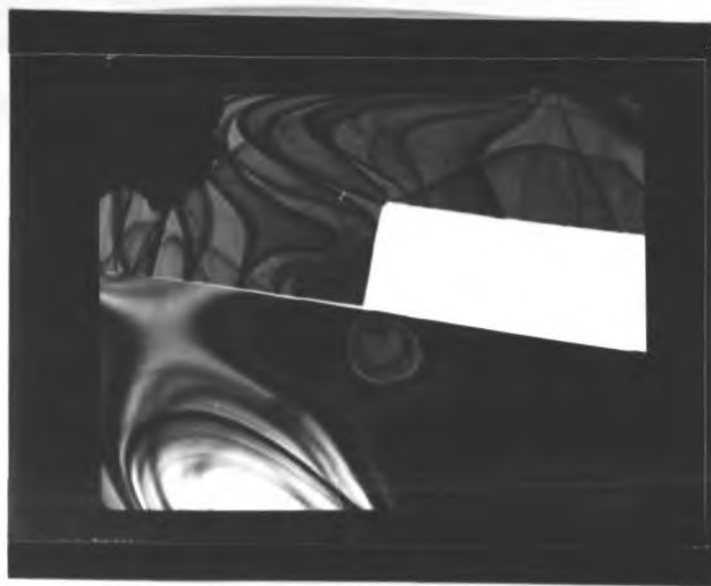
theories of the growth mechanism depend on the initial formation of screw dislocations. CHIKAWA and NAKAYAMA (1964) examined the dislocations by adding impurities which prevented them slipping out during growth.

Several of the crystals also exhibited Kikuchi lines which are due to second and higher order diffraction effects which can only occur when the internal structure of the crystal is highly perfect.

The optical transmission spectrum of a typical crystal obtained on a Perkin-Elmer spectrometer is shown in fig. 2.15. The sharp absorption edge indicates that the crystal is of good quality and is highly stochiometric.

On illumination of the crystals with ultraviolet radiation ($2,537A^{\circ}$) at $77^{\circ}K$ a green edge emission was observed indicating the presence of sulphur vacancies (KULP and KELLY 1960).

2.8. GROWTH IN A SEALED TUBE

A short study was made of the iodine transport method of growth in a sealed tube (NITSCHE 1960) and an interesting method of crystal growth was discovered. A charge of sintered cadmium sulphide powder was placed in a silica tube which was then connected to a multi-head vacuum set. The tube was evacuated to a pressure less than 10^{-5} Torr. Iodine was leaked in by gently heating
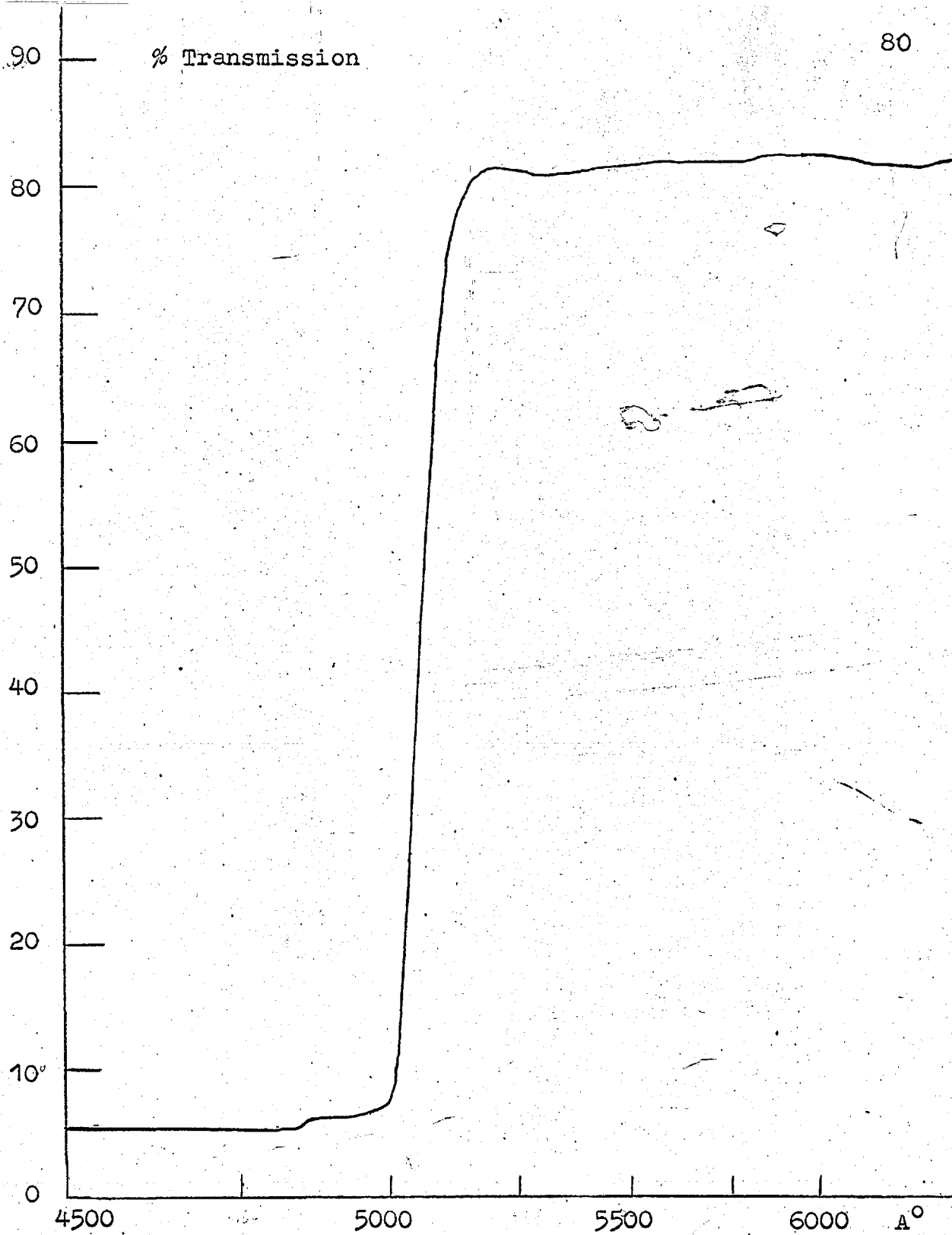
Fig. 2.15.

Absorption Spectrum of CdS Platelet

a silica tube containing iodine attached to another head on the vacuum set. The silica tube was sealed off, under vacuum, with an oxy-hydrogen torch.

The silica tube was placed, in a furnace, in a temperature gradient of about $5^{\circ}C/cm$. The temperature of the charge at one end of the silica tube was about $900^{\circ}C$ and the temperature of the other end of the silica tube about $800^{\circ}C$. The tube was left in position for a week.

A single crystal grew at the cooler end of the tube which had been brought to a fine point to facilitate the growth of only one crystal. An interesting effect occurred at the hotter end containing the initial charge, for the initial charge itself had changed into a single crystal with several well defined facets. One of these crystals is shown in fig. 2.16. The crystal could have been the result of a sintering mechanism going to completion but a more likely explanation is that the crystal was formed by successive evaporation and condensation aided by the iodine. The reaction is likely to proceed according to the following equations:

$$CdS_s + I_{2g} = CdI_2(g) + \tfrac{1}{2}S_2(g) \quad ....2.2$$

$$CdI_{2s} + \tfrac{1}{2}S_{2g} = CdS(s) + I_2(g) \quad ....2.3$$
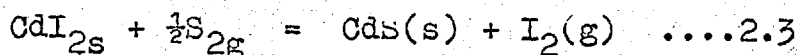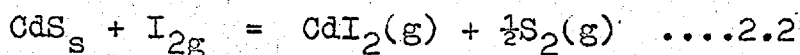
which also apply to the main growth process (NITSCHE and RICHMAN 1962).

Fig. 2.16

Iodine doped crystal
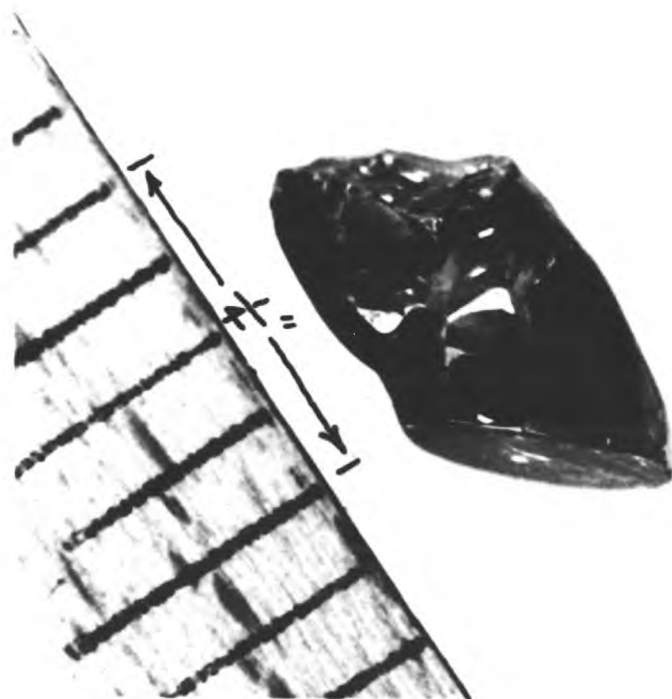
The crystals exhibited a low resistivity of less than 1 ohm-cm, due to the incorporation of iodine, which acts as a donor, into the lattice.

An attempt was made to reduce the iodine content by growing in an atmosphere containing excess sulphur. No transport or crystal formation occurred. The presence of sulphur vacancies appears to be an essential ingredient for both evaporation and crystal growth of cadmium sulphide.

Since the crystals were of too low a resistivity they were not used for subsequent electrical measurements.

2.9. SUMMARY

Highly perfect single crystal platelets of cadmium sulphide have been grown which are very suitable for the study of injected current carriers. Their growth appears to depend on high degrees of supersaturation obtainable with a flow technique. X-rays, electron microscopy and optical spectrometry have been used to examine some of their physical properties.

Low resistive crystals grown by conversion of a sintered charge into single crystal by means of iodine transport technique had too low a resistivity for injected charge carriers to be significant.

C H A P T E R   III

DEVICE   FABRICATION

3.1.   INTRODUCTION

The devices that were studied, consisted of flat
platelets of cadmium sulphide with electrodes on the two
large area faces. The ratio of the surface to bulk con-
duction path length, between contacts on the two opposite
faces, was of the order of one hundred to one.

The majority of the devices had two terminals but
a few three terminal devices, with two electrodes on one
of the flat faces, were made.

Cuprous sulphide, silicon monoxide, gold, cuprous
iodide, indium and gallium were all used as electrode
materials. The majority of the devices that were
investigated had a gold/cuprous sulphide contact on one
face and an indium one on the other face.

3.2.   DEVICES WITH A CUPROUS SULPHIDE CONTACT

3.2.1.   PREPARATION OF CUPROUS SULPHIDE

Commercially prepared cuprous sulphide is available
but since its purity is unknown and a number of modifica-
tions exist, cuprous sulphide was specially prepared for
use in these experiments.

The cuprous sulphide was prepared by the thermal
decomposition of cupric sulphide. At first the cupric

sulphide was prepared by precipitation from solutions of ammonium sulphide and acidified cupric sulphate. Purer cupric sulphide was later prepared by homogeneous precipitation from solutions of cupric sulphate and thioacetamide. In the latter method the cupric sulphate solution was mixed with ammonium hydroxide to form the complex cupro-ammonium ion before addition of the thioacetamide. The correct pH was obtained when adding the ammonium hydroxide by adding until a blue precipitate formed and then just disappeared.

The cupric sulphide precipitate which was obtained by the latter method appeared in the form of large flakes instead of a fine powder and so reduced the amount of contamination by absorption of ions from solution.

The cupric sulphide was thermally decomposed by heating it in a quartz crucible, in a stream of argon for about fifteen minutes at a temperature greater than $1150^\circ C$. If the temperature was too low the decomposition did not procede to completion. Intermediate sulphides, including those of the form $Cu_{9-x}S_5$, were formed. The various sulphides were identified by X-ray powder photography and the diffraction lines obtained were checked with the ASTM index. The powder photograph of the composition obtained at $1150^\circ C$ exhibited the same lines as that of commercially obtained (BDH) cuprous sulphide (Cu_2S).

The powder photograph did not change when the commercially obtained cuprous sulphide was heated above $1150^\circ C$ and this was assumed to be the terminal composition.

The cuprous sulphide was ground into a powder and remelted (melting point $1100^\circ C$) into the form of small ingots by heating in argon or under vacuum. The ingots were suitable for evaporation as they did not tend to spit on heating.

3.2.2. THE EVAPORATION OF CUPROUS SULPHIDE

The evaporation of cuprous sulphide has been studied extensively mainly because of its use in photovoltaic devices (VOHL et al 1967, MYTON 1968, SPAKOWSKI 1965, CUSANO 1963). The main requirements of the evaporated film were that it was transparent to solar radiation and had a small value of sheet resistance. If the film was too thick then too much radiation was absorbed whereas if it was too thin the resistance was high due to incomplete film formation (island structure SWANSON 1967).

SOROKIN et al (1966) studied the evaporation from single crystals of cuprous sulphide. The films obtained had large variations in their properties such as photoconductivity and resistivity, which were also affected by the atmosphere. The variations were probably due to differences in stochiometry, which is difficult to control

in the evaporation of a two component compound, and also due to the formation of cuprous oxide.

ELLIS (1967) decreased the resistivity of cuprous sulphide films by exposing them to ammonium sulphide fumes. The resistivity ceased to decrease when the terminal composition Cu_9S_5 had formed according to the equation

$$9Cu_2S + S = 2Cu_9S_5 \quad \ldots\ldots 3.1$$
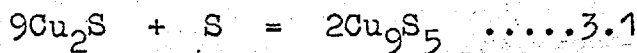
Stochiometric films were obtained by the flash evaporation of material of composition Cu_9S_5.

The conductivity of cuprous sulphide is almost entirely due to the motion of free holes caused by copper vacancies and is very dependent on composition. The reported resistivity values, which varied between 10^2 and 10^{-4} ohm-cm, are many orders of magnitude lower than the resistivity of the cadmium sulphide crystals used in the present investigation. The most important consideration for the measurements in this investigation, was the nature of the cuprous sulphide directly in contact with the cadmium sulphide which would determine the injection mechanism for holes. Results of measurements on chemically deposited films of cuprous sulphide indicated it is almost certainly of composition Cu_2S.

SPAKOWSKI (1965) performed measurements on thin and thick layers of cuprous sulphide. Electron diffraction measurements of very thin layers of cuprous sulphide put down on cadmium sulphide showed the cuprous sulphide to be of the hexagonal high temperature (460°C) modification of Cu_2S with a close match to the cadmium sulphide lattice. X-ray measurements on thicker deposits away from the cadmium sulphide surface indicated the formation of the low temperature (20°C) orthorhombic chalcocite structure.

The evaporated layers of cuprous sulphide are also likely to tend towards the composition Cu_2S at the cadmium sulphide surface due to the transference of sulphur atoms to fill sulphur vacancies in the cadmium sulphide. Further evidence is the exact formation of Cu_2S when copper is diffused into cadmium sulphide.

The evaporation of the cuprous sulphide, for the devices fabricated here, was performed in an Edwards 12E vacuum set. A cuprous sulphide ingot placed in a tantalum boat was evaporated upwards onto the face of a cadmium sulphide crystal at pressures less than 10^{-5} Torr. The cadmium sulphide crystal rested on top of a mask; a microscope slide having holes drilled in it ultrasonically. The hole size varied between 1 and 2 mm. depending on the area of contact desired. The film thickness could

be estimated, during deposition, by observation of its transmission colour on the surface of the slide near to the crystal. The colour changed from a light yellow (of the order of $100A^{\circ}$) to a red brown (of the order of $1000A^{\circ}$) and became highly reflecting and metallic for films greater than $5000A^{\circ}$. The thickness of the various films on the microscope slide could be measured accurately by means of a Talysurf. Films thicker than $3000A^{\circ}$ were generally used on most of the devices since the variation of their properties with thickness ceases at that value (SOROKIN et al 1966). The film thickness by necessity was kept below $500A^{\circ}$ for contacts to very thin crystals (less than 5 microns thick) to avoid severe buckling produced by the stress in the evaporated film (TURNER and TRUBY 1951, WILLCOCKS 1968).

Thermoelectric power measurements on the thin film showed the material to be p-type. The small value of voltage produced indicated a high carrier concentration of a degenerate nature $10^{19} - 10^{22}/cm^3$.

A layer of gold was evaporated over the cuprous sulphide since it was known to provide a low resistance contact (KEATING 1963). The gold layer was evaporated through the same mask but from a greater distance in order to produce a smaller area film than the cuprous sulphide.

3.2.3. MOUNTING OF THE CRYSTAL

Gallium which melts just above room temperature (melting point 29°C) was first used to provide contact to the side of crystal opposite the cuprous sulphide contact. The gallium was also used to attach the crystal to a power transistor header on which it was to be mounted.

The gallium (5N pure) was slightly warmed and stroked onto the surface of the transistor header using a pair of stainless steel tweezers. The crystal was held suspended over the header, by a vacuum tweezer, with the evaporated contact face facing upwards. The gallium surface was continuously stroked to remove any oxide layer which had formed and the crystal allowed to drop onto the surface of the gallium to which it adhered.

The gallium did not solidify completely and in order to obtain a more rigid structure gallium was replaced by indium (melting point 150°C) in later devices.

The higher melting point of indium required the heating of the transistor header prior to application. A tantalum strip heater was used for this purpose (see fig. 3.1.) The indium (6N pure) was stroked on as the temperature reached its melting point. The current through the strip heater was reduced to zero when the indium was molten. The indium remained molten for a

Fig. 3.1

Strip heater
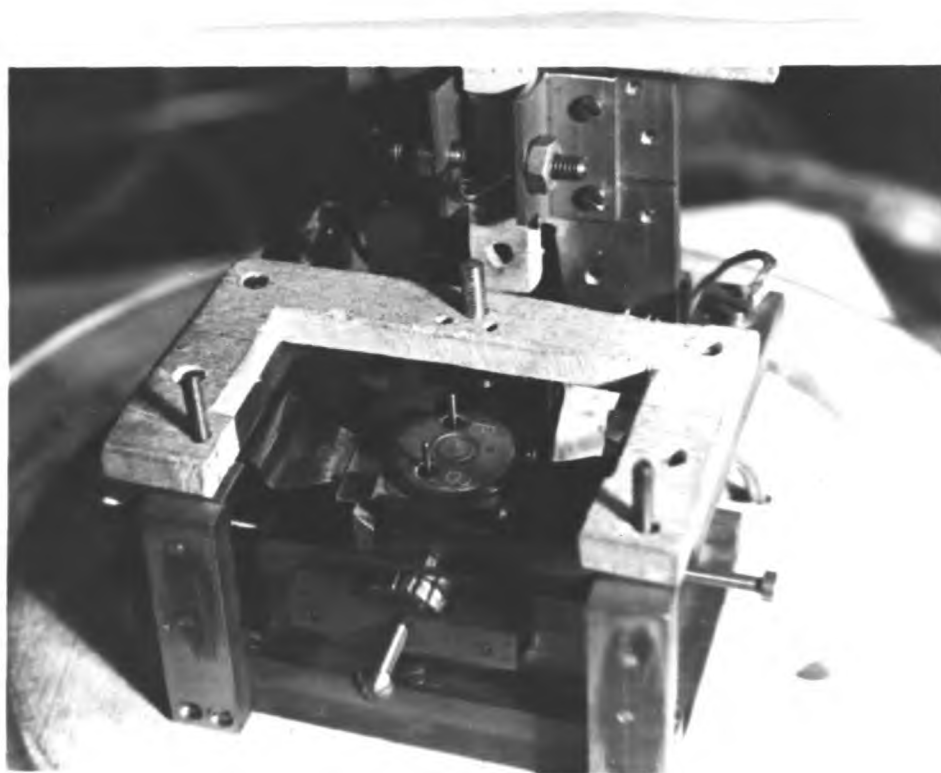
short time due to the thermal capacity of the transistor
header. During this time the indium was stroked contin-
uously to remove any oxide film. The crystal was dropped
onto the freshly cleaned shiny indium surface just before
solidification occurred. The above procedure reduced
contamination with indium oxide. In later device fabric-
ation forming gas was also blown over the surface to
reduce oxidation.

3.2.4. CONTACT TO THE EVAPORATED LAYER

Contact to the evaporated gold layer was made with
fifty microns thick gold wire. At first the devices
were made with a press contact. The gold wire was
fashioned into a simple spring and positioned using a
micromanipulator. The gold wire was soldered with indium
(tin dissolves gold) to a copper bar attached to one of
the transistor header terminals. A device of this con-
struction is shown diagrammatically in fig. 3.2.

Since measurements were to be performed at low
temperatures it was necessary to have a more permanent
form of contact. An attempt was made to solder the gold
wire to the gold layer using indium solder. The gold
wire was positioned with a micromanipulator and the
soldering performed under a microscope. A low tempera-
ture soldering iron was used to prevent too much oxide

Fig. 3.2

Press contact device

Fig. 3.2

Press contact device
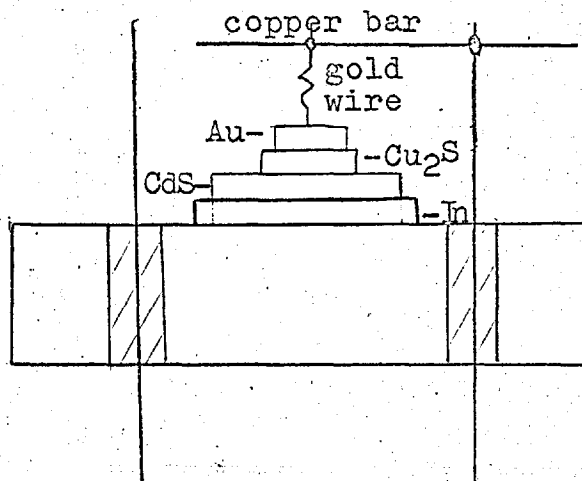
formation on the surface of the indium. The soldering
was not successful because the indium did not wet the
surface easily and the use of a flux such as zinc chloride
contaminated the surface of the crystal and removed the
evaporated film. The undue heating of the crystal in
air was also undesirable.

A technique based on the radiation wetting method
of BARBER (1965) was successfully developed for putting
on indium contacts to the evaporated layer and also
directly to the cadmium sulphide crystal. The system
used is shown in fig. 3.3. The transistor header, with
the crystal fixed to it, was placed in a mount underneath
a tungsten filament. The mount was adjustable in three
dimensions for accurate positioning under the filament.
Indium was compacted onto the end of a fifty micron gold
wire by pressing between two microscope slides. The
indium was then shaped to the desired size with a scalpel.
The compacting procedure was preferred to melting the
indium onto the gold wire since it avoided the formation
of an oxide skin. The gold wire (about 1.5cm long) was
placed on the crystal so that the indium pellet lay on
the evaporated gold layer. The header was then positioned
so that the indium pellet was directly under and a milli-
metre below the filament. The indium tended to rise up
when it was molten and a millimetre was the closest

Fig. 3.3

Radiation wetting apparatus
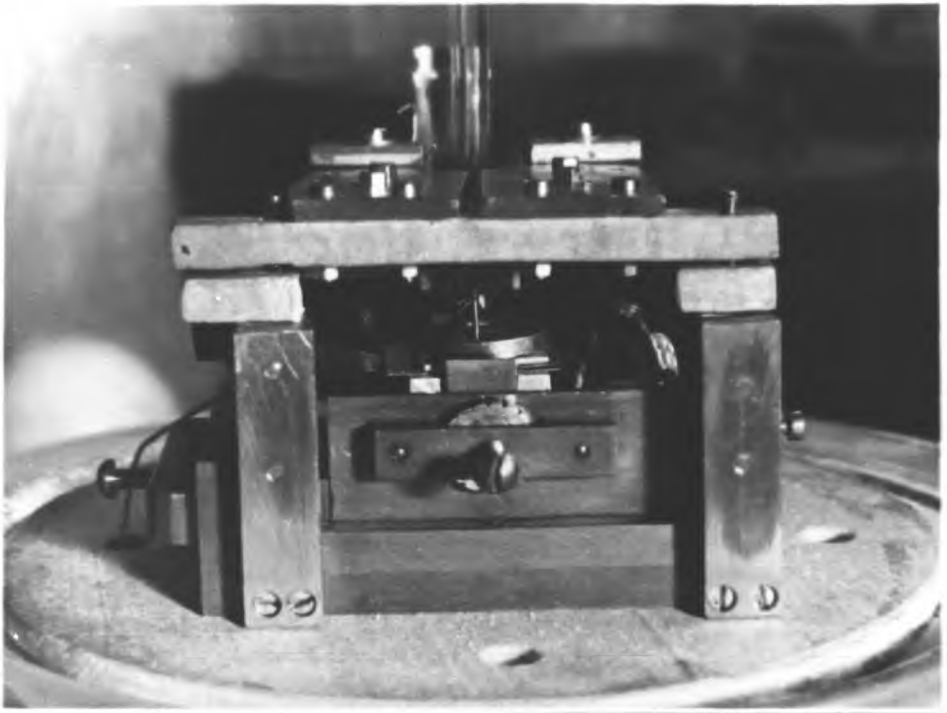
distance the indium could be positioned without the risk

of shorting to the filament on melting. A glass cover

with a ground base was then placed on the apparatus and

hydrogen passed through the system for several minutes.

Current was then passed through the wire causing it to

become white hot. The radiated heat from the wire

melted the indium almost instantaneously. The intense

heat from the wire also caused the hydrogen, about a

millimetre from the wire, to break down from the molecular

state according to the relation:

$$H_2 \quad = \quad 2H \quad \ldots\ldots\ldots 3.2$$
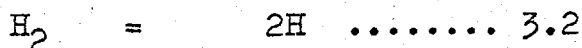
to form atomic hydrogen (LAIDER 1951). Atomic hydrogen

is a very powerful reducing agent even at low tempera-

tures. The reducing action probably removed oxygen from

the surface of the indium and from the surface of the

cadmium sulphide which could otherwise contribute to

current decay in the electrical measurements (MARLOR and

WOODS 1963). The molten pellet of indium was pulled into

a sphere by the action of surface tension. The surface

of the indium became very shiny which indicated the sur-

face oxide had been removed. The spherical state was

very unstable because the critical wetting conditions such

as temperature and oxide removal were reached downwards

from the top of the pellet to the point where contact

was made to the crystal. When wetting started it proceeded almost instantaneously so that the pellet collapsed onto the crystal. The crystal temperature was below that of the pellet as the crystal was effectively resting on a heat sink. When the pellet wetted the surface it now made good thermal contact so that it assumed the temperature of the crystal and solidified. The current through the filament was then reduced to zero.

When direct contact was to be made between indium and cadmium sulphide excessive heating was undesirable due to the rapid diffusion of indium. When contact was made to the gold layer no diffusion of indium was observed on heating. The device was often heated further in the above apparatus after wetting had occurred in order to "form" the cuprous sulphide contact. If the further heating in hydrogen went on for more than one or two minutes the surface of the cadmium became black due to the removal of sulphur and the formation of free cadmium.

A finished device is shown in fig. 3.4. The gold wire was joined to one of the terminals of the transistor header with silver conducting point. The devices could be kept in the dark by means of a press fit cap which fitted on the transistor header.

Fig. 3.4

Fixed contact device

3.3. OTHER DEVICES

The smaller band gap of cuprous sulphide (see 1.5.3) than cadmium sulphide results in efficient carrier injection due to the large injection barrier and the ease of majority carrier extraction. Wider band gap semiconductors and thin insulating films have been used here to try and improve the injection efficiency.

The forming process mentioned in 3.2.4. could have resulted in a thin insulating layer at the surface of the cadmium sulphide through which tunnel injection could have occurred. Copper is known to increase the resistivity of cadmium sulphide (SIMHONEY et al 1967). The temperature of the top surface of the crystal reached about 250°C for about one minute and this may have been sufficient to cause sufficient diffusion of copper.

Several investigators have used silicon monoxide as the insulator for tunnel injection in cadmium sulphide metal-oxide-semiconductor types of device (JAKLEVIC et al 1963, O'SULLIVAN and MALARKEY 1965, YEE and CONDAS 1968). Only low resistivity doped and undoped cadmium sulphide was investigated.

In the present work devices were fabricated with a thin silicon monoxide layer (about hundred angstroms) between a cuprous sulphide or gold layer and the cadmium sulphide crystal.

The silicon monoxide was evaporated from a tantalum boat. The amount of material evaporated was controlled by a shutter. The thickness of the film was measured, with a Talysurf, on the microscope slide which had acted as a mask.

A few three terminal devices were fabricated with a gold/cuprous sulphide and a gold/silicon monoxide contact on the top surface. The device was mounted on an indium contact on the transistor header. The two contacts on the large area faces were separated by around 0.5cm (see fig. 3.5).

The cuprous halides are wide band gap semiconductors and usually exhibit p-type conduction. Cuprous iodide was used in device fabrication and evaporated layers on microscope slides of the bromide and chloride were also prepared. The evaporated cuprous iodide appeared as a white opaque film (due to particle size). Thermal probe measurements showed it to be p-type. Contact was made to the evaporated layer on the cadmium sulphide crystal with a gold film.

The cuprous bromide and chloride both appeared as transparent colourless films indicating they had high band gaps. The bromide exhibited p-type behaviour with the thermal probe but the chloride showed neither sign of conductivity.
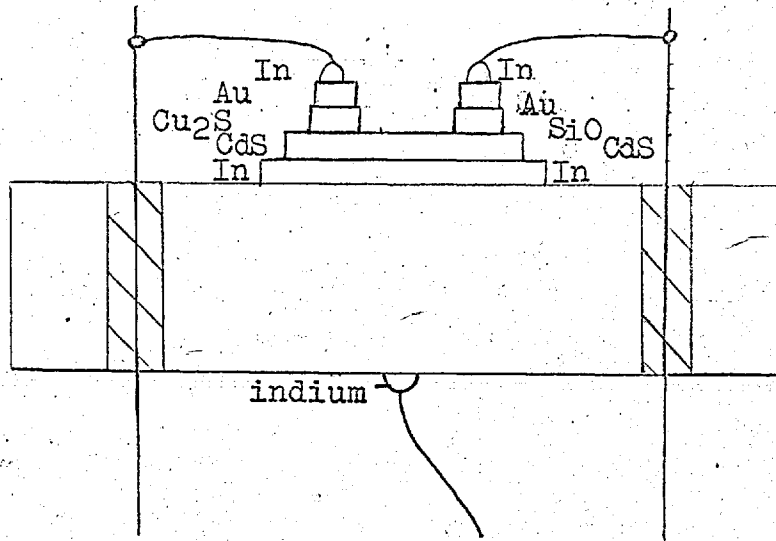
Fig. 3.5

Three terminal device

The cuprous sulphide contact was investigated further by putting it down by chemical deposition. A cadmium sulphide crystal was floated on the surface of a solution of cupric sulphate for a few minutes during which time a layer of cuprous sulphide deposited on the surface of the crystal.

A few devices were fabricated with a gold/cadmium sulphide contact similar to the ones examined by RUSHBY and WOODS (1966) in order to examine the performance of gold as an injecting contact.

The nature of the indium contact was studied by fabricating devices with an indium contact on both the large area faces. The top contact was put on by means of the radiation wetting procedure. A short heating time was used to prevent excessive diffusion. (see 3.2.4).

3.4. SUMMARY

The following devices were prepared and studied.

1a.   Goldwire/Au/Cu_2S/CdS/Ga
           (Cu_2S - evaporated)

1b.   In/Au/Cu_2S/CdS/In
           (Cu_2S - evaporated)

1c.   In/Au/Cu_2S/CdS/In
           (Cu_2S - chemically deposited)

2.   In/Au/Cu_2S/SiO/CdS/In

3.   In/Au/CuI/CdS/In

4.   In/Au/CdS/In

5.   In/CdS/In

6.   In/Au/Cu_2S

                CdS/In

In/Au/SiO

C H A P T E R   IV

MEASUREMENTS AND RESULTS

4.1.   INTRODUCTION

Many devices have been fabricated by the methods
described in Chapter III. Due to the fragile nature of
the cadmium sulphide platelets, a high proportion were
initially damaged in handling, as experience was gained
in the fabrication technique, and had to be discarded.
Others which were successfully completed were later de-
stroyed, during the course of electrical measurements,
by the passage of too large a current.

Measurements were made in a temperature range
between 77°K and 300°K. The measurements, which were
mainly electrical in nature, were performed in order to
gain an insight into the injection mechanism. Phenomena,
such as light emission and current oscillations, due to
the presence of the injected carriers were also observed.
The measurements were performed in the dark except in
the cases where observation of the effect of illumination
was desired.

4.2.   TEMPERATURE VARIATION

Low temperature measurements, on the original
devices which had been fabricated, were performed by

immersion of the device in liquid nitrogen in a simple
split silvered glass dewar. The formation of ice on
the surface of the crystal on heating to room temperature
and the lack of control over temperature led to the use
of a stainless steel optical cryostat supplied by the
British Oxygen Company. The cryostat was of the cold
finger type of construction. The cold finger formed the
base of the inner dewar in a double dewar system intended
for use with liquid helium. Liquid nitrogen was used
in both dewars during the course of the measurements
discussed here. A copper screw-on adaptor was fabricated
for mounting the device on the copper cold finger so
that the device was at the same level as the windows of
the cryostat. The adaptor was fabricated with heater
wires (eureka or constantan) between the base of the
cold finger and the device to raise the temperature of
the device above that of liquid nitrogen. Electrical
insulation between the device and the cryostat was ob-
tained by use of a thin layer of varnish or thin strips
of mica. The transistor header was screwed onto the
adaptor with polythene screws.

The working chamber was evacuated to near 10^{-6} Torr
during the course of measurements preventing the formation
of ice at low temperatures. The effect of the atmosphere
could be observed by performing measurements at room

temperature with and without the chamber being evacuated.

Electrical connections, to the device, to the heaters and to thermocouples were made with a special multi pin adaptor constructed from a valve base which fitted by means of an o-ring seal into the side of the cryostat.

4.3. MEASUREMENT OF THE DEVICE CHARACTERISTICS.

The specific properties of the devices which effectively acted as high resistance diodes necessitated taking several precautions in the measuring circuit and allied apparatus.

The devices were to be characterized by a high rate of rise of current with voltage over several orders of magnitude, often accompanied by a negative resistance, in the forward direction. A range of series resistances was incorporated into the measuring circuit in order to obtain a continuous plot of the characteristics using a constant current supply and also to prevent destruction of the device by passage of too large a current.

The devices were very susceptible to the pick-up of 50c/s voltages emitted by mains operated measuring instruments and power supplies. The pick-up voltage was rectified by the device and opposed the applied measuring voltage. The effects of pick-up were reduced to negligible

proportions by using a bank of batteries as the power supply and in later experiments by the use of a Fluke 412B high voltage (2100V maximum) high stability power supply.

The high resistance of the devices at low currents led to the use of a cathode follower circuit to prevent the loading of the device by measuring instruments. Fig. 4.1. shows the measuring circuit used with battery operated power supplies. The valve was biased (-18V supply) so that it was always switched off to prevent the passage of leakage currents which would have caused errors in the measured value of sample current. Coaxial cable was used for all connections and jack plugs used for convenient interchange of instruments. Two positions were provided for the device, one in the grid and one in the anode circuit. The former was the normal position for d-c measurements. The second position allowed the valve to be used as a pulse amplifier in pulse measurements. In practice this facility was not used, the device being directly connected to the output of the pulse generator.

The device characteristics were studied between 77°K and 300°K using a variety of techniques:-

1) Point by point measurements.

2) Continuous measurements.

3) Pulse measurements.

The point by point measurements were performed using the circuit of fig. 4.1. The device current was measured using a Vibron electrometer (lowest range 10^{-12}A) or a Keithley electrometer (lowest range 10^{-14}A) or a Pye galvanometer (lowest range 2.5 x 10^{-9}A/division). The device voltage was measured using a Phillips voltmeter type GM6020 having an input impedance of 10^{8} ohms.

Continuous traces of the characteristics at higher currents (greater than 10^{-5}A) were obtained using a Tektronix type 575 curve tracer or a Bryans type 22000 autoplotter. The continuous trace could only be studied over one decade of current at a time.

The Tektronix curve tracer was generally used in the diode testing mode with a maximum applied voltage of $\pm$1.5Kv in series with a resistance of 1.5 megohms. For currents greater than a milli-amp the device was connected between the emitter and base connections the curve tracer output with a possible maximum applied voltage of 400V and a series resistance range from zero to 10^{5} ohms. The device characteristic was retraced fifty times a second when it was examined in this manner.

The Bryans X - Y recorder enabled observation of the device characteristic at slow plotting speeds. The device voltage was fed from the output of the cathode follower into the X input and the voltage across a series

109

Fig. 4.1

Cathode-Follower Circuit
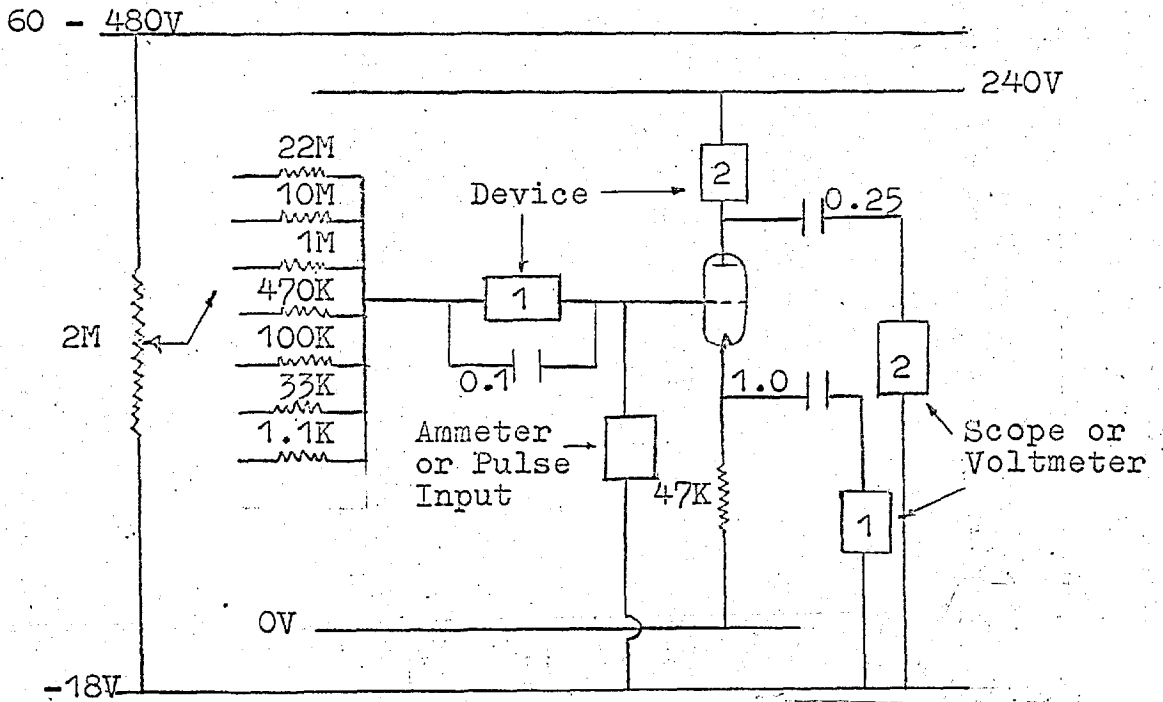
Fig. 4.2

Pulsing Circuit
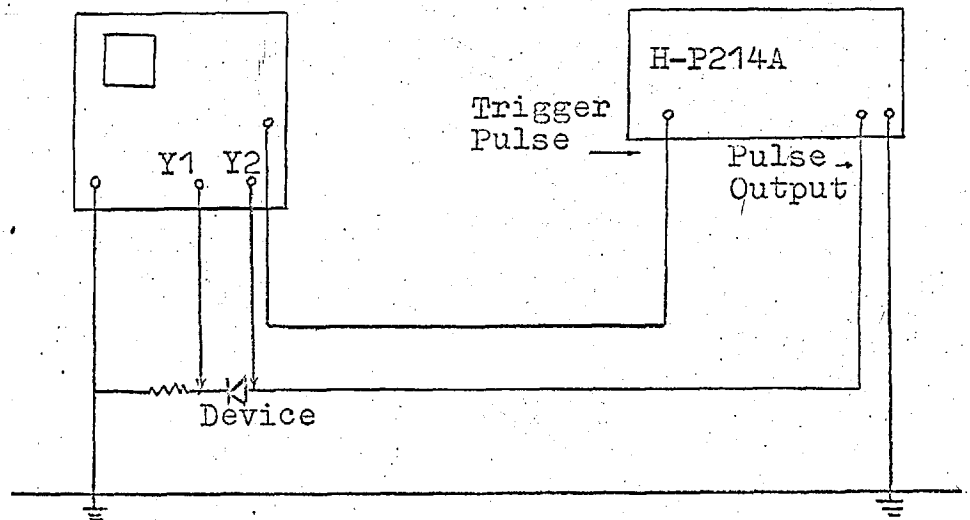
resistance, corresponding to the current, was fed into the Y input. The voltage across the device was increased by manually operating a potentiometer. Slow variations (of the order of seconds) of the voltage across the device as a function of time could be observed by using the autoplotter in the Y - T mode. The plotting speed could be varied between .05 and 20 cm/sec.

Pulse voltages applied to the device enabled high currents to be passed and also the transient response of the device to be studied. A Hewlett-Packard type 214A pulse generator was used for this purpose. Pulse amplitudes up to a maximum of 200 volts and 2 amps. could be passed. The arrangement used for pulsing is shown in fig. 4.2. The pulses were displayed on a Tektronix type 545A or 585 oscilloscope, the time base of which was triggered externally by the pulse generator. Simult- aneous display of the current and voltage pulse was obtained using a type D differential amplifier plug-in unit.

Measurements were performed in the dark by using a press-fit cap over the transistor header or else by covering the windows of the cryostat with black photo- graphic wrapping paper. The devices were kept in the dark for at least a day before measurements.

Fig. 4.3 shows a general view of the measuring apparatus.

Fig. 4.3

Measuring apparatus

4.4. PRESS CONTACT DEVICES

The initial devices which utilized a press contact were all fabricated with gallium as the electron inject-ing contact. The devices fabricated in this manner at first showed a low resistance characteristic in both directions. After heat treatment for several hours at $100^{\circ}C$ the characteristic changed considerably. The devices now exhibited rectification, the low resistance direction being when positive voltage was applied to the gold/cuprous sulphide contact. The forward, dark, room temperature characteristic of such a device, LF/PA, about 30 microns thick is shown in fig. 4.4. A pronounced negative resistance appeared in the forward characteristic. The reverse current at 30V was less than 10^{-8}A giving a rectification ratio of the order of 10^6 at this voltage.

The low current portion of the characteristic of the present device was a complicated function of applied voltage. An exponential law would be expected for the injection of carriers over a barrier. The device under consideration, however, did not consist of a simple p-n homojunction, but of a heterojunction complicated by the presence of surface states and tunnel barriers. The pre-sence of space charge due to injected carriers in the cad-mium sulphide bulk would also complicate the characteristic.

Fig. 4.4

Forward Characteristic
Device LF/PA   300°K
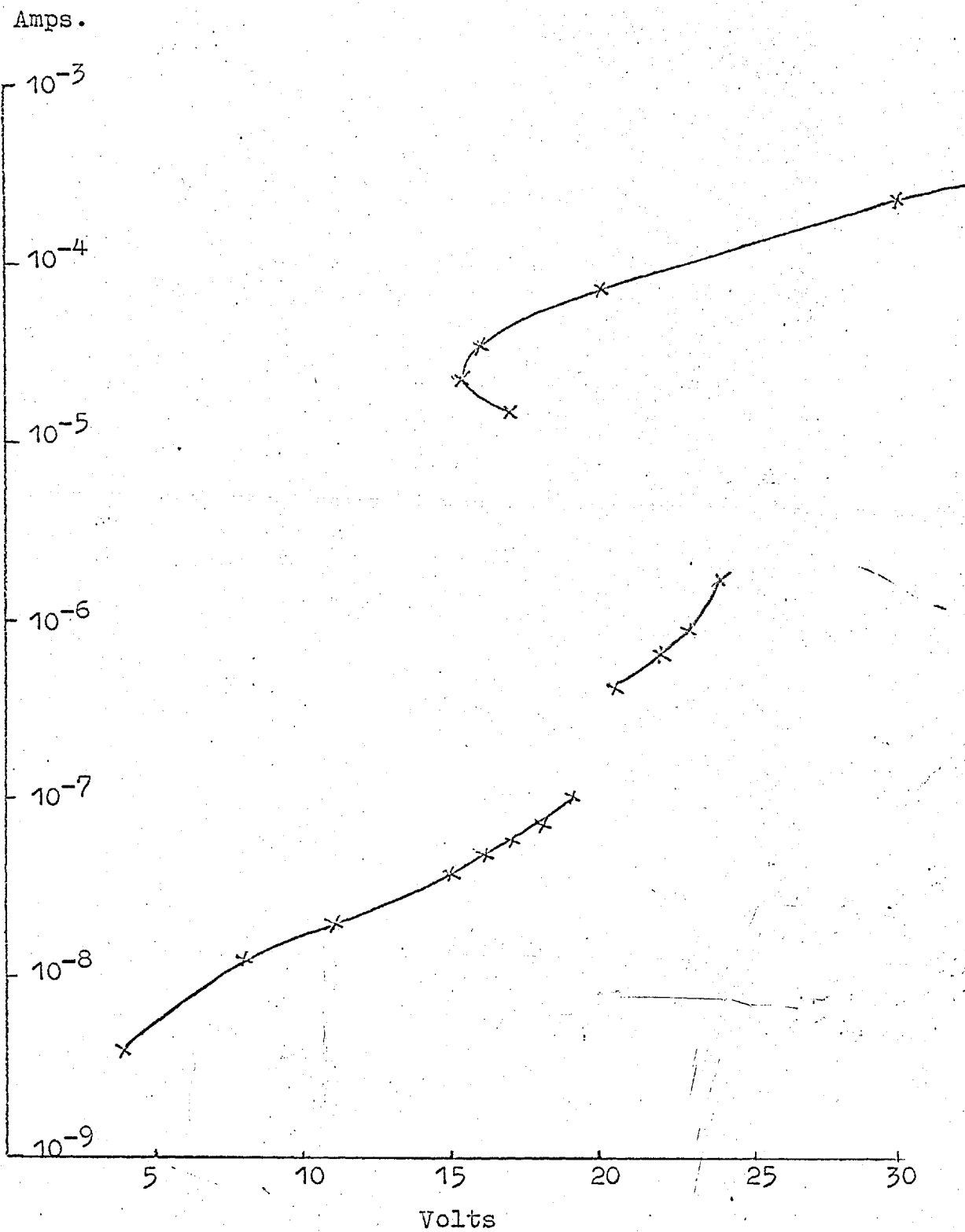
A discontinuity was observed in the characteristic (fig. 4.4.) at about 10^{-7}A and may have been due to filamentary injection (see 1.4 and 4.6.2.).

The portion of the characteristic after the negative resistance regime followed a current proportional to the third power of the voltage law, see fig. 4.5. LAMPERT (1962) obtained the same law following the analysis of a simple model for double injection into an insulator having a single recombination centre in the band gap. A negative resistance was also predicted by this theory due to the increase of hole lifetime with injection level. The current proportional to voltage cubed section of the characteristic was predicted for high injection levels in the presence of space charge. The theory of LAMPERT (1962) will be dealt with in more detail in CHAPTER V together with other theories on double injection.

No visible luminescence was observed using an EMI 9558 BQ photomultiplier at room temperature contrary to the results of KEATING (1963) on similar devices, where a weak long-wavelength red electroluminescence was observed. It is possible that recombination between electrons and holes did occur but that the recombination transition was in the infra-red in the present devices. KEATING (1963) did observe a negative resistance in the

Fig. 4.5

Characteristic after negative resistance
Device LF/PA
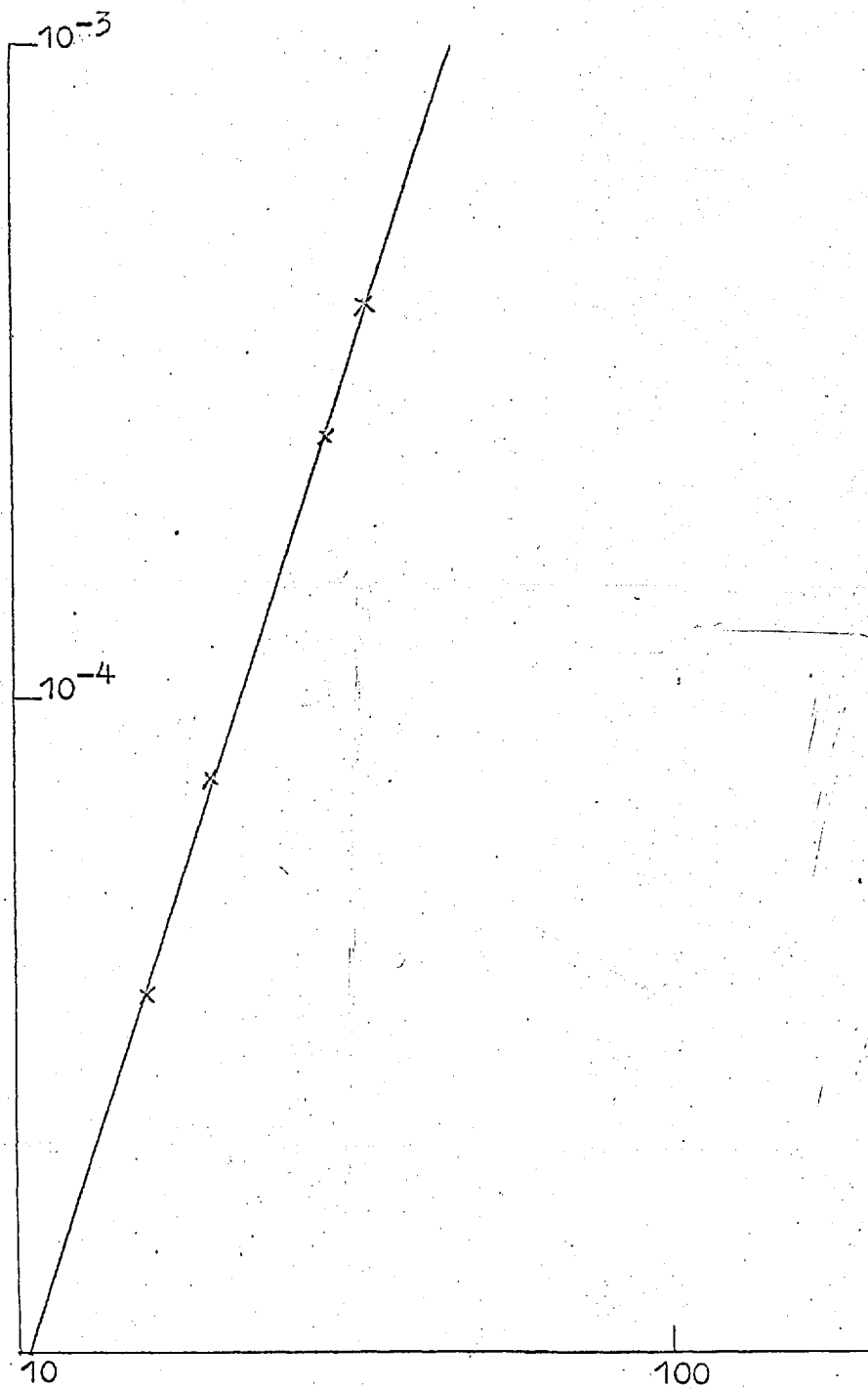
forward direction in some of his devices and explained it as due to a double injection mechanism.

The press-contact did not appear reliable at low temperatures and no measurements were taken on this type of device below room temperature.

4.5. FIXED CONTACT DEVICES.

The majority of the devices, on which measurements were performed, were fabricated with the gold wire fixed to the evaporated gold layer by the method described in section 3.2.4.

The heating of the device in hydrogen during the course of the above procedure elimated the need for heat treatment experienced with the press-contact devices. The fixed contact devices did not exhibit the irreversible changes observed with press-contact devices before heat treatment. The press-contact devices had been fabricated with a gallium electron injecting contact. The temperature at which the original devices were mounted on the gallium was only just above room temperature. Heat treatment was probably necessary in order to produce an ohmic contact between the gallium and the cadmium sulphide (KRÖGER et al 1956) as well as to "form" the cuprous sulphide contact (BRAÜNLICH 1967).

4.6. DEVICES OF THE FORM In/CdS/Cu$_2$S/Au/In

4.6.1. ROOM TEMPERATURE CHARACTERISTICS.

The dark, room temperature, forward characteristics
of devices of the form In/CdS/Cu$_2$S/Au/In were obtained
and some of these are plotted in fig. 4.6. The thick-
ness of these devices was more than 20 microns but less
than 50 microns. A negative resistance was observed in
the forward characteristics of all the devices in the
above thickness range. The negative resistance was
followed in most of the devices by a region where the
current increased at a constant voltage and was limited
by the series resistance in the circuit. A character-
istic of this form is predicted by the theory of ASHLEY
and MILNES (1964) for the analysis of a model for double
injection into a solid having a partially compensated
trapping centre for holes in the band gap. The theory
of ASHLEY and MILNES will be considered in more detail
in CHAPTER V.

The devices exhibited rectification with rectifica-
tion ratios up to 10^6 similar to that observed with the
press-contact devices. Breakdown occurred in the reverse
direction at sufficiently high voltages (were often more
than 100V.) The actual cause of the reverse breakdown is
uncertain as most of the voltage probably appeared across
the junction. A probable mechanism is the avalanche

118

Fig. 4.6

Forward Characteristics
Devices of the form In/CdS/Cu$_2$S/Au/In
300°K
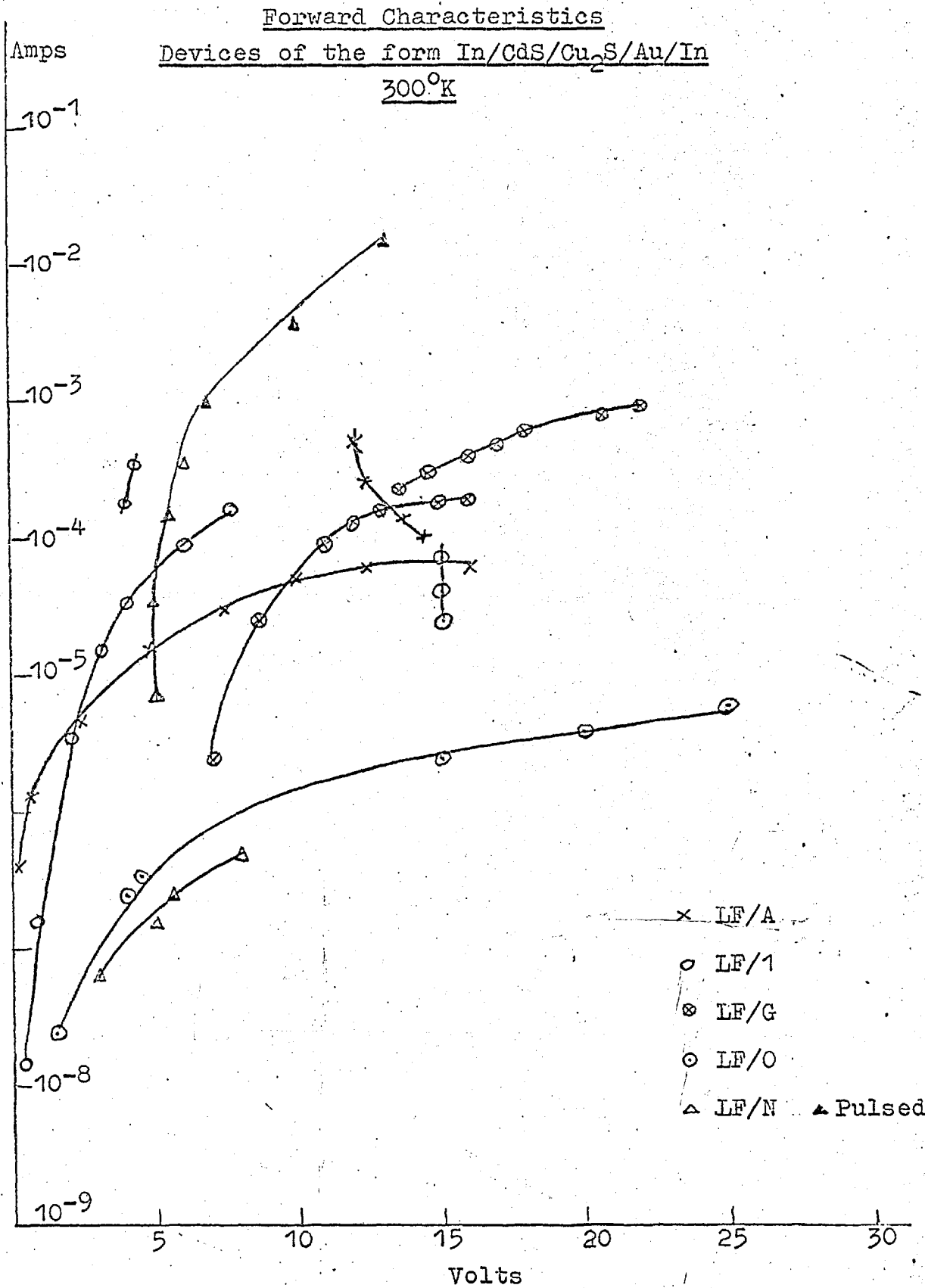
breakdown injection of carriers discussed by STEELE et
al (1962).

4.6.2. HIGH CURRENT DAMAGE

The devices were permanently altered to a low
resistance state by the passage of too high a current.
Observation of the device showed a dark region had formed
on the gold/cuprous sulphide contact at one point where
breakthrough had occurred. The probable mechanism of
this breakthrough was the diffusion of the indium contact.
At room temperature continuous currents of more than a
few milliamps were sufficient to cause the irreversible
change. The corresponding power input to the device was
of the order of .1 watt into a volume less than 10^{-3}cm^3
which should cause a significant temperature rise. The
input power increased rapidly with applied voltage due
to the rapid increase of current with voltage.

Indium is known to diffuse rapidly in cadmium
sulphide. Diffusion of the indium electrode would have
a twofold effect on the current. The theory of LAMPERT
(1962) for example, predicts the current to be inversely
proportional to the fifth power of the electrode spacing
at high currents for the model mentioned in section 4.4.
MOORE (1967) observed that the exponent in the power
law variation of current with voltage was a function of

Fig. 4.7

Double Negative Resistance
300°K

Device LF/T
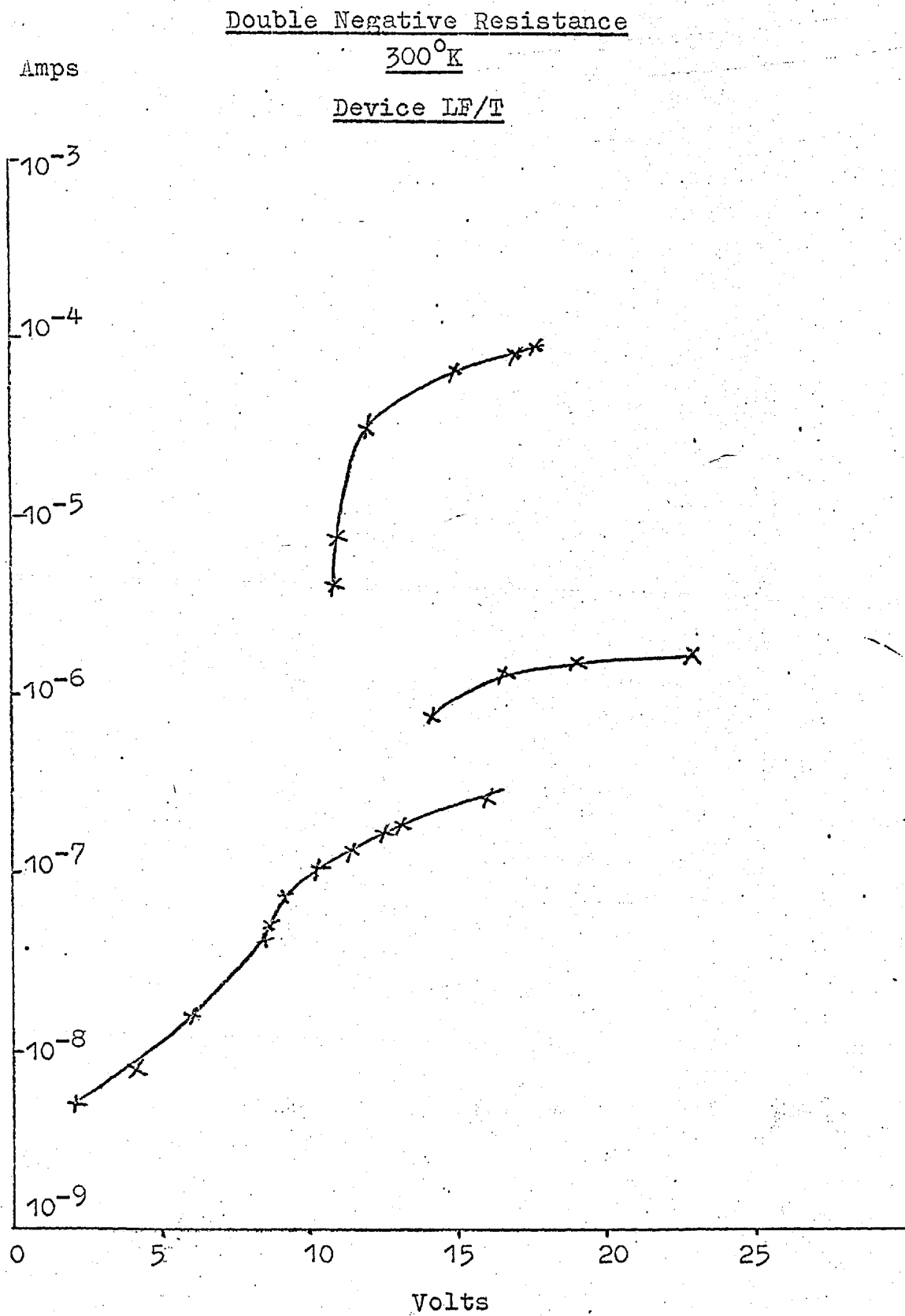
the length of the insulating region in silicon p-i-n devices. The exponent varied from 2 or 3 for thicknesses of more than 100 microns to greater than 10 for devices less than 20 microns thick. The above two effects were probably occurring in the present devices and would be acting as a positive feedback mechanism to cause very rapid thermal breakdown.

The fact that breakthrough appeared to occur at only one point indicated that the current may have been carried by a filamentary mechanism similar to that proposed by BARNETT (1966) which will be discussed in more detail in CHAPTER V. Some devices exhibited multiple negative resistance regions indicating the possible formation of more than one filament. Fig. 4.7 shows the forward characteristic of a device exhibiting two negative resistance regions.

4.6.3.   EFFECTS OF CARRIER TRAPPING

Carrier trapping was an important mechanism which affected the device characteristics. Hysteresis was always observed in the forward characteristic because of the change in the trap population due to carrier injection or the action of the applied field. The reversion to the original state of trap occupancy was time dependent and this was more easily observed by continuous tracing of the characteristic either with the

Tektronix curve tracer or the Bryans Autoplotter.

Using the Tetronix curve tracer the characteristic was completely retraced fifty times a second. Once the device had switched from the high resistance to the low resistance state after negative resistance on the first trace it generally stayed in the low resistance state. The short 20 msec. retrace time did not allow the cadmium sulphide to return to the initial trapping state which led to the negative resistance. Fig. 4.8. shows the trace of such a device (LF/1) at room temperature. After the low resistance state had been reached the hysteresis became more pronounced. The reverse characteristic is also shown demonstrating pronounced rectification.

Using the Bryans Autoplotter with a retrace time of several seconds using manual operation the negative resistance could be easily demonstrated. The curve replotted after a few minutes showed a significant change due to the effect of slow traps. Fig. 4.9 shows the result for a device LF/A left in the dark overnight and the curve plotted three times with a lapse of the order of a minute between successive traces.

A current decay observed at low currents below 10^{-6}A was probably due to injected carriers falling into traps associated both with the surface and the bulk of the cadmium sulphide (SMITH and ROSE 1955, ROSE 1955).
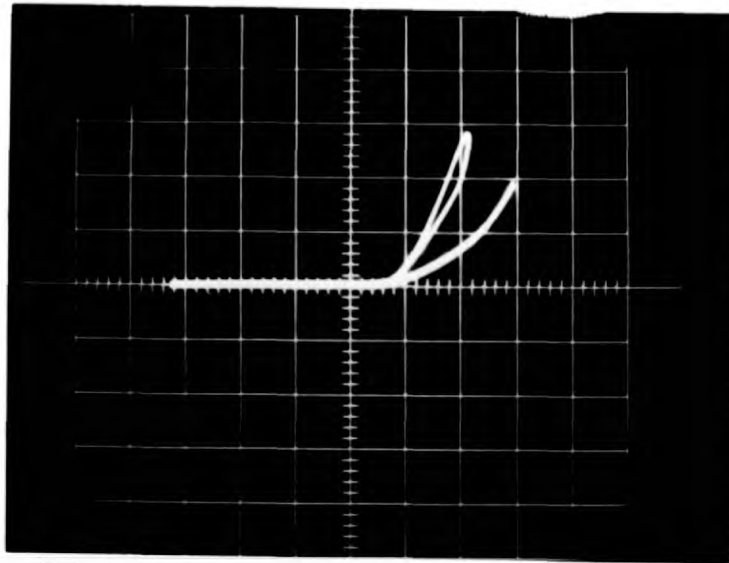
0.05mA/div.

5V/div.   2V/div.

Fig. 4.8

Room temperature characteristics device LF/1

Fig. 4.9

Repeated traces
Device LF/A 300°K

2×10^{-5}A/cm

2 V/cm
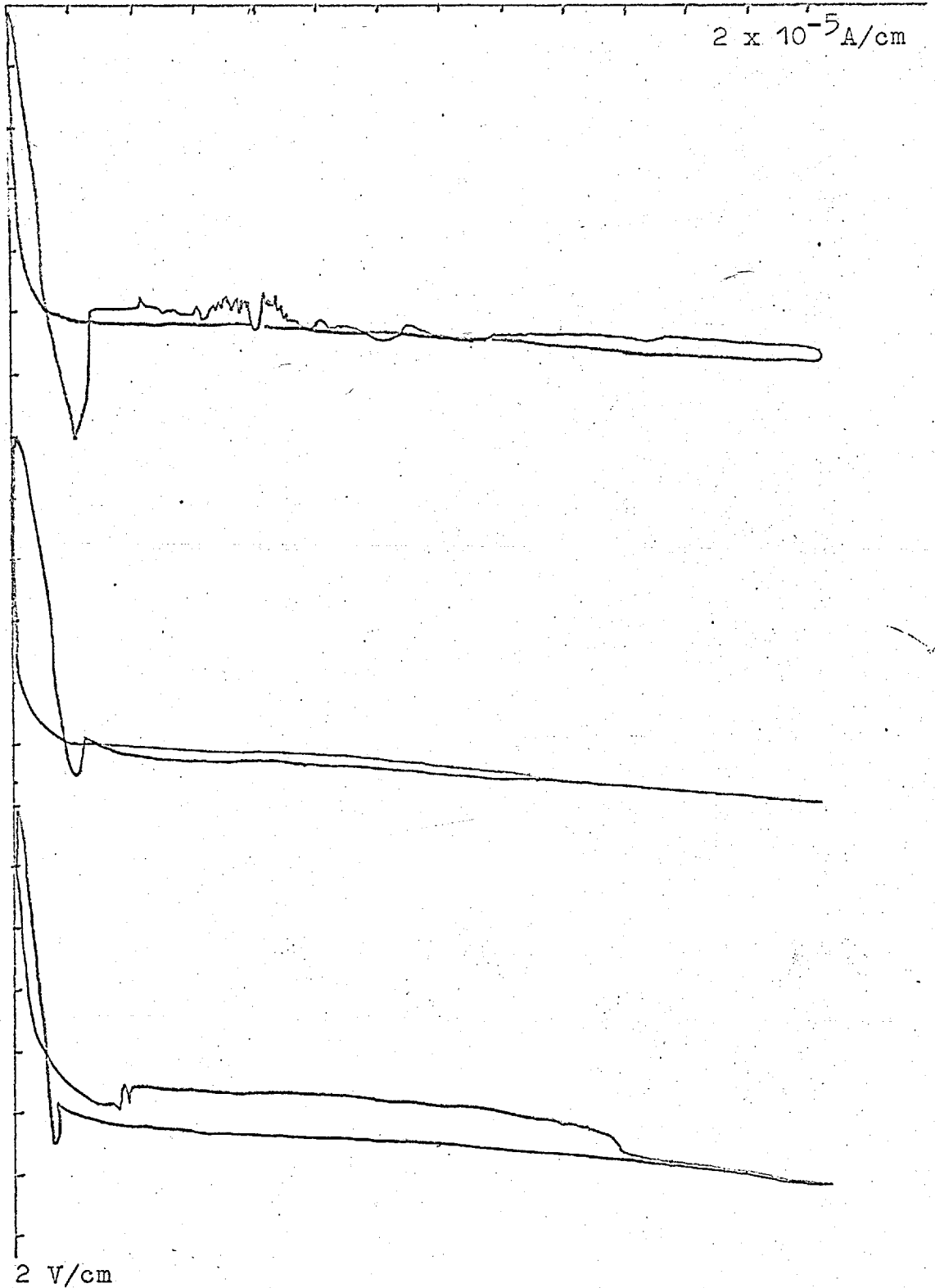
The low current points in the device characteristics
which have been presented represent the equilibrium values
of current.

4.6.4.   PULSE CHARACTERISTICS

Pulse measurements were performed using the circuit
of fig. 4.2. The current pulse always exhibited an
initial capacitive spike. The duration of the spike was
of the order of 1 microsecond and limited the minimum
width of the pulse that could be applied to the sample.
The maximum pulse width was limited by the pulse generator
overload mechanism depending on the amplitude and the
duty cycle of the pulse. The maximum input power to the
device was limited by the high current damage described
in section 4.6.2.

Fig. 4.10 shows the current pulse for device LF/o,
see fig. 4.6, at a current above the negative resistance
regime. After the initial capacitive spike the current
was an increasing function of pulse width. With a duty
cycle of 0.1 seconds the device eventually suffered
catastrophic breakdown when the pulse width was increased
to 50 microseconds. The series resistance in this partic-
ular case was only 1 K-ohm and was insufficient to control
the current.

Prior to the final breakdown a hysteresis was observed
in the relationship between the width and the height of

Fig. 4.10

Current pulse device LF/0
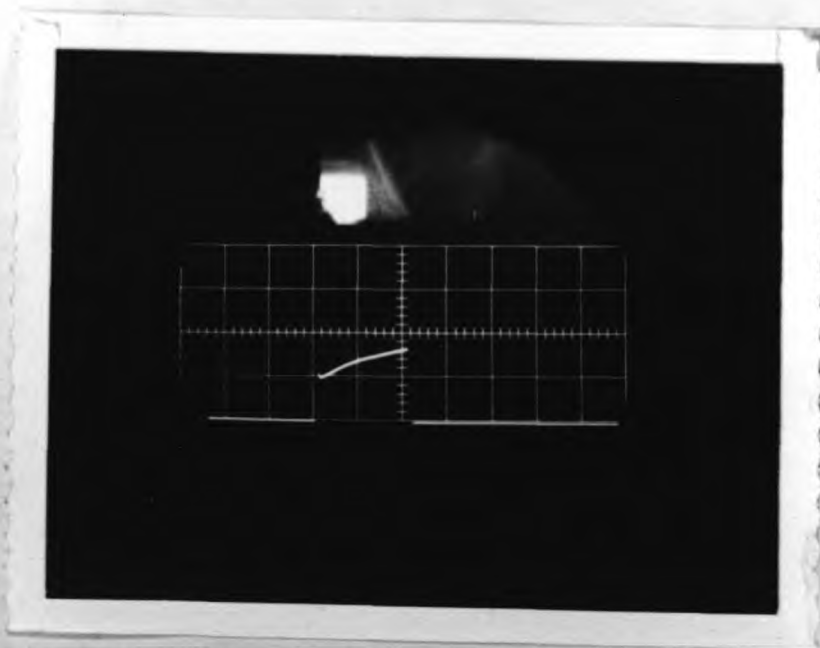
1mA/div.

10μsec/div.
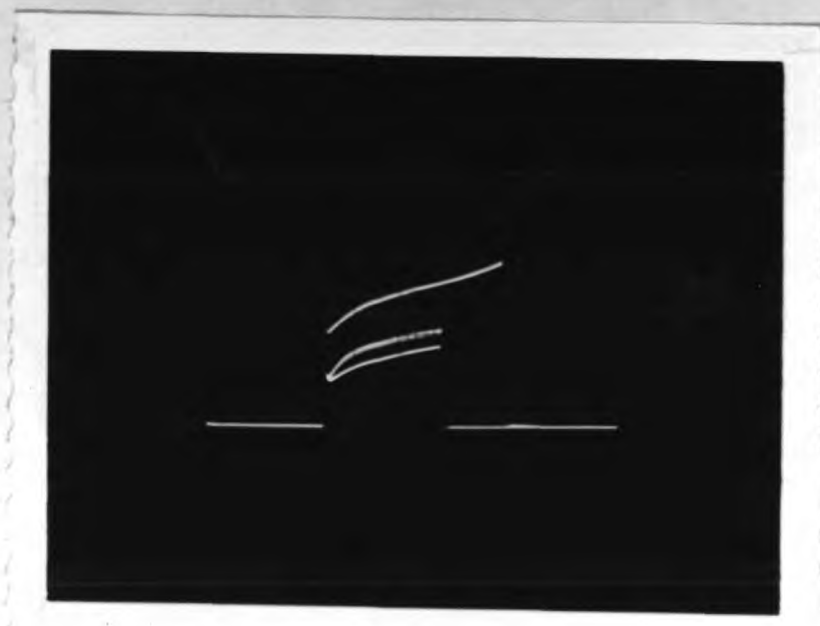
Fig. 4.11

Hysteresis with pulse width device LF/0

the current pulse, see fig. 4.11. The lowest trace was
for a pulse width of 20 microseconds, the highest trace
occurred after the pulse width was increased from 20 to
30 microseconds and the middle trace when the pulse width
was reduced from 30 to 20 microseconds. The applied
voltage pulse amplitude was kept constant throughout.

The hysteresis could have been due to changes in
the trap occupancy, however, at the high currents
(2 - 3 mA) which were passed it was possible that the
actual trap distribution in the crystal was altered.
KORSUNSKAYA et al (1968) have shown that the presence
of free electrons and holes in cadmium sulphide single
crystals can cause the formation of new local centres.
A further explanation is that the indium contact has
diffused due to local heating so decreasing the electrode
spacing and increasing the applied field strength (see
4.6.2).

Using a higher series resistance it was possible
to study the effect of the transition through the nega-
tive resistance region of the characteristic on the shape
of current pulse. The effect of increasing pulse ampli-
tude on device LF/A is shown in fig. 4.12. At low cur-
rents the current pulse had the shape expected for a
capacitive circuit element. At the switch-on point of
the pulse there was an initial sharp rise of current which

Fig. 4.12

Current pulse variation device LF/A

75μA/div.
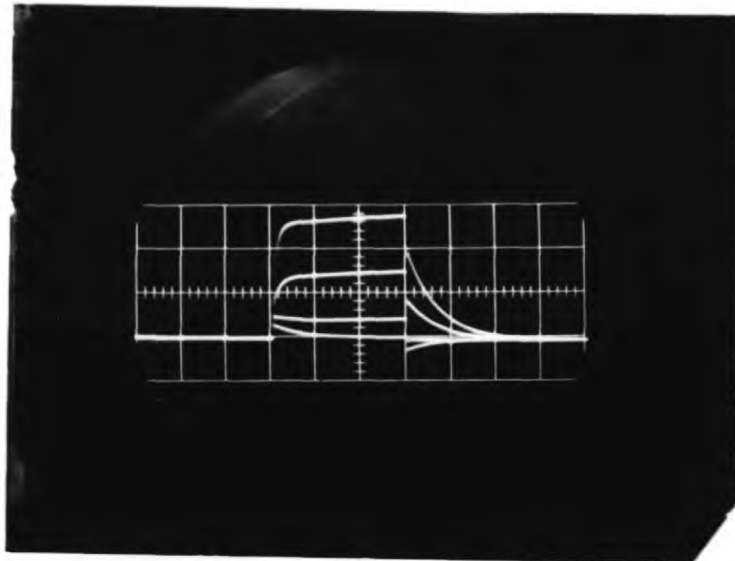
10μsec/div.

Fig. 4.13

Voltage pulse variation with applied voltage device LF/A
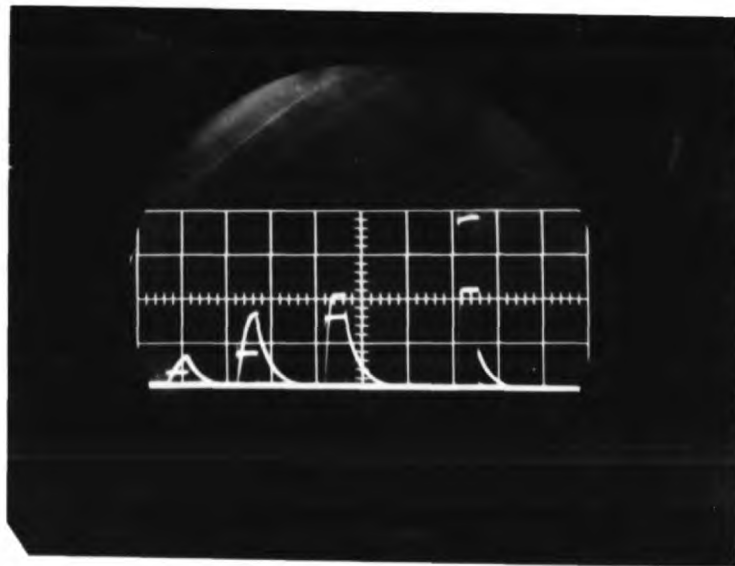
5V/div.

20V/div.

10μsec/div.

was followed by a gradual decay probably due to trap filling. At the switch-off point of the pulse there was a sharp decrease of current causing the current to go negative and slowly decay back to zero. As the applied pulse amplitude was increased the decay, following the initial sharp rise, became less pronounced until a square current pulse occurred near the negative resistance region. Further increase of the applied pulse amplitude now caused a gradual rise of current to occur after the sharp initial increase of current. When the pulse was switched off a sharp decrease in current occurred equal and opposite to the initial sharp rise. The current now decayed slowly from a positive value to zero.

The variation of voltage across the sample with the total applied voltage is shown in fig. 4.13. The pulse characteristic was probably a combination of the capacitive action of the device, including the action of traps, and the double injection of free carriers leading to a complicated variation of the impedance of the device with voltage. BINGGELI and KIESS (1967), for example, have shown that appreciable increases in capacitance can occur in thin cadmium sulphide crystals under d - c bias. One of the reasons for performing pulse measurements in the present case was to pass high

currents without destruction of the device. It was
noted that at relatively high currents (up to 1 mA)
the voltages required to produce a given current under
pulsed or continuous voltage conditions were nearly
equal indicating undue heating of the devices was not
occuring under the continuous voltage conditions.

4.6.5. MEASUREMENTS BELOW ROOM TEMPERATURE

No electroluminescence had been observed at room
temperature. Competition with non radiative ("killer")
centres is much more significant near room temperature
(MANDEL et al 1964). Electroluminescence is also known
to be thermally quenched, the efficiency generally
decreasing with temperature according to the relation
$A(1 + B \exp -\frac{W}{KT})^{-1}$. RUSHBY and WOODS (1966), for
example, observed electroluminescence in devices of the
form gold/cadmium sulphide/indium at $77^{\circ}K$. The emission
effectively decreased to zero at $130^{\circ}K$. Assuming the
above relationship they obtained a value for the activa-
tion energy W of 0.15eV. The crystals of RUSHBY and WOODS
were at least five times as thick as those used in the
present investigation.

Measurements were performed on the present devices
below room temperature in order to observe if electro-
luminescence had occurred and also to study the change
in the electrical characteristics.

No luminescence was observed when the present devices were operated at the temperature of liquid nitrogen. The geometry of the devices, however, did not easily allow observation due to their thinness and the opaque nature of the top electrode. The presence of "killer" centres was also probable since spectrographic examination of the crystals revealed the presence of several parts per million of the elements, likely to produce these centres, iron, nickel and cobalt. The electrical characteristics of the devices were significantly altered by reducing the temperature to $77^{\circ}K$. The room temperature and $77^{\circ}K$ forward characteristics for device LF/A, which was a typical device, are shown in fig. 4.14. The negative resistance which occurred at room temperature did not appear at $77^{\circ}K$ for the current range covered. Over most of the current range the effective resistance of the device was increased by reducing the temperature.

The disappearance of the negative resistance region and the effective increase of resistivity is shown for device LF/9 over a range of temperatures between $245^{\circ}K$ and $77^{\circ}K$ in fig. 4.15. In the temperature range 175° – $140^{\circ}K$ where the negative resistance disappeared there also appeared a reversal in the resistivity increase at currents below 10^{-4} Amps. Between 140° and $77^{\circ}K$ the resistivity increased once more.

132

Fig. 4.14

Forward Characteristics
Device LF/A
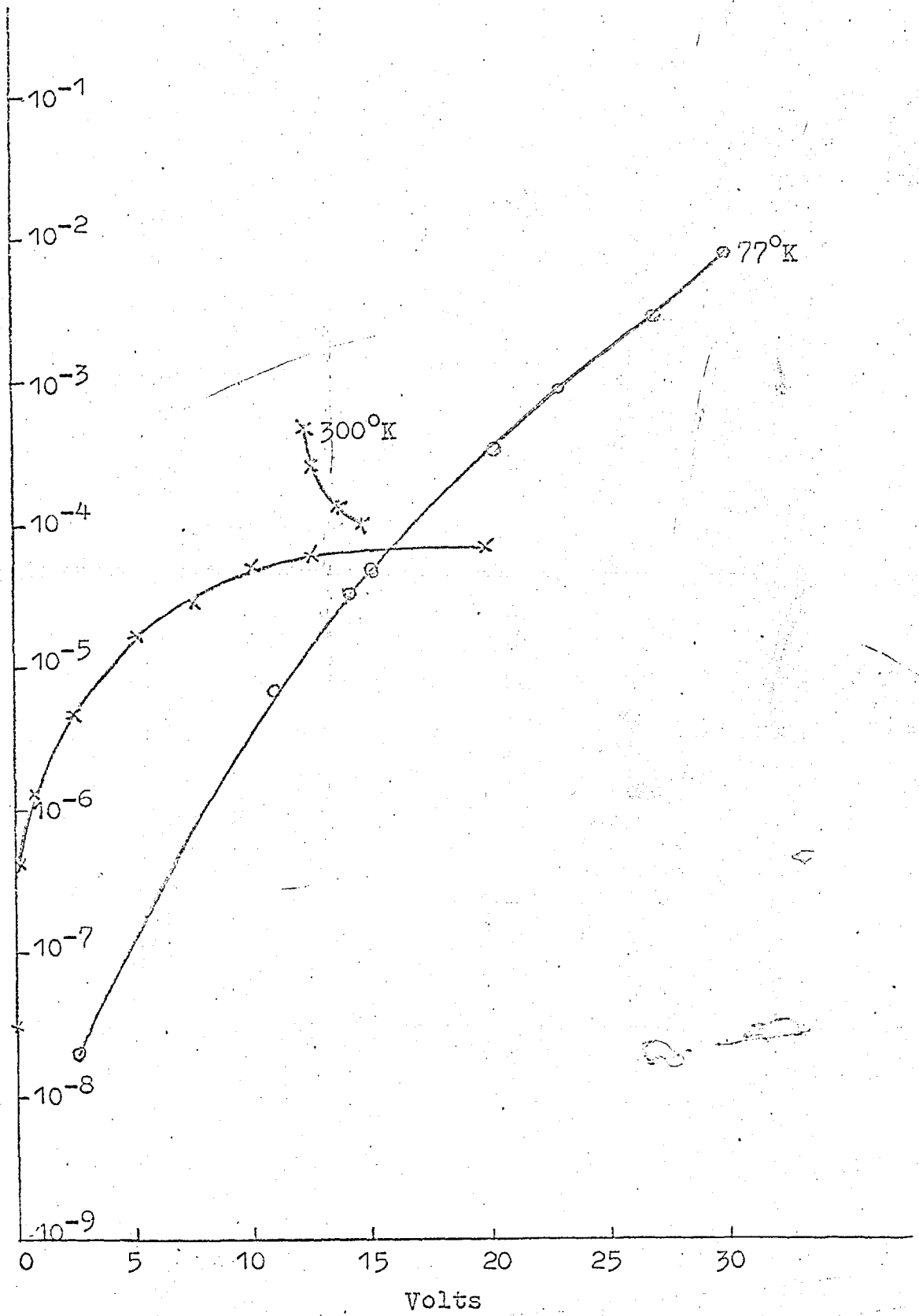
Fig. 4.15

Variation of Characteristic
with Temperature
Device LF/9
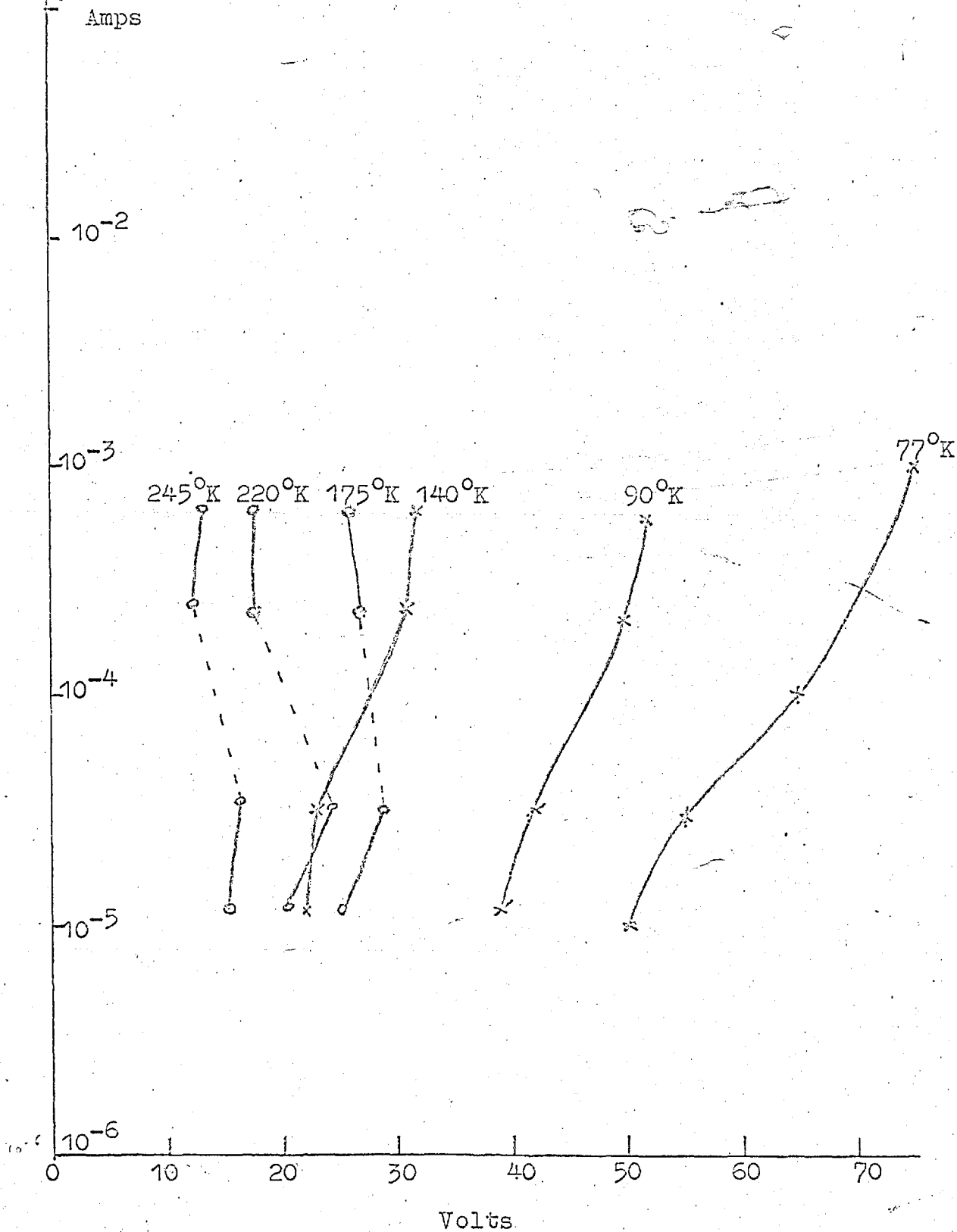
Negative resistance was however observed in several devices at 77°K when the current was increased to a few milliamps - and is shown for device LF/3 in fig. 4.16. RUSHBY and WOODS (1966) observed negative resistance in the above current range at 77°K and ascribed it to a double injection mechanism.

The devices all exhibited rectification which was more pronounced than at room temperature.

At high injection levels under pulsed conditions the room temperature and 77°K characteristics tended to approach one another.

4.6.6. OSCILLATIONS AT LOW TEMPERATURE

At temperatures near that of liquid nitrogen many of the devices exhibited oscillations in the voltage across the device in certain ranges of current. The electrical circuit only contained the device, a d - c supply and a series resistance. The oscillations occurred in the absence of illumination. Most of the oscillations occurred in a positive resistance region of the characteristic.

The positive resistance region oscillations were of two main types, ones which occurred at currents of the order of milliamps and those which occurred at currents between 1 and 100 microamps.
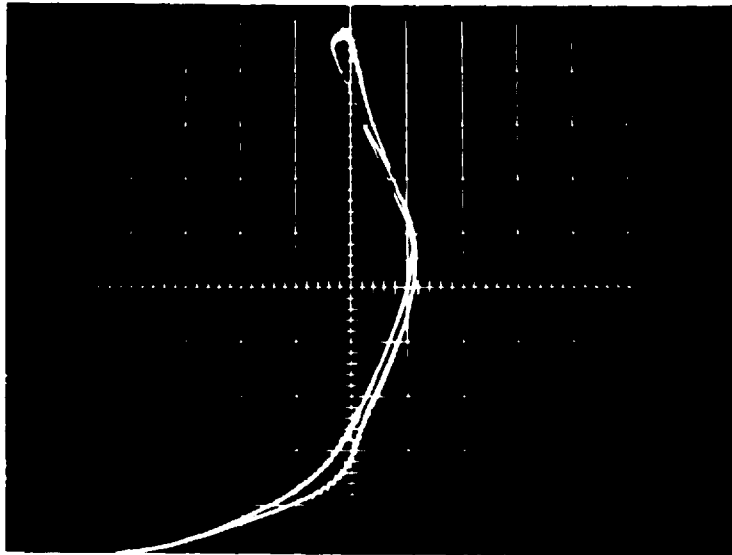
0.5mA/div.

20V/div.

Fig. 4.16

Forward characteristic device LF/3   77°K

The high current oscillations occurred near the limit of operation of the devices and it was often discovered that raising the current could significantly alter the frequency and amplitude. The cause of this change may be due to thermal diffusion of the contact into the crystal or a change in the imperfection distribution in the cadmium sulphide.

Close examination of fig. 4.16, the forward characteristic of device LF/3 at 77°K revealed the presence of oscillations at currents between 0.5 and 1.5 mA. An expanded portion of this section of the characteristic is shown in fig. 4.17. Changing the series resistance in the circuit had no effect on the oscillation frequency which indicated that it was a fundamental property of the device.

The oscillations only appeared within a limited current range. As the limits of the range were approached the oscillations became incoherent and finally disappeared altogether. As the current was increased from the lower limit the oscillations became complicated by the presence of harmonics, see fig. 4.18.

An analysis of the oscillations was performed using a Wayne Kerr wave analyser. It was found that the frequency of the fundamental increased with applied field see fig. 4.19. The analysis of the oscillation

Fig. 4.17

Oscillations in forward characteristic device LF/3
77°K
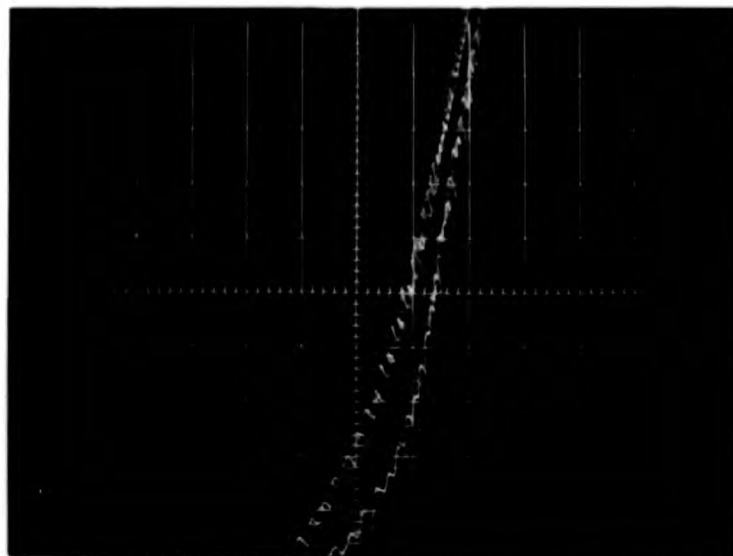
0.1mA/div.

10V/div.

Fig.4.18

Harmonics in oscillation device LF/3 77°K
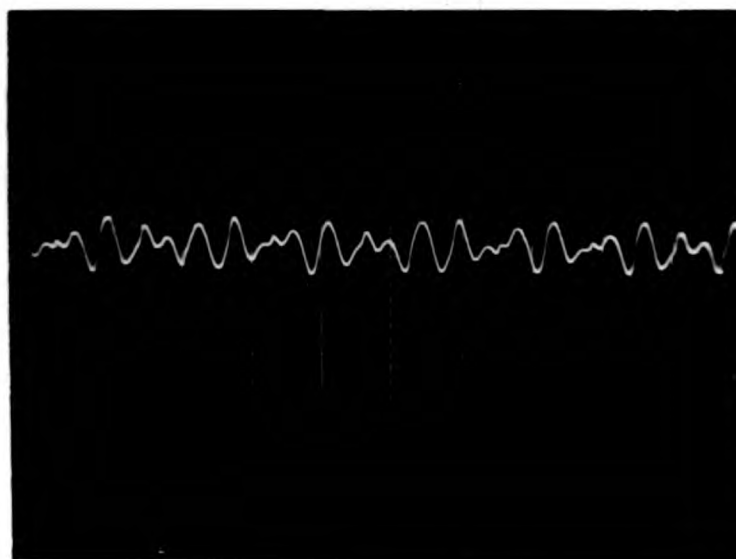
1V/div.

0.2msec/div.
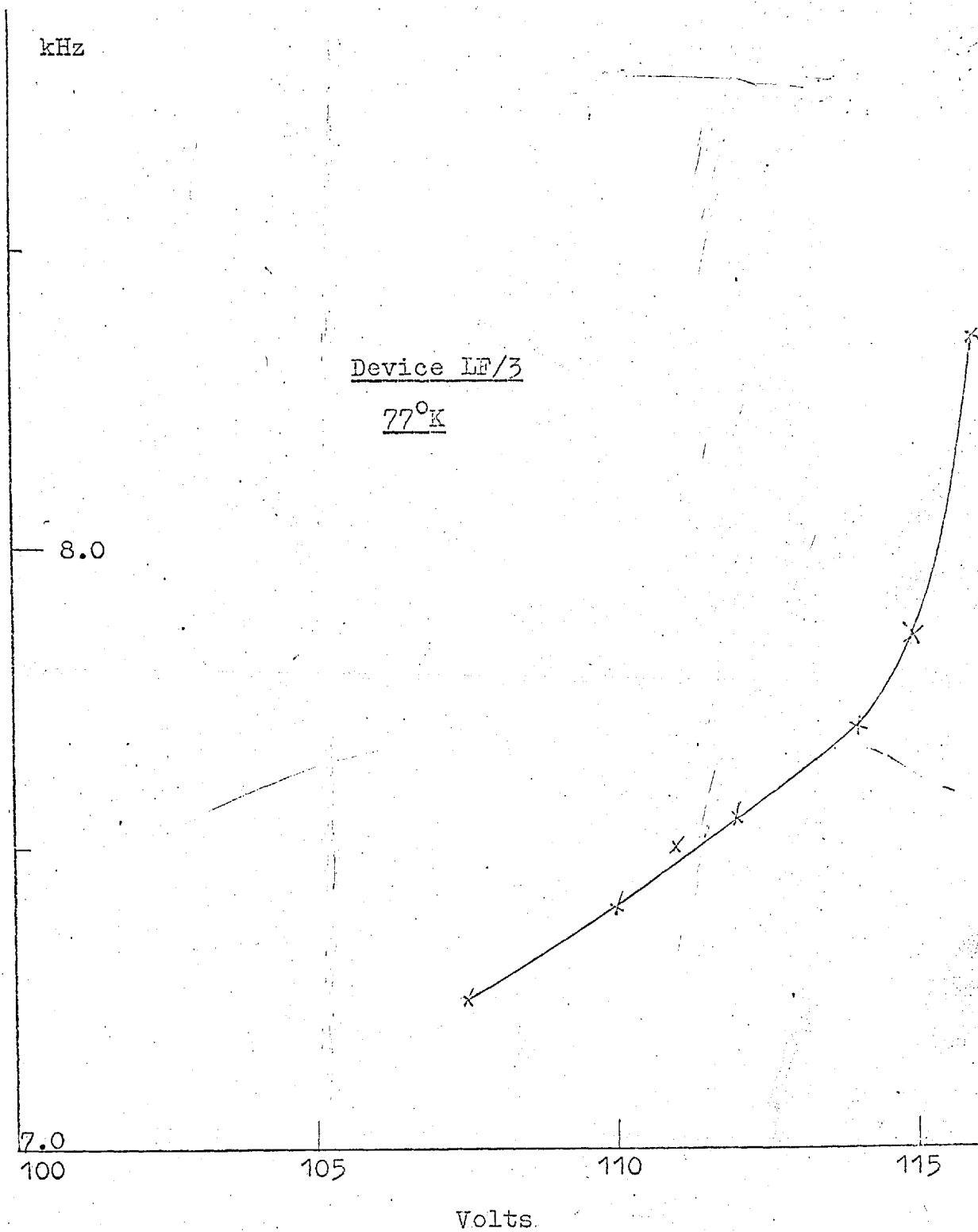
Fig. 4.19

Fundamental frequency of oscillation

versus applied voltage

Fig. 4.20

Analysis of Oscillation at 1mA

Device LF/3 77°K
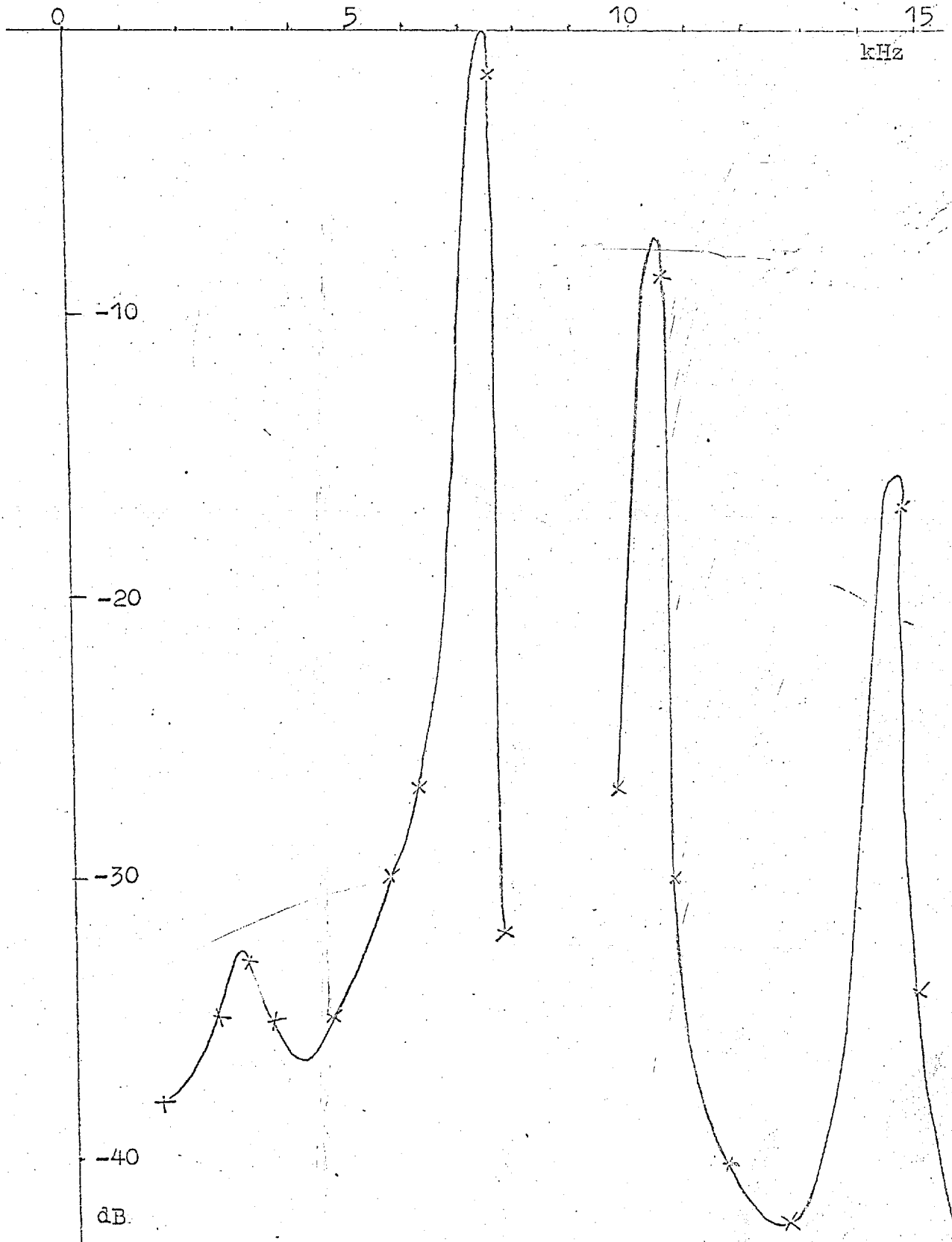
at a particular fixed current is shown in fig. 4.20.

The high current type oscillations were often not of a simple form. Fig. 4.21, for example, shows the oscillations observed in device LF/6 at 77°K at a current of 4mA. The oscillation showed an upward peak at the end.

Most of the high current oscillations observed were in the frequency range 1 - 10 kHz. However, oscillation frequencies up to 100 kHz were observed in devices through which very high currents had previously been passed.

The low current oscillations were more uniform and exhibited different characteristics in their relation- ship to the applied field. The low current oscillations did not occur in a region of negative resistance. The portion of the characteristic for device LF/12 in which this type of oscillation occurred is shown in fig. 4.22. A slight saturation in current occurred between 32 and 36 V. Oscillations occurred throughout the whole of the part of the characteristic shown. The oscillation period increased linearly with applied field, see fig. 4.23. The period of high current oscillations had shown a slight decrease with applied field (fig. 4.19). The amplitude of the oscillation also increased with applied field, see fig. 4.24. The oscillation amplitude was
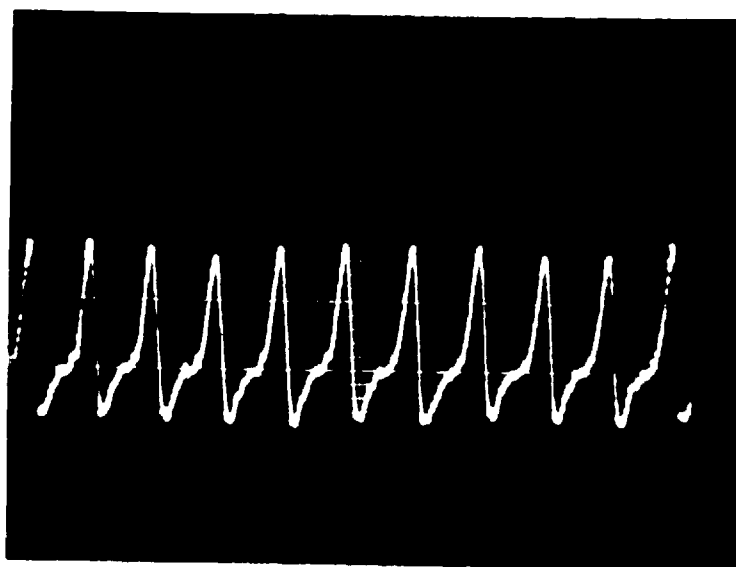
1V/div.

1msec/div.

Fig. 4.21

Oscillation in device IF/6   77°K
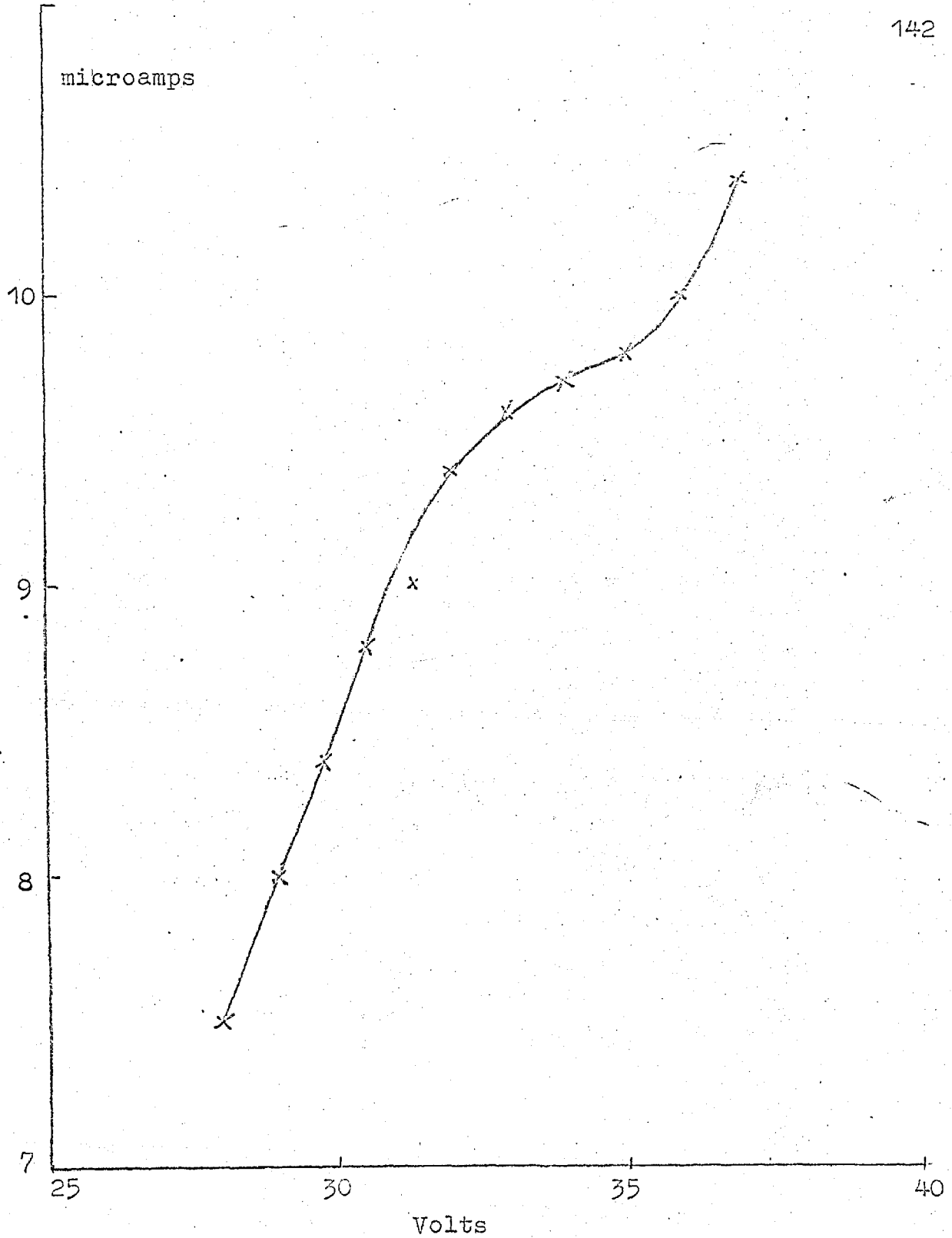
Fig. 4.22

Oscillation region

Device LF/12

77°K
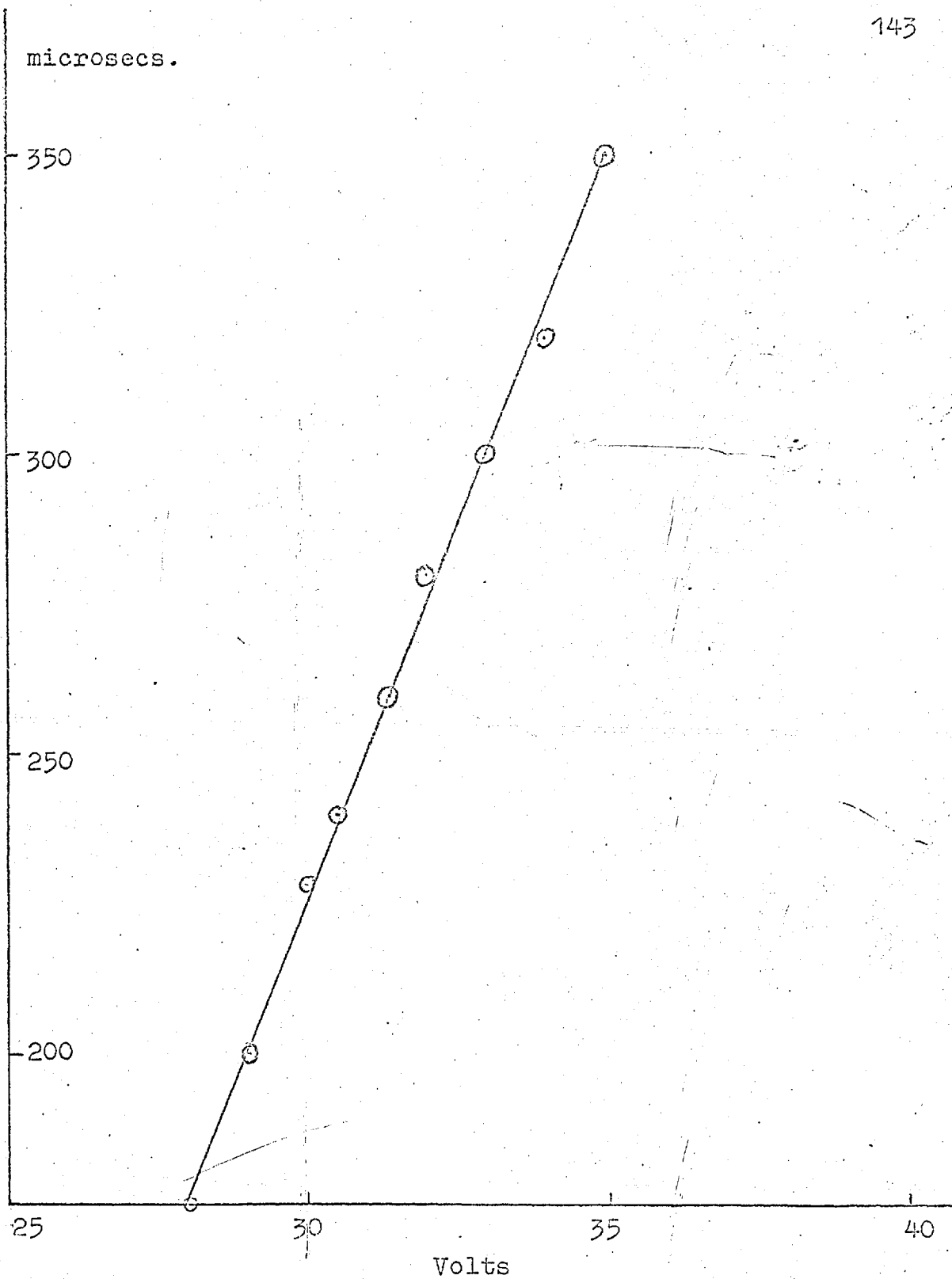
Fig. 4.23

Period of oscillation versus applied field

Device LF/12   77°K
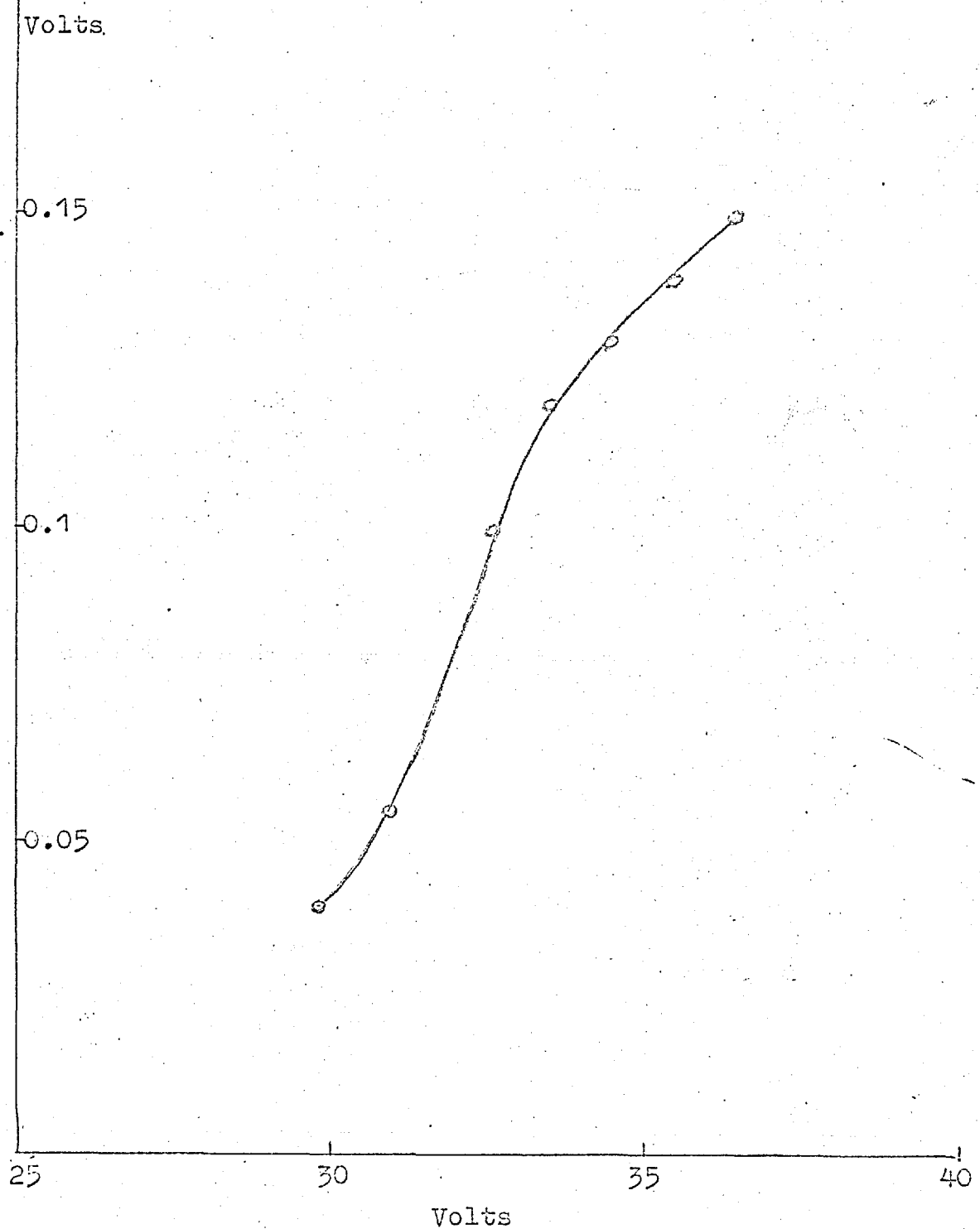
Fig. 4.24

Amplitude of oscillation versus applied voltage

Device LF/12   77°K

less than 1% of the total voltage across the device.

On close examination of the oscillation it appeared to be a combination of two exponential curves. Fig. 4.25 shows the oscillation at applied voltages of 30 and 33.7V.

On raising the temperature from 77°K the amplitude of the oscillation gradually decreased. No oscillations could be observed above 100°K. The oscillations were observed both when the sample was directly immersed in liquid nitrogen and when attached to the cold finger of the cryostat at a pressure of the order of 10^{-6} Torr.

Slight illumination of the device with white light reduced the amplitude of the oscillations. Strong illumination completely removed them.

Several mechanisms involving two carrier currents are known to lead to oscillations in compensated semi-conductors. Some of these mechanisms are discussed in section 1.6. The applicability of these theories to the oscillations observed in the present devices is discussed in CHAPTER V.

Oscillations were also observed at 77°K following a negative resistance region in the characteristic and were of a large amplitude and sinusoidal. Device LF/8 exhibited particularly spectacular oscillations under reverse bias conditions following a negative resistance

breakdown. Fig. 4.26 shows these oscillations as they
appear as part of the characteristic and 4.27 as they
appear as a function of time. The amplitude was an
increasing function of the applied field and was about
70V when the applied voltage was 95V. The frequency
was around 27kHz. The same device also exhibited the
positive resistance low current type of oscillation
in the forward direction.

Although coherent oscillations were not observed
at room temperature, monitoring of the voltage across
the device revealed a significant increase of the noise
in the device when the sharply rising or negative resist-
ance portion of the characteristic was reached. Observ-
ation on the oscilloscope or autoplotter revealed com-
ponents varying from a few Hz to several hundred kHz.

Cooling the device whilst a constant current was
being passed had the effect of reducing the noise to a
low level at 77°K and often resulted in the appearance
of the oscillations previously discussed.

The observed noise at room temperature associated
with the negative resistance breakdown may have been due
to the action of current filaments which had formed and
only existed for a short period similar to microplasma
breakdown.

Fig. 4.26

Oscillations under reverse bias device LF/8 77°K
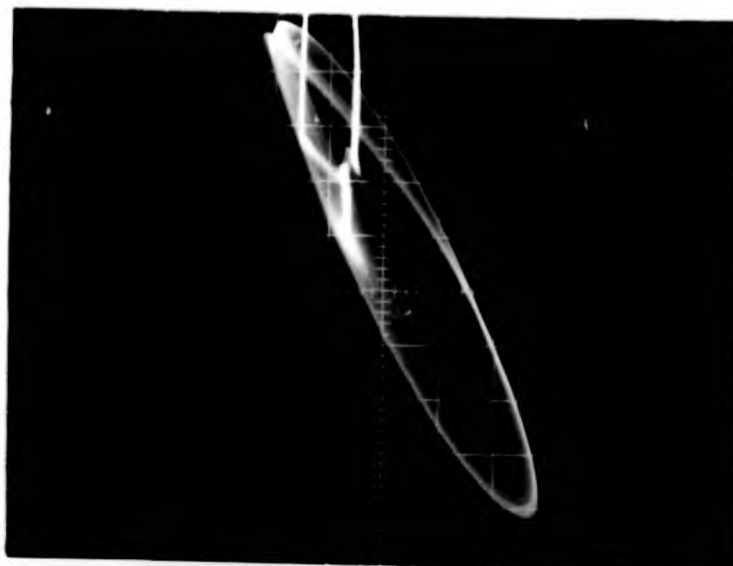
0.2mA/div.

10V/div.

Fig. 4.27

Large amplitude oscillations device LF/8 77°K
Reverse current 2mA
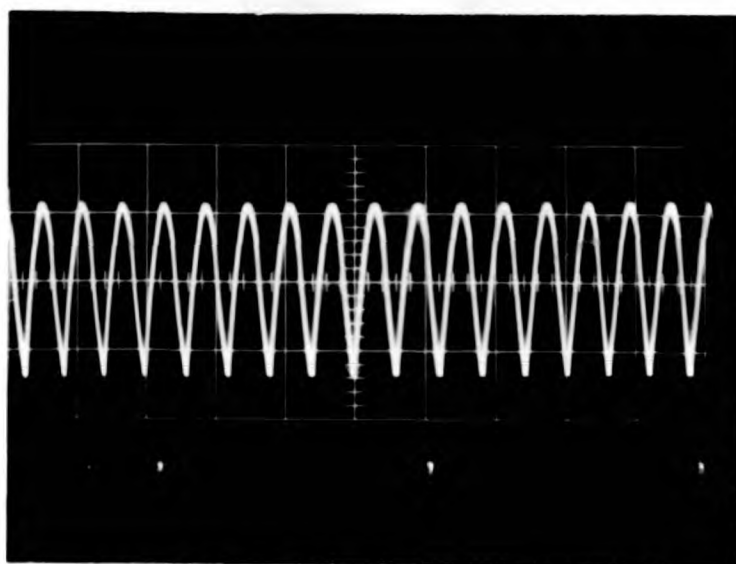
20V/div.

50μsec/div.

4.6.7. HARDENING AND SWITCHING EFFECTS

It is possible to increase the breakdown strength of diodes by applying a high value of reverse bias, a process known as hardening. BARBER (1965), for example, has observed the effect in diodes fabricated from indium antimonide. In the present devices this phenomena was used to reverse a switching effect in both the forward and reverse directions.

When high currents were passed through the devices near their limit of operation the device switched from a power law characteristic, which may contain a negative resistance, to an ohmic characteristic. When reverse bias was applied the ohmic characteristic still persisted. On increasing the reverse bias, however, the characteristic became non-ohmic. At first the resistance decreased but on further increase of the reverse bias the resistance of the device started to increase again to give a high value of reverse breakdown voltage. When the forward bias was reapplied the original power law characteristic was obtained. The series of operations was reproducible.

At room temperature the power law gradually decayed to the ohmic characteristic at voltages just below the threshhold for switching, probably due to heating.

A device which was in the ohmic state at room temp-
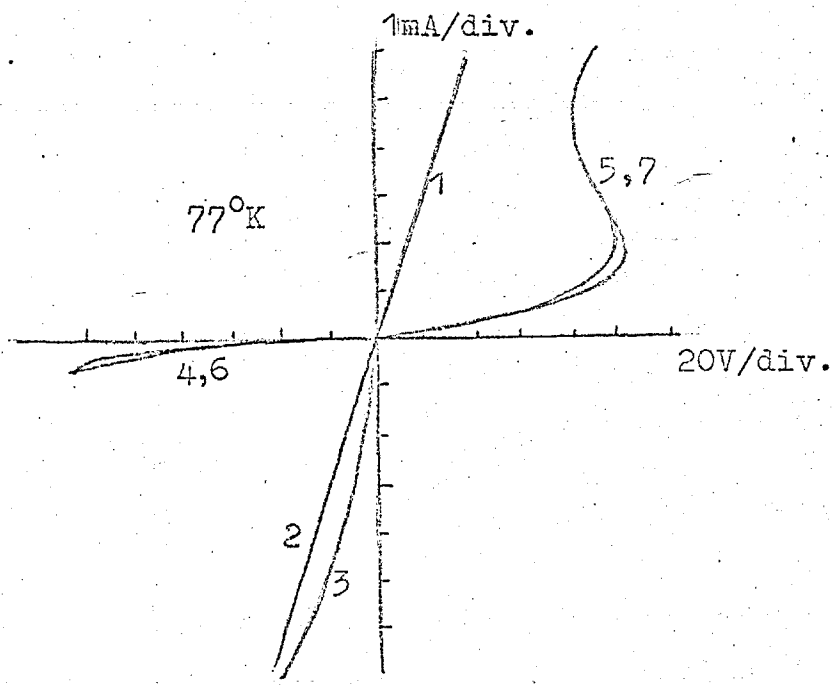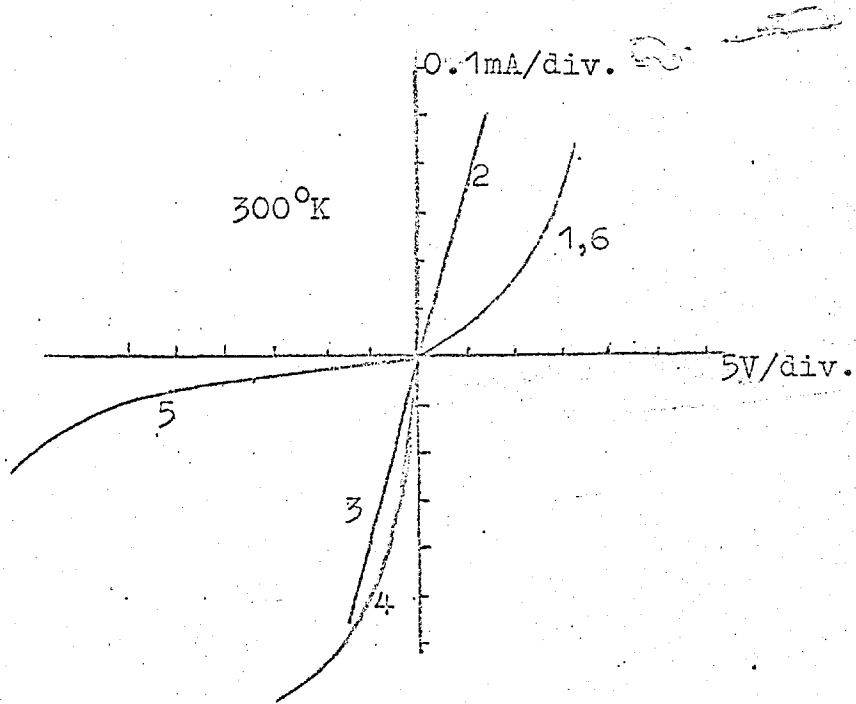
Fig. 4.28

Hardening and switching observed in device LF/3

erature would remain in that state when cooled to 77°K. On repeating the above series of operations a final non-ohmic state was obtained. At liquid nitrogen temperature the final state was stable with time. The series of events for a device both at room temperature and at 77°K is shown in fig. 4.28.

A possible explanation for the observed effect at high forward currents is that local heating could have caused enhanced diffusion of indium into the cadmium sulphide doping it n-type. The application of the reverse bias, however, could not have caused the indium to be removed by the action of solid state electrolysis since the applied field was now in the wrong direction. Indium becomes a cation in cadmium sulphide and would normally be attracted to the negative terminal.

The phenomenon could have been due to a surface effect whereby a low resistance surface path was made high resistance by the field dependant diffusion of copper observed by SIMHONY et al (1967).

4.6.8.   THERMALLY STIMULATED CURRENT.

Thermally stimulated current is a method of observing trapping levels in the forbidden gap. When a semiconductor is cooled and free carriers generated, usually by optical stimulation, the majority of carriers will be trapped. If the stimulation is removed and the semi-
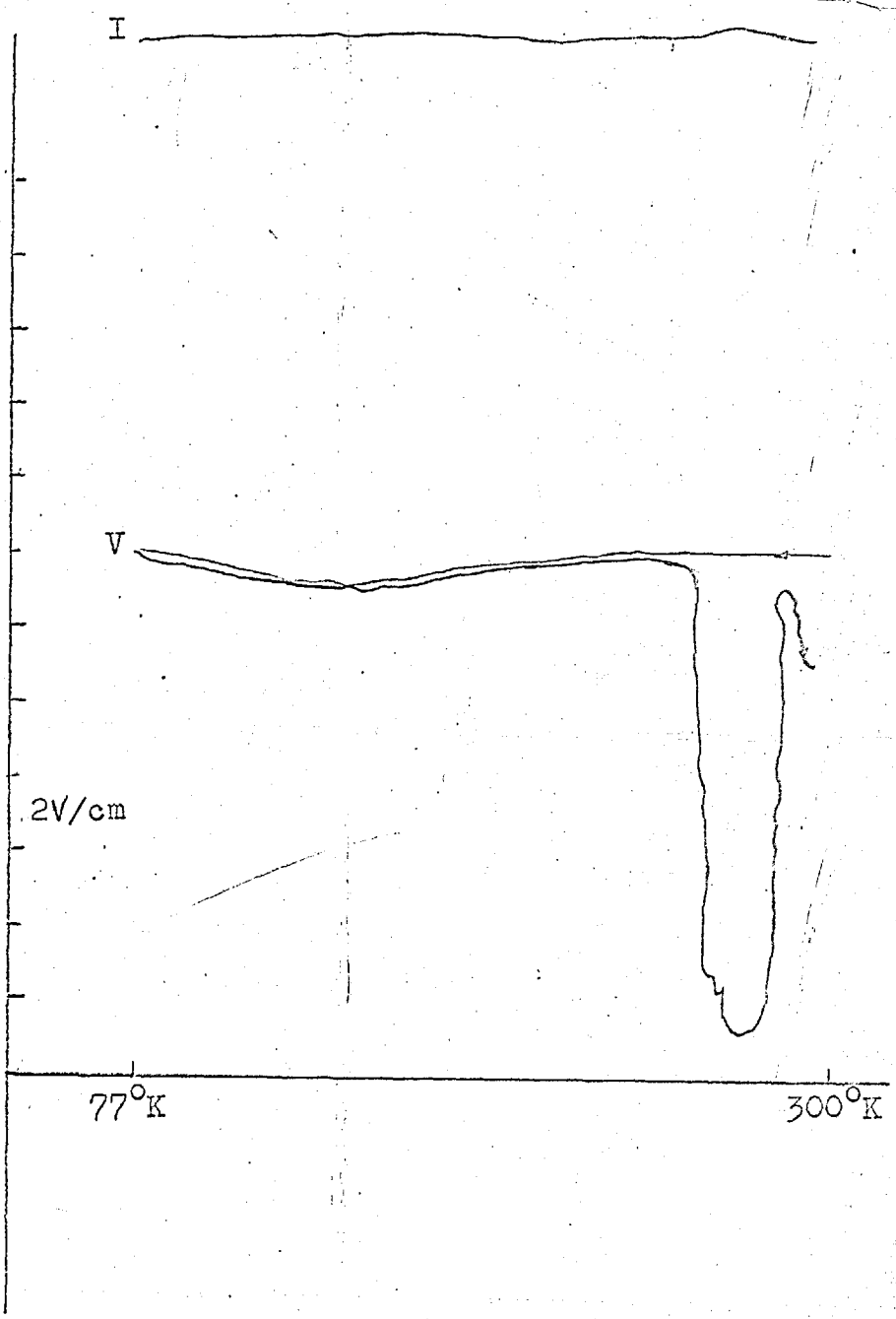
Fig. 4.29

Resistivity decrease due to thermal
emptying of a traping level

conductor is warmed quickly the traps will empty into
the appropriate conduction band. The phenomenon may be
observed by a temporarily enhanced conductivity. With
the present devices the phenomen was observed by cooling
the device whilst under the influence of a forward bias
which provided injected carriers. On warming the pre-
sence of a trapping level was indicated by a large
decrease in resistance which occurred around $270^{\circ}K$ and
is shown for one device in fig. 4.29 as it was observed
on the Bryans Autoplotter.

No quantitative measurements of trap depths and
related parameters were attempted as it was necessary
to be able to heat the device at constant rate to enable
the interpretation of the results to performed (WRIGHT
and ALLEN 1965). The cryostat used had a large thermal
inertia and did not lend itself to simple temperature
control.

4.6.9. THIN DEVICES

Thin devices, that is, devices less than 10 microns
in thickness did not in general exhibit a negative resist-
ance in the forward characteristic at room temperature.
The room temperature characteristic of such a device,
LF/2, which was below 5 microns thick is shown in fig.4.30.
KEATING (1963) also did not observe a negative resistance
in his thinner devices. SHOHNO (1965) observed a similar
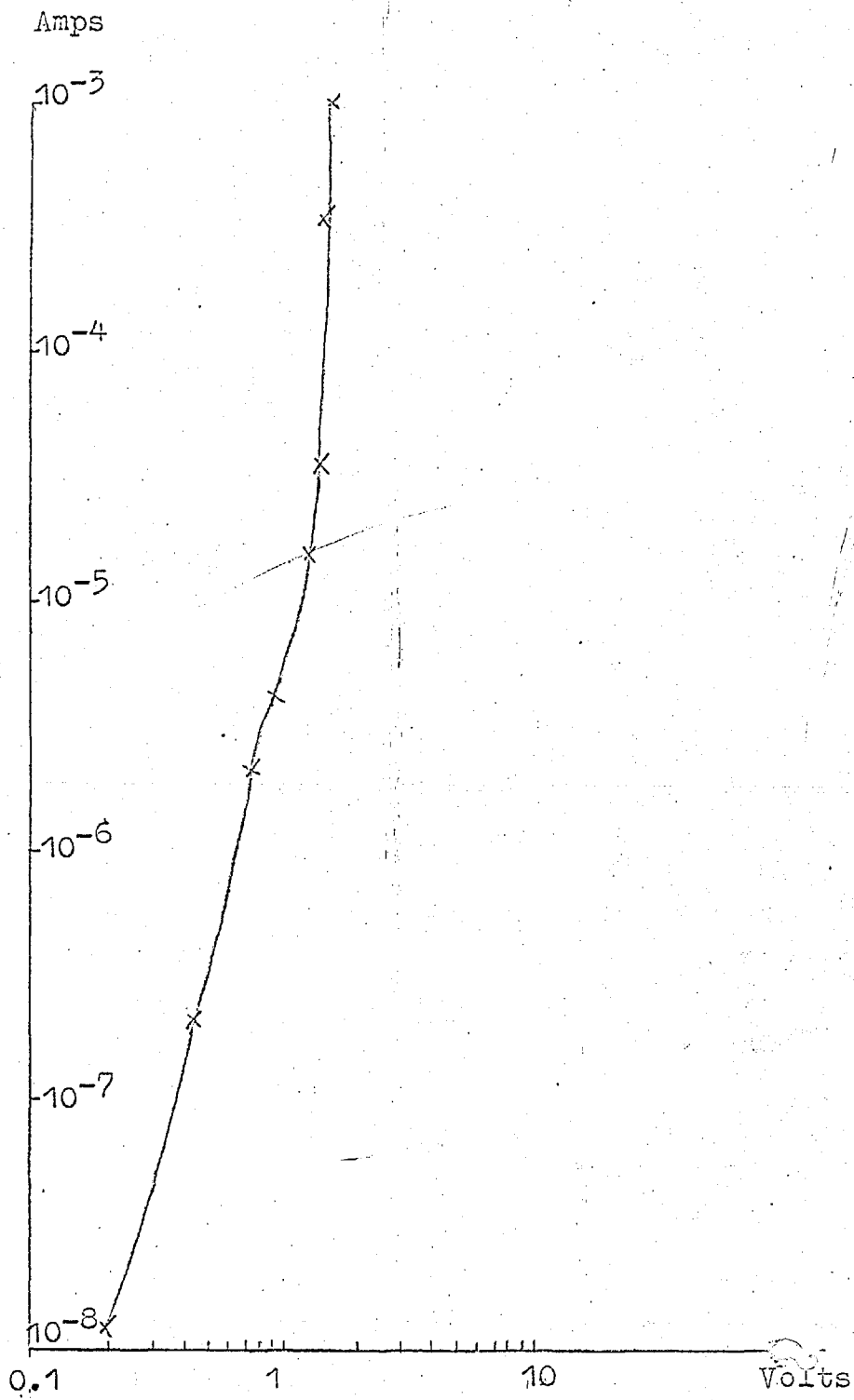
Fig. 4.30

Forward Characteristic
Thin Device
LF72 300°K

result with silicon p-i-n devices.

The diffusion length of holes in cadmium sulphide
is of the order of 1 - 5 microns (SPEAR and MORT 1962,
AUTH 1961). If holes were injected they could traverse
the crystal immediately and hence remove the criterion,
for negative resistance, of changing hole lifetime
discussed in section 1.4.

Only thin contacts could be evaporated on thin
crystals to prevent buckling due to the stress in the
film. The thin contact permitted illumination of the
crystal directly beneath the contact. A photovoltage
was observed in these crystals. Device LF/2, for example,
exhibited a photovoltage of 0.25V when illuminated with
light from a medium power mercury vapour lamp. The
photovoltage indicated the presence of a p - n junction
or hetero-junction.

Simultaneous illumination and forward bias of the
crystals resulted in a current composed of a photocurrent
and an injection current. Fig. 4.31 shows the dark
current compared to current under illumination by the
mercury vapour lamp for device LF/11 at 300°K. At
currents above 10^{-4}A the injection current predominated.
BRAÜNLICH (1967) has since observed the same effect in
similar devices illuminated in a similar manner, that is,
with light which did not interact directly with the

Fig. 4.31
The effect of air
and illumination
on device LF/11
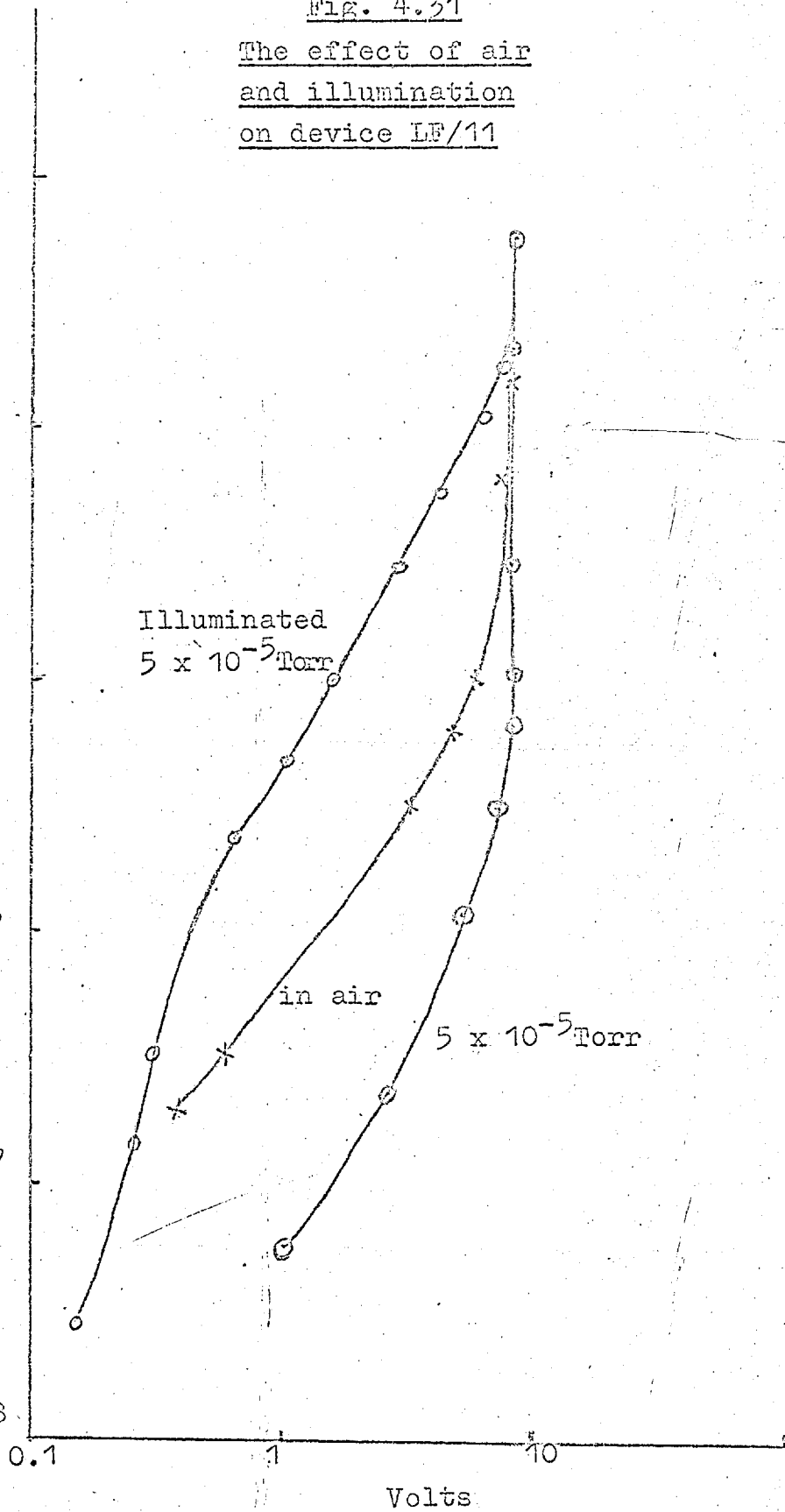
injected carriers. Using infra-red light he also observed an interaction which reduced the conductivity by exciting electrons to the copper centres probably produced by diffusion from the cuprous sulphide contact.

At low currents the devices in common with the thicker devices exhibited a lower resistance characteristic in air than under a vacuum. The effect of the ambient on device LF/11 is also shown in fig. 4.31. At high currents (greater than 5×10^{-5}A in this case) the characteristic in air was identical to that in the vacuum. The above result indicated the low current characteristic was affected by surface states which could be altered by the adsorption of gas molecules.

4.6.10 CUPROUS SULPHIDE LAYER FROM CUPRIC SULPHATE SOLUTION

Devices prepared with a cuprous sulphide layer deposited by floating a crystal on the surface of a solution of cupric sulphate (cupric ions) exhibited similar properties to those prepared with an evaporated layer. A negative resistance was observed in the forward direction at room temperature and low current oscillations at 77°K with a frequency of the order of 10kHz.

The fact that similar results were obtained with chemically deposited and evaporated layers of cuprous sulphide indicated the layer of cuprous sulphide in contact with the cadmium sulphide may have assumed the same

modification independent of the method of application.

The use of chemical deposition was discontinued
due to the difficulty of masking the area on which the
contact was to be applied and of preventing the cupric
sulphate solution wetting both large area faces of the
crystal.

4.7. OTHER DEVICES

4.7.1. DEVICES OF THE FORM In/CdS/SiO/Cu$_2$S/Au/In

The devices of the form In/CdS/SiO/Cu$_2$S/Au/In were
prepared as described in section 3.3. The samples did
not exhibit the current decay observed at low currents
in devices which did not have the silicon monoxide layer.
The decay was probably associated with surface states at
the junction. The introduction of the silicon monoxide
layer had probably caused bending of the energy band
edges at the surface causing carrier repulsion (FISCHER
1964).

The devices with the silicon monoxide layer exhibited
a negative resistance in their forward characteristic at
room temperature but not at 77°K. The forward character-
istic for such a device LF/S/1 at both these temperatures
is shown in fig. 4.32.

The devices exhibited rectification and this is
shown, together with the switching corresponding to the
negative resistance for device LF/S/1, as it was observed
on the curve tracer, in fig.4.33. Hysterisis occurred

159

Fig. 4.32

Forward Characteristics
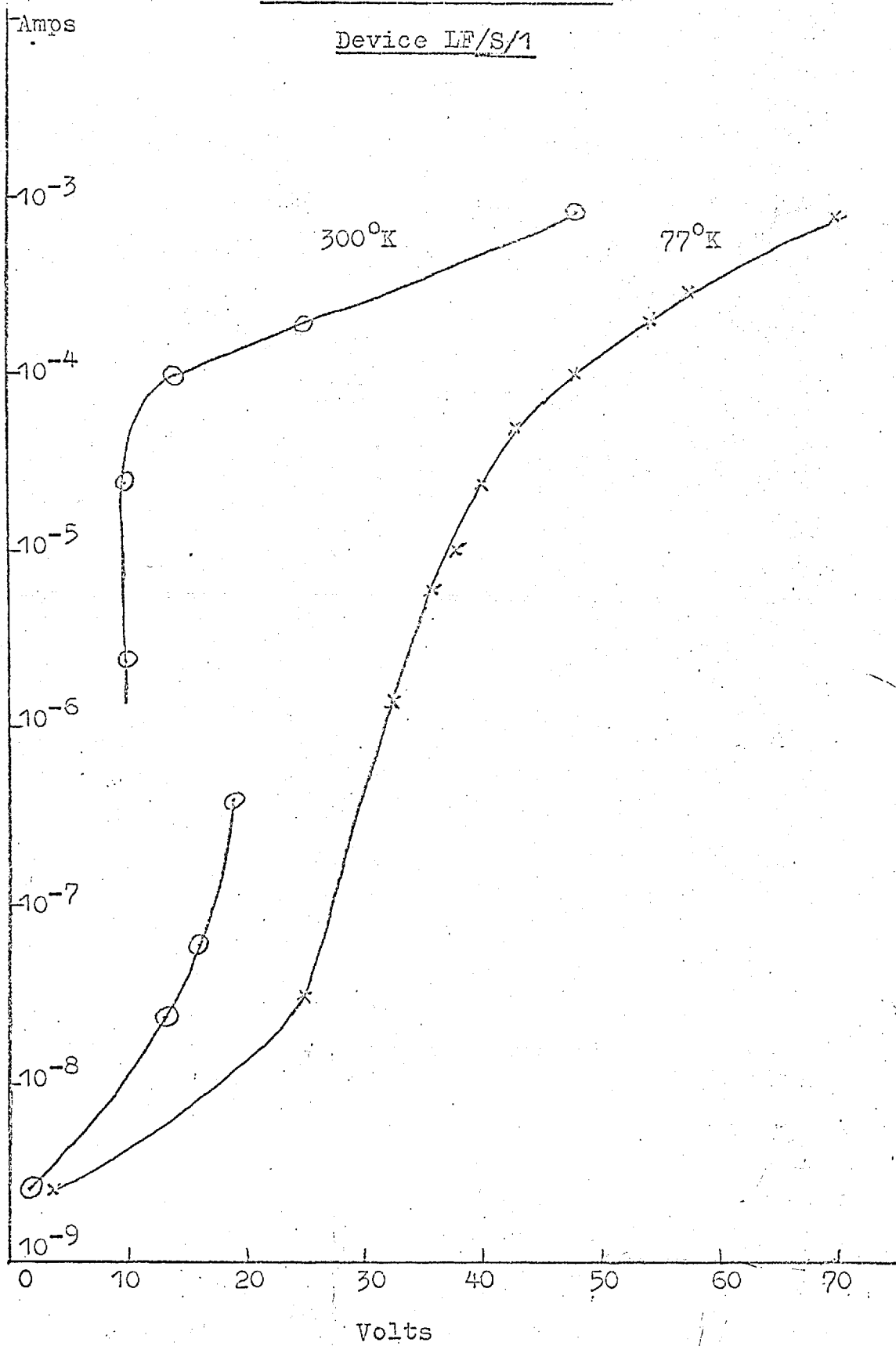
Device LF/S/1

Fig. 4.33

Switching in the forward characteristic device LF/S/1
300°K
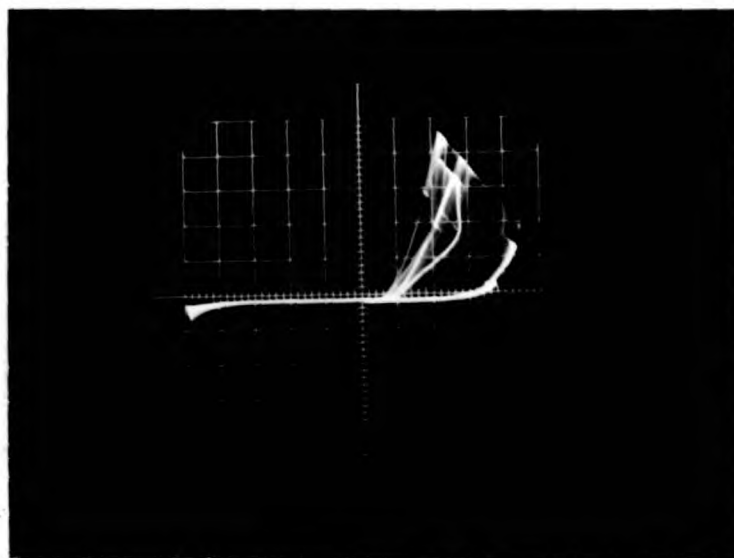
0.05mA/div.

−20V/div.   +5V/div.

Fig. 4.34
Switching oscillations in device LF/S/1   300°K

2V/div.

5msec/div.

after the negative resistance region.

In the region of negative resistance the devices
exhibited oscillations at room temperature. The oscilla-
tions which occurred in the voltage across device LF/S/1
are shown in fig.4.34. The amplitude of the oscillation
was about 5V and the frequency about 8Hz for this device.
The oscillation corresponded to the switching between
the two regions of fig. 4.33. A possible explanation
is that before the negative resistance breakdown most of
the applied voltage was across the cadmium sulphide.
After the breakdown a large current flowed which charged
up the silicon monoxide layer, which in turn reduced
the current flow through the cadmium sulphide and switched
it back to the high resistance state.

The oscillation threshhold could be initiated by
either reducing the current from a high value or raising
it from a low value.

The oscillations associated with the devices where
the cuprous sulphide was directly in contact with cadmium
sulphide were not observed when the silicon monoxide
layer was inserted.

4.7.2. DEVICES WITH A CUPROUS HALIDE CONTACT.

Only devices utilizing a cuprous iodide contact
were fabricated (see 3.3). The room temperature forward
and reverse characteristics of a device LF/H/1 of the

162

Fig. 4.35

Forward and reverse characteristics

Device LF/H/1

300°K
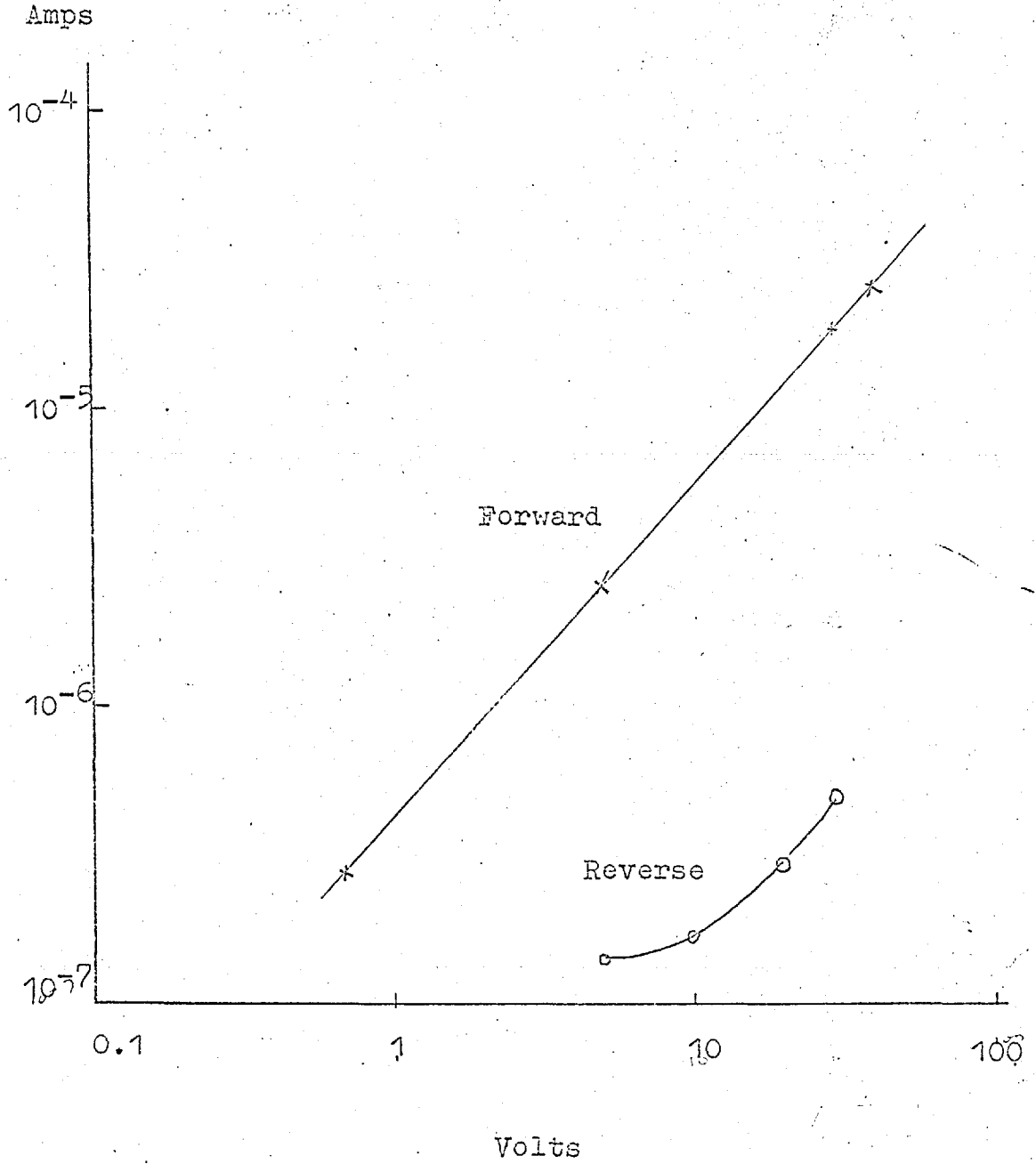
form In/Au/CuI/CdS/In are plotted in fig. 4.35. The forward characteristic followed an ohmic law whereas the reverse characteristic followed an exponential law.

In the forward direction most of the applied field was appearing across the series resistance provided by the cuprous iodide/cadmium sulphide junction and the effects of any injection were completely masked. The reverse characteristic may have been the result of tunnel injection.

4.7.3. DEVICES OF THE FORM In/CdS/Au/In

The devices having a gold/cadmium sulphide contact exhibited similar characteristics to those with a cuprous sulphide/cadmium sulphide contact. The characteristics of a gold/cadmium sulphide device LF/5G as observed on the curve tracer is shown in fig. 4.36. At room temperature rectification was observed together with a negative resistance in the forward direction. The negative resistance was exhibited on the curve tracer as a switch between two characteristics. No negative resistance was observed at 77°K even up to currents of several milliamps contrary to the result of RUSHBY and WOODS (1966) on thicker devices.

No luminescence was observed either at room temperature or at 77°K in the current ranges examined.

Fig. 4.36

Characteristic device LF/5G   300°K
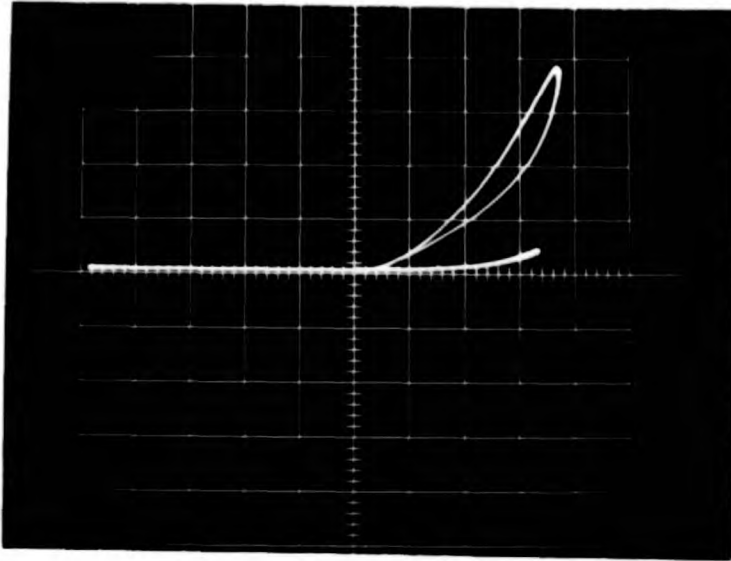
0.1mA/div.

5V/div.

Characteristic device LF/5G   77°K
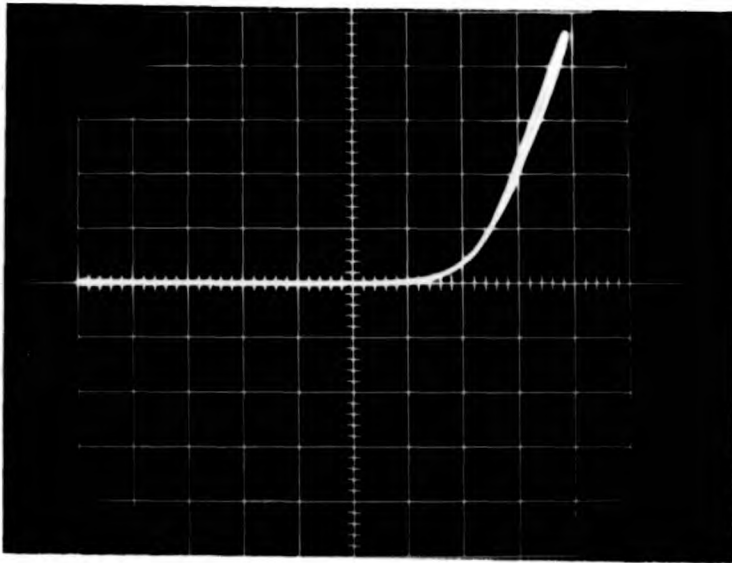
0.5mA/div.

20V/div.

4.7.4. DEVICES OF THE FORM In/CdS/In

Devices with indium contacts on both large area
faces exhibited the same characteristic independent of
the direction of the applied bias from room temperature
to 77°K. The symettry of the characteristic indicated
the contacts were ohmic.

No negative resistance or oscillations were observed
with devices of the above form. The functional variation
of current with voltage was dependent on the thickness
and trap density.

For currents where the thermal free carrier density
exceeded the injected free carrier density a linear
variation was observed between current and voltage.
At higher currents a power law variation was observed.
Fig. 4.37 illustrates the transition from a linear to
a power law characteristic for device LF/IN/A by reduction
of the temperature from 300°K to 77°K and hence the
reduction of the thermal free carrier density.

4.7.5. THREE TERMINAL DEVICES

No luminescence had been observed in devices with
one contact on each of the opposite large area faces.
In order to study whether the absence of luminescence
was partly due to the contact geometry, devices with two
contacts on one large area face were fabricated as
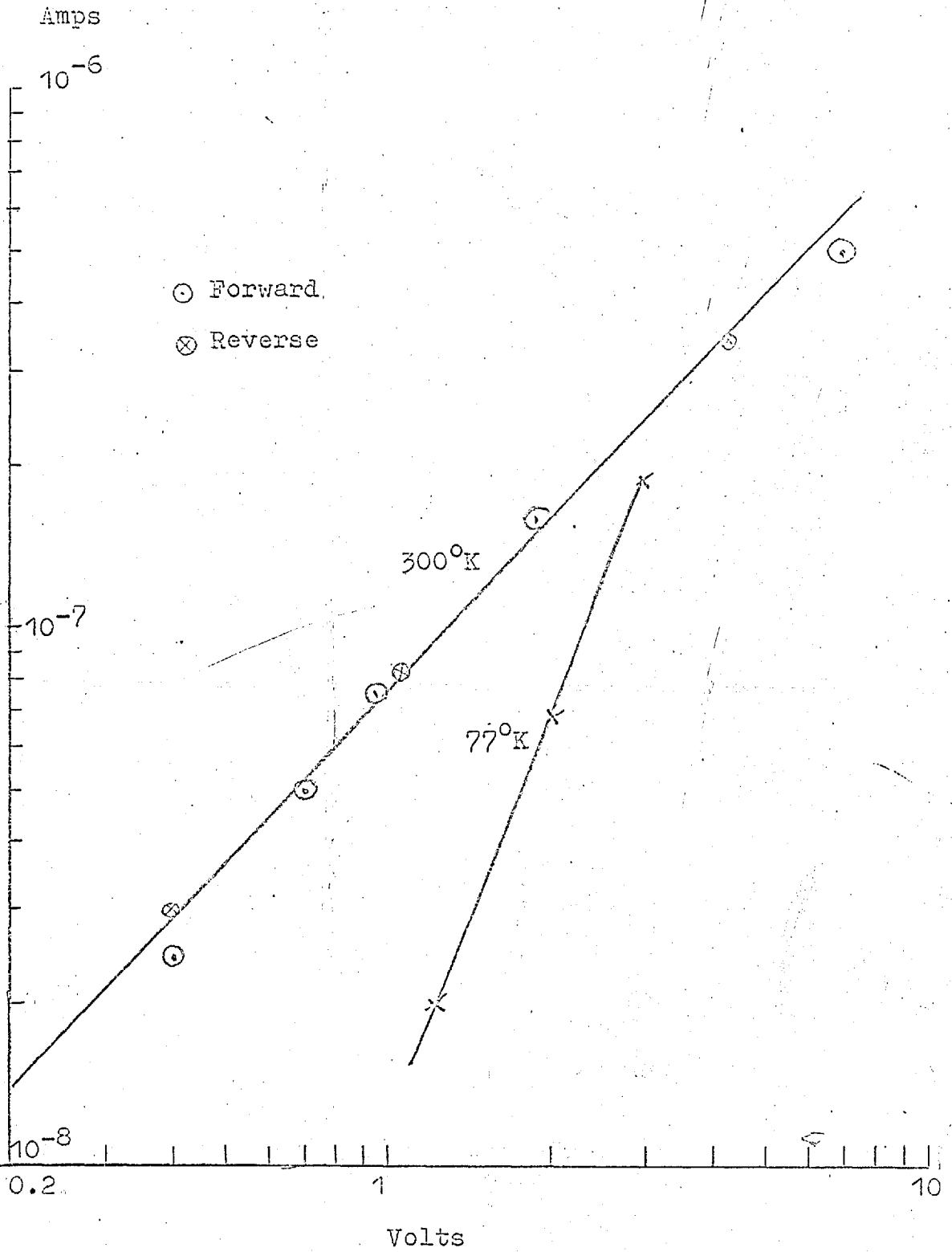
Fig. 4.37

Forward Characteristics

Device LF/IN/A

described in section 3.3.

The characteristic with voltage applied between the cuprous sulphide/cadmium sulphide and the cadmium sulphide/indium contacts showed a lower resistance path than with voltage applied between the silicon monoxide/cadmium sulphide and cadmium sulphide/indium contacts. Fig. 4.38 shows the characteristics for the two paths at 77°K for device LF/1/A. (The crystal was uniformly thick).

The devices exhibited unity current gain when operated as a three terminal device on the curve tracer. Fig. 4.39 shows the collector characteristic for device LF/1/A operating in the NPN mode. Loops occurred in the characteristic due to trapping effects.

When the devices were operated with bias only between the two contacts on the top surface they exhibited a relatively low field (order 10^3 V/cm) breakdown at 77°K with the cuprous sulphide/cadmium sulphide contact positively biased. The current increased almost at constant voltage. A green-blue light (probably edge emission) was seen emitting from between the contacts in the breakdown region, 1 - 10mA. The light appeared to be emanating from isolated spots rather than as a continuous stream. After the device had been left in the dark for over a day the luminescence emitted when the device was first switched on was extremely bright and could easily be observed in daylight. The luminescence
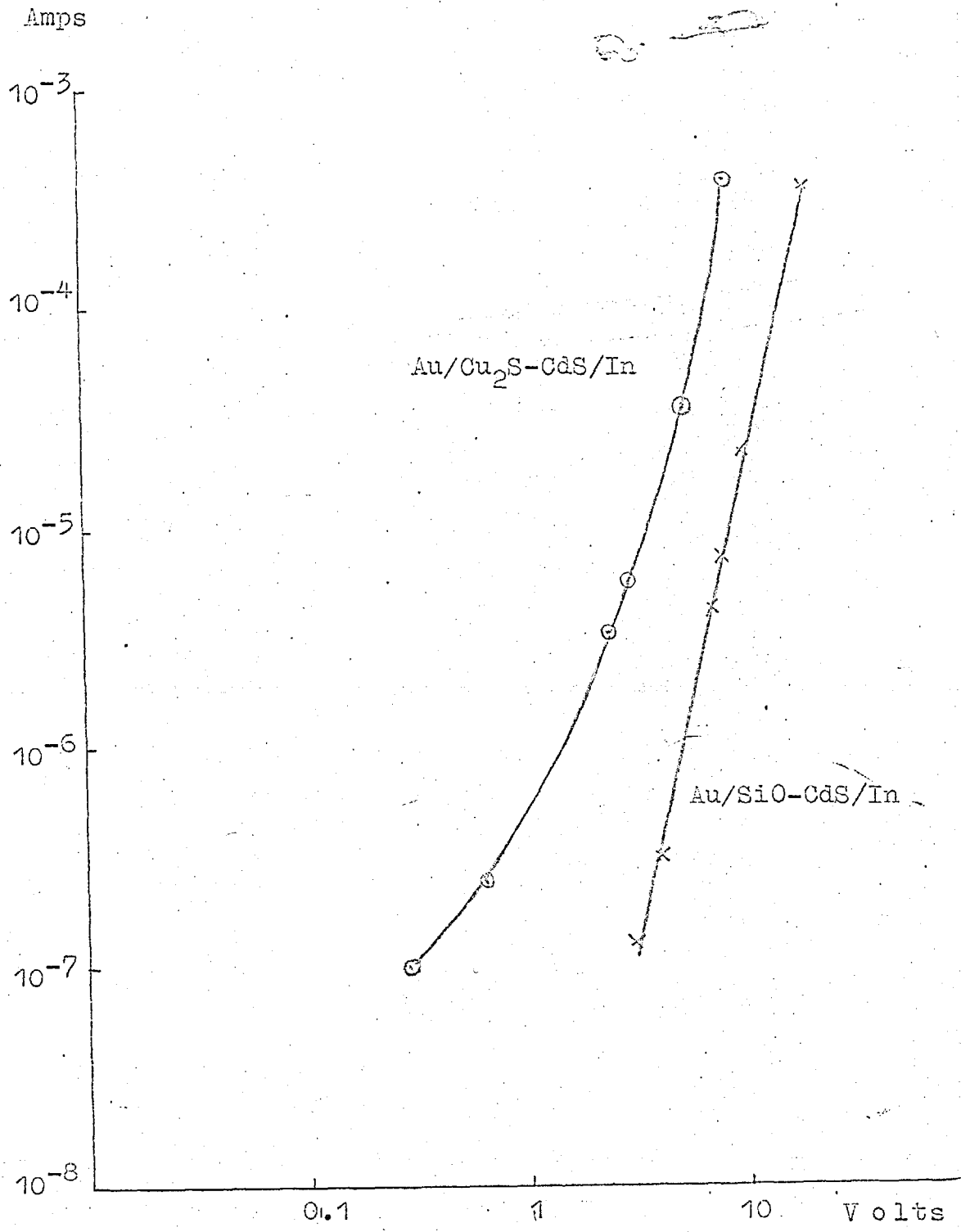
Fig. 4.38

Device LF/1/A

Alternate current paths 77°K

Fig. 4.39

Collector characteristics device LF/1/A
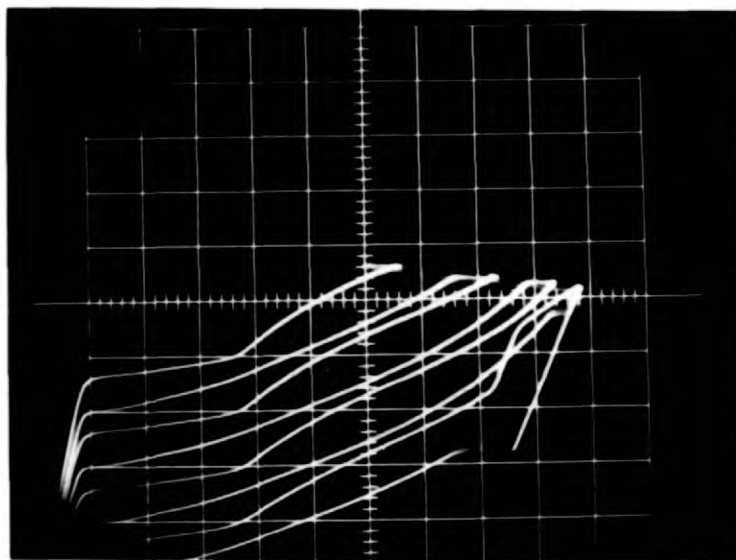
I_C 2mA/div.

I_B 1mA/step

V_{CE} 2v/div.

Cuprous sulphide contact positive

appeared again but greatly reduced in intensity when the device was switched off and then switched on again.

All the devices fabricated in the above manner exhibited luminescence at 77°K when a bias was applied between the two top surface contacts.

4.8   SUMMARY

Measurements have been performed on a number of cadmium sulphide devices made from thin single crystal platelets with different electrical contact materials on their large area faces.   All the devices had one contact of indium or gallium, which could be considered to be ohmic.   The results obtained with different contacts on the opposite face are summarized below:-

1)   Gold/cuprous sulphide contact

These devices exhibit:

a) Rectification with rectification ratios up to 10^{6};   the low current direction corresponds to a positive bias on the gold/cuprous sulphide contact.

b) Negative resistance in the forward direction at 300°K if the devices are of sufficient thickness.

c) Disappearance of negative resistance on cooling to 77°K.

d) Positive resistance oscillations below 100°K.

e) Oscillations associated with negative resistance.

f) No visible luminescence in the temperature range 77°K to 300°K.

g) The results of trapping, hysteresis, current decay, and thermally stimulated current.

h) Switching at high current.

i) Photocurrents plus an injection current when illuminated under bias.

2) <u>Gold/cuprous sulphide/silicon monoxide contact</u>
These devices exhibit:

a) Rectification; rectification ratios greater than 10^6.

b) Negative resistance in the forward characteristic at 300°K.

c) Disappearance of negative resistance on cooling at 77°K.

d) Oscillations associated with negative resistance at 300°K.

e) No current decay.

f) No positive resistance oscillations.

g) No visible luminescence in the temperature range 77°K to 300°K.

3) <u>Gold/cuprous iodide contact</u>
These devices exhibit:

a) Rectification; rectification ratio up to 10^2.

b) Ohmic behaviour in the forward characteristic at 300°K.

c) Exponential characteristic in reverse direction at 300°K.

4)   Gold contact

These devices exhibit:

a) Rectification.

b) Negative resistance in forward characteristic at 300°K.

c) Disappearance of negative resistance on cooling at 77°K.

d) No visible luminescence in the temperature range 77°K to 300°K.

5)   Indium contact

These devices exhibit:

a) No rectification; these devices appeared to be ohmic in both directions.

b) No oscillations in the temperature range 77°K to 300°K.

c) No luminescence in the temperature range 77°K to 300°K.

6)   Gold/cuprous sulphide plus gold/silicon monoxide contact

These devices exhibit:

a) Lower resistance path via the gold/cuprous sulphide contact.

b) Low field electroluminescence at 77°K when bias applied between two contacts on one side; gold/cuprous sulphide positively biased.

CHAPTER V

DISCUSSION OF RESULTS AND CONCLUSION

5.1. Devices with a cuprous sulphide contact.

5.1.1. Nature of the contact.

The occurrence of negative resistance at room temperature and the observation of positive resistance oscillations below $100°$K, in the device characteristic, indicated the participation of both electrons and holes in the conduction mechanism (see 1.4. and 1.6). Electrons can be introduced into the cadmium sulphide bulk through the ohmic indium or gallium electrode. The mechanism for the injection of holes is not so simple to understand, however, due to the complicated nature of the cuprous sulphide/cadmium sulphide contact.

Cuprous sulphide has a smaller band gap than cadmium sulphide and is unlikely to be an efficient source of holes by injection to the valence band, because of the competing process of electron extractions. There is considerable disagreement in the reported measured values of band gap of cuprous sulphide (see table 1.5) due to differences in stoichiometry, degeneracy and the effects of free carrier absorption on optical measurements. Since the electron affinity of cuprous sulphide and the work function of cadmium sulphide are also not known, a

simple energy band diagram of an abrupt heterojunction
cannot be accurately constructed. An abrupt heterojunction
is unlikely, however, due to the presence of interfacial
surface states, and the effect of heat treatment during
fabrication of the devices (see 3.2.4).

Copper is known to diffuse rapidly in cadmium sulphide
(CLARKE 1959, SZETO and SAMORJAI 1966, SIMHONY et al 1967).
SHITAYA and SATO (1968) have performed electron micro-
probe analysis on the surface of a cadmium sulphide crystal
prepared by electroplating at room temperature in a
cupric sulphate solution. A transition was observed from
a cadmium rich cuprous sulphide layer to a copper rich
cadmium sulphide layer over a region of about 3 microns.
Electron microprobe analysis could not be performed on
the present devices due to the difficulty of lapping the
thin devices used. It is probable, however, that copper
had diffused the order of a micron into the cadmium sulphide.
The rapid diffusion of copper indicates an interstitial
diffusion mechanism. The relatively small atomic radius
of $Cu^+(0.96A^o)$ would permit interstitial diffusion. An
interstitial copper atom can react with ionized cadmium
vacancies to settle on a substitutional site.

$$Cu_i \;+\; V_{cd}^- \;=\; Cu_s^- \quad \ldots\ldots\ldots 5.1$$
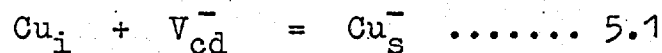
Substitutional copper ions are more soluble in cadmium
sulphide than cadmium vacancies (SZETO and SAMORJAI 1966)

leading to a reduction in the cadmium vacancy concentration. Any excess copper has to dissolve in the lattice by a self compensation mechanism (see 1.2.4) producing sulphur vacancies.

$$Cu = Cu_S^- + V_S^+ \quad \ldots\ldots\ldots 5.2$$
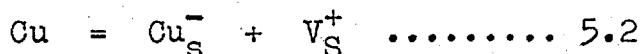
Cadmium sulphide crystal platelets grown by a vapour transport technique exhibit a high degree of self compensation. The degree of self compensation is not complete, even though the resistivity is high, and in general will vary from crystal to crystal. Undoped cadmium sulphide crystals are always n-type at room temperature indicating an excess of sulphur vacancies over cadmium vacancies. The n-type nature is caused by an excess of the cadmium partial pressure during the growth process and subsequent quenching to room temperature (KRÖGER and VINK 1956). Evidence of excess cadmium was observed during the growth of crystals examined here by the deposition of free cadmium at the cool end of the growth tube. The addition of copper is known to increase the resistivity of cadmium sulphide (SIMHONY et al 1967) due to the compensation of shallow donors by deep acceptor levels. Copper increases the resistivity of relatively highly self compensated cadmium sulphide because it reduces the ratio of shallow donor to deep acceptor concentration towards unity.

Copper, however, is not very soluble in cadmium sulphide at room temperature and precipitates as crystallites of

cuprous sulphide at concentrations greater than 100ppm
(STURNER and BLEIL 1964, SINGER and FAETH 1967).

From the above considerations a simplified model can
be proposed for the cuprous sulphide/cadmium sulphide
junction (see fig. 5.1). Region A represents the simple
band model for a p-n heterojunction proposed by ANDERSON
(1962) for a p-type semiconductor with a smaller band gap
than that of the n-type semiconductor and neglecting the
effect of interfacial surface states. The discontinuities
at the interface are due to the difference in dielectric
constants of the two materials. Region B represents
cadmium sulphide containing copper. The concentration
of copper will be graded across region B. At small values
of distance x, the copper concentration is high and
precipitation of cuprous sulphide occurs. As x increases
there is a gradual transition from highly resistive copper
compensated cadmium sulphide to the less highly resistive
cadmium sulphide bulk, region C.

On the other side of the crystal diffusion will have
occurred from the indium or gallium contact. Indium is
known to diffuse rapidly in cadmium sulphide (WOODBURY 1964)
and produces n-type conductivity. The relatively small
ionic radius of In^{3+} ($0.81A^{o}$) indicates both a substitutional
and interstitial diffusion mechanism are possible. Indium
has a segregation coefficient of about unity in cadmium
sulphide grown from the melt (MEDCALF and FAHRIG 1958) which

Fig. 5.1

Model for the cuprous sulphide/cadmium sulphide junction region
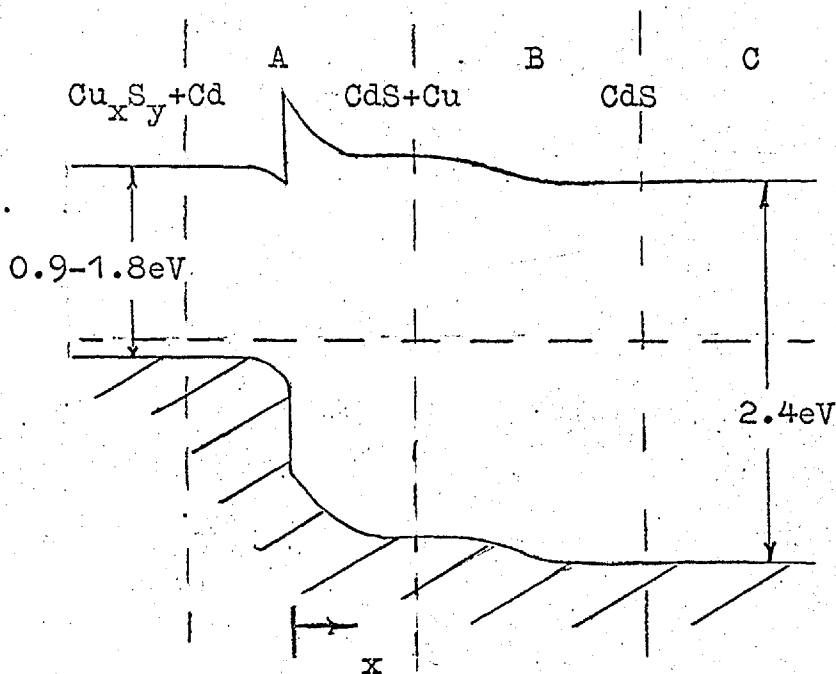
Fig. 5.2

Model for the cadmium sulphide/indium junction region
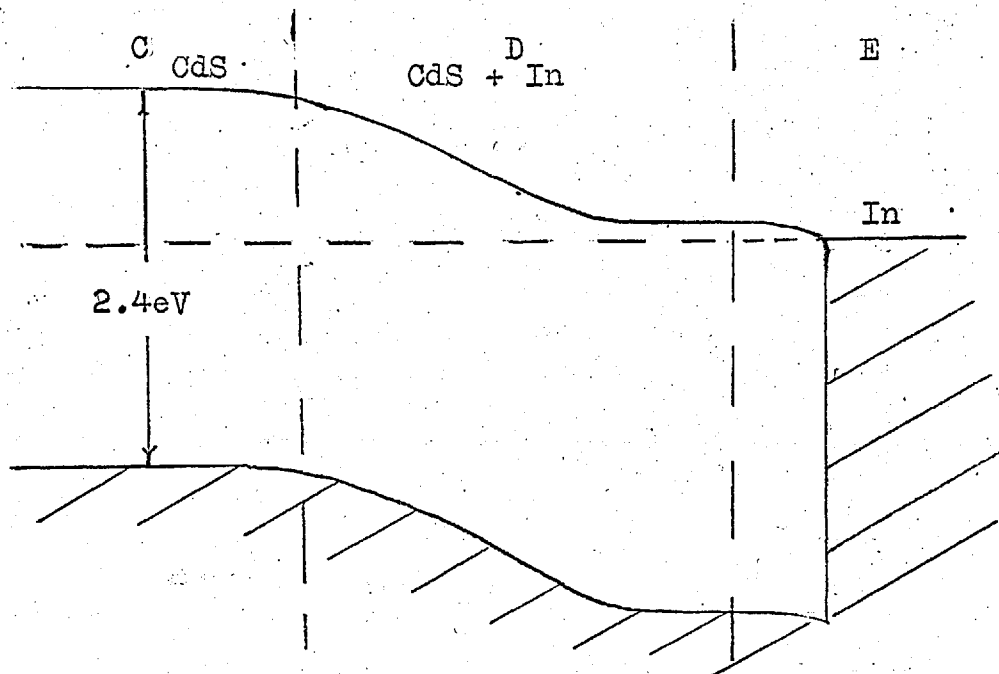
implies a high solubility.

It was possible to diffuse indium right through the cadmium sulphide platelets used here by heating a crystal containing two indium contacts for more than five minutes at around $300^{\circ}C$ in the radiation wetting apparatus.

Indium and gallium in cadmium sulphide lead to donor levels on substitution for cadmium, around 0.03eV below the conduction band (PIPER and HALSTED 1961) which are not compensated for by cadmium vacancies, a consequence of the fact that cadmium vacancy formation requires more energy than that gained by compensation (see 1.2.4.).

The n-type character observed in the cadmium sulphide and discussed above could also be due to uncompensated donors due to diffusion from the indium contact. A further possibility is the incorporation of halogens, which may have been present in the initial charge, into the crystals during growth can also lead to uncompensated donor levels in cadmium sulphide by substitution for sulphur. The chemical impurities responsible are likely to be of low concentration, because the crystals are high resistive, and below the limits of detection of conventional analytical techniques.

In the region close to the indium contact a high conductivity n-type cadmium sulphide layer will exist, see fig. 5.2. Region C is continued from fig. 5.1. Region D represents a graded indium doped cadmium sulphide layer.

Region E represents the ohmic indium cadmium sulphide contact. The transition region between D and E will contain degenerate indium doped cadmium sulphide (KRÖGER et al 1956) where impurity band conduction can occur.

The open circuit photovoltage of 250mV obtained under relatively high light intensities, (see 4.6.9) indicates the presence of a barrier. The barrier responsible is in the conduction band edge, between region B and region A of figure 5.1. For a p-n heterojunction the open circuit photovoltage is a function of the conduction band barrier height, the difference between the quasi-Fermi levels in the two semiconductors and the ratio of density of states and carrier lifetimes (KEATING 1965). Since none of the above parameters are known, no calculation of the barrier height can be attempted. MYTTON (1968) obtained a value of 480mV at $300^{\circ}K$ for a cuprous sulphide/cadmium sulphide photocell. The cadmium sulphide, however, had a high conductivity and consequently a higher barrier occurred under equilibrium conditions (Fermi-levels lined up).

For a simple Schottky barrier between metals and cadmium sulphide the open circuit photovoltage saturates to a value equal to the conduction band barrier height at high light intensities (BUJATTI (1967), (1968),). A Schottky barrier is unlikely to have occurred in the present devices due to diffusion of the contact.

Contact barriers on insulating semiconductors are difficult to measure because of the properties of the bulk material. Bulk effects can be separated from contact effects by the use of pulsed light (nanosecond pulses) having a small penetration depth (COURTENS and CHERNOW 1966).

The fact that similar results were obtained on devices prepared with evaporated and chemically deposited layers is evidence for the device characteristics being independent of the composition of the cuprous sulphide layer. The properties of the devices appear to be determined by a complicated region containing copper, cadmium and sulphur. SHITAYA and SATO (1968) have suggested that the barrier height at the junction does not depend on the work function of the cuprous sulphide but on the position of the Fermi-level in the copper compensated surface layers of the cadmium sulphide. Evidence for the above is that:

a) the photocurrent versus wavelength relation of cuprous sulphide/cadmium sulphide photocells was the same as that for copper doped cadmium sulphide (BUBE 1960).

b) the reverse bias capacitance was independent of applied voltage which suggested a high resistance (MOTT) layer had formed in the cadmium sulphide bulk due to copper, confirming the result of SIMHONY et al (1967) for copper diffused layers in cadmium sulphide.

5.1.2. THE ANALYSIS OF THE DEVICE CHARACTERISTIC

Several mechanisms can lead to a current controlled (S-type) negative resistance:

1) Avalanche breakdown
2) Electroluminescence – photoconductivity feedback
3) Heating effects
4) Double injection

Avalanche breakdown requires field strengths greater than 5×10^5V/cm in cadmium sulphide (SIMHONY et al 1967). The low average fields observed at the onset of negative resistance in the present devices ($10^3 - 10^4$V/cm) indicate avalanche breakdown does not occur. The average field in very thin devices was of the same order of magnitude as thick devices, which indicated that most of the applied voltage was not across a high field region. Furthermore, avalanche breakdown should still occur at 77°K and the disappearance of negative resistance cannot be explained on this basis. Negative resistance observed in the reverse direction (see fig. 4.26), however, is almost certainly due to avalanche breakdown when most of the applied voltage appears across the junction region.

The electroluminescence-photoconductivity mechanism can lead to negative resistance (DUMKE 1964) and appears to be the mechanism in gallium arsenide p-i-n diodes. Before negative resistance breakdown the conductivity is

dominated by an electronic space-charge limited current
and in the simplest case of no diffusion currents or
contact limitation will be of the form J proportional to
V^2 (MOTT and GURNEY 1940). Electrons recombining with
holes in the anode can generate photons at a rate depend-
ent on the internal quantum efficiency. In a semiconductor
containing deep levels there is a strong possibility that
a photon will be reabsorbed in the anode region producing
a free electron and a hole bound to a deep level. Until
this hole decays, another electron can be present in
addition to the electrons contributing to the net space
charge. Assuming that the photoconductivity produced
current can be added to the space charge limited current
it can be shown that breakdown will occur when at least
one of the (τ_n/t_n) electrons, that traverse from cathode
to anode during the lifetime of the bound hole, recombines
producing a photon which can produce another free electron-
bound hole pair. τ_n/t_n is the ratio of electron lifetime
to electron transit time. If the quantum efficiency
depends superlinearly on current then breakdown may be
maintained at progressively lower values of voltage leading
to a negative resistance.

The absence of visible luminescence in the present
devices, however, indicates that the above mechanism did
not occur.

A simple analysis shows that heating of a semiconductor can lead to negative resistance. The temperature dependence of resistivity of intrinsic semiconductors generally obeys a relationship of the form:

$$\rho = \rho_0 \exp (B/T) \quad \ldots\ldots\ldots 5.3$$

Assuming the resistance of the semiconductor is determined by the active region below the contact of area A, then the resistance R/unit length is given approximately by:

$$R = 1/A\rho_0 \exp B/T \quad \ldots\ldots\ldots 5.4$$

Assuming Newtons law of cooling the thermal balance equation for the active region is given by:

$$I^2 R = V^2/R = C(T-T_0) \quad \ldots\ldots\ldots 5.5$$

where C is the dissipation coefficient per unit length, T is the temperature of the active region and T_0 the ambient temperature.

Hence using 5.4 and 5.5:

$$I = \left\{A\rho_0 C(T-T_0)\right\}^{\frac{1}{2}} \exp (-B/2T)$$
$$\ldots\ldots\ldots 5.6$$
$$V = \left\{C(T-T_0)/A\rho_0\right\}^{\frac{1}{2}} \exp B/2T$$

Differentiating V with respect to temperature it can be shown by equating dV/dT to zero that a maximum will

occur in the voltage at a temperature:

$$T_m = B/2 \pm \left\{ B(B-4T_o) \right\}^{\frac{1}{2}}/2 \quad \dots\dots\dots 5.7$$

Negative resistance can appear for the above simple analysis if the condition:

$$B > 4T_o \quad \dots\dots\dots 5.8$$

is satisfied. Assuming B is given by $E_G/2k$ where E_G is the band gap and k is Boltzmann's constant then the above condition would be satisfied for cadmium sulphide at room temperature.

The power input to the devices at the onset of negative resistance was of the order of 0.5mW and unlikely to cause a significant temperature rise. The above analysis would be more applicable to ceramic materials (LOTOTSKII and CHIRKIN 1968).

The relatively low fields (SMITH 1957) at which negative resistance occurred and the large concentration of holes in the cuprous sulphide indicates that a double injection mechanism can be used to explain the device characteristics.

In a wide band gap semiconductor containing a deep impurity level which acts as a hole trap the simultaneous injection of holes into the valence band at the anode and electrons into the conduction band at the cathode from ohmic contacts, results in electronic current since the holes will be trapped. The resistance of the semiconductor

is determined by the space charge barrier, due to the free injected carriers, to further injection. The hole lifetime will be shorter than the electron lifetime. As the injection level increases the hole traps will become increasingly populated by holes (equivalent to a transfer of electrons to the conduction band) and hence the hole lifetime can increase. As the applied voltage increases the hole transit time decreases and the hole lifetime increases. When the hole lifetime is of the order of the transit time the hole traps will have been filled between the anode and cathode. The space charge barrier at the cathode to electron injection is reduced and higher currents can flow.

A negative resistance will occur because the hole lifetime when the hole traps have all been filled will have increased to a value approximately equal to the electron lifetime. Hence the condition that the hole lifetime equals the transit time can be maintained at a lower applied voltage.

For devices where there is no limitation on the supply of electrons at the cathode and the supply of holes at the anode the device characteristic can be obtained by the simultaneous solution of the following equations for one dimensional current flow:

a) Current flow equation

$$J = J_n + J_p$$

$$J = e\left\{\mu_n(n+n_o)E + D_n dn/dx\right\}$$

$$+ e\left\{\mu_p(p+p_o)E - D_p dp/dx\right\} \dots \dots 5.9$$

b) Particle conservation equation

$$1/e \, dJ_n/dx = -1/e \, dJ_p/dx$$

$$= n/\tau_n \qquad \dots \dots 5.10$$

$$= p/\tau_p$$

c) Poissons equation

$$\epsilon/e \, dE/dx = (p-n) + \delta q \qquad \dots \dots 5.11$$

Where p and n are the injected free hole and electron densities, p_o and n_o the holes and electrons present in thermal equilibrium, μ_p and μ_n the hole and electron mobilities, τ_p and τ_n the hole and electron lifetimes, D_p and D_n the hole and electron diffusion coefficients, δq is a term which accounts for charge redistribution on impurity levels in the band gap and ϵ is the dielectric constant of the material.

The equations for various models will have to satisfy different boundary conditions. They are, using present techniques, insoluble when diffusion currents and drift currents are taken into account. Most models consider only one current flow mechanism and hence only one boundary condition is required. Common boundary conditions are that the field is uniform; or else that it is zero at the

contact (implying an infinite supply of carriers). Analysis of the characteristics of the present devices cannot be performed quantitatively since both diffusion and drift currents occur and the boundary conditions are unknown due to the complex nature of the anode contact. Consideration of various simplified models, however, leads to an explanation of the characteristics observed in the present devices.

LAMPERT (1962) considered a wide band gap semi-conductor or semi-insulator where a deep impurity level was completely compensated by shallow donors, see fig. 5.3. He only considered drift currents and neglected contact potentials. The main results of the analysis were:

a) At low currents the current was ohmic and carried by carriers present in thermal equilibrium.

b) At a threshhold when the injected free carrier density exceeded the thermal density the current became space charge limited and obeyed a J proportional to V^2 law.

c) A negative resistance occurred at a threshhold voltage (V_B) when the hole transit time (t_p) was twice the hole lifetime (τ_p)

$$t_p = 2\tau_p \quad \dots\dots\dots 5.12$$

$$\tau_p = d^2/2\mu_p V_B \quad \dots\dots\dots 5.13$$

where d is the effective thickness of the device.

Fig. 5.3

Complete compensation of deep level by shallow donors
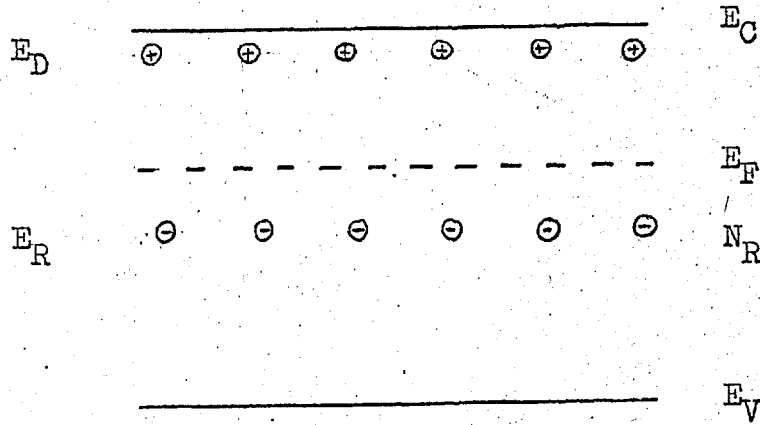
Fig. 5.4

Partial compensation of deep level by shallow donors
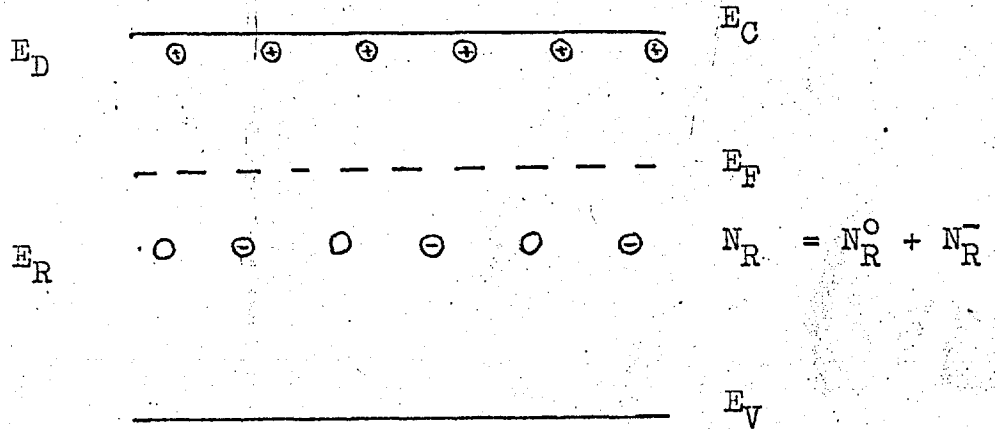
d) The voltage after threshhold drops to a minimum value V_M given approximately by:

$$V_M = \tau_{p,low}/\tau_{p,high} \cdot (V_B)$$

$$= \tau_{p,low}/\tau_n \cdot (V_B)$$

$$= \sigma_p^-/\sigma_n^o \cdot (V_B) \quad \ldots\ldots 5.14$$

where $\tau_{p,low}$ is the hole lifetime below the negative resistance threshhold, $\tau_{p,high}$ the hole lifetime after the threshhold, σ_p^- is the capture cross-section of a negatively charged centre for holes and σ_n^o the capture cross-section of a neutral centre for electrons.

e) Above V_M a $J \propto V^2$ law again applies the current being recombination limited in the bulk.

f) At higher currents still a $J \propto V^3$ applies due to two-carrier space charge limited current.

ASHLEY and MILNES (1964) considered partial compensation and partial occupation of the deep levels, see fig. 5.4.

The net result is that the space charge barrier to injection is due to trapped rather than free carriers, leading to higher values of negative resistance breakdown voltage. By equating the hole transit time to the low injection level hole lifetime the following form of relationship was obtained for V_B.

$$V_B = Ad^2(N_R^0/N_R)N_R^- \quad \ldots \ldots \; 5.15$$

where N_R is the deep level density, N_R^- is the negatively charged deep level density, N_R^0 the neutrally charged deep level density and A is a constant containing terms for capture cross-sections and mobilities. For a sample where $N_D \gg N_R$ then:

$$V_B \longrightarrow Ad^2N_D \quad \ldots \ldots \; 5.16$$

Hence the breakdown voltage is a function not only of the thickness but of the donor concentration. BARNETT (1966) has postulated that variations in donor concentration could lead to conditions favourable for double injection breakdown to occur preferentially along filaments, the variation in N_D providing the filament nucleation point. RIDLEY (1963) has predicted filamentary breakdown for current-controlled negative resistance devices from thermo-dynamic considerations. Voltage-controlled negative resistance leads to domain formation. Filamentary breakdown occurs along a critical path satisfying equation 5.16, where the hole traps have been filled whilst the rest of the device still supports a pre-breakdown current. A second negative resistance region occurs at higher current when another filament forms. Devices which undergo filamentary breakdown exhibit a current rise at constant voltage after the negative resistance, the increase of current being accomodated by widening of the filament.

BARNETT (1966) considered radial diffusion of carriers from the filament and predicted a power law variation of current such that J is proportional to $V^{1.5}$ to $V^{1.9}$ depending on the device area.

KEATING (1964) has shown that consideration of shallow trapping can considerably modify the characteristic particularly in the negative resistance region.

The characteristics observed in the present devices will now be discussed with reference to figs. 5.1, 5.2 and the above considerations. The characteristics can be divided into three regions:- pre-negative resistance, negative resistance and post-negative resistance.

a) Pre-negative resistance region

The pre-negative resistance region (see fig. 4.6) was generally characterised by an exponential rise of current with voltage at low currents which merged into a region of decreasing slope as the negative resistance was approached. At low currents the resistance of the cuprous sulphide/cadmium sulphide heterojunction predominates over that of the cadmium sulphide bulk and the currents are a diffusion current of electrons from B to A over the barrier in the conduction band and a diffusion current of holes from A to B in the valence band. Since the barrier in the conduction band is considerably less than that in the valence band (ANDERSON 1962) the current will be mainly due to electron extraction from the cadmium sulphide. Electrons will be supplied to the cadmium

sulphide bulk by the ohmic indium electrode. As the electronic current increases a space charge barrier builds up in region C to further electron injection from the indium electrode. The region of decreasing slope in the characteristic, see fig. 4.6 is due to a progressively increasing voltage drop across region C. For pure drift current a J proportional to V^2 characteristic should occur in this region. In the present devices the characteristic is complicated by the contact potential drop and diffusion currents.

Since the resistivity of the bulk region C is limited by space charge effects more voltage can be applied to the device without destroying it with a high electronic current. The increasing field across the device tilts the band diagram of fig. 5.1 anti-clockwise so increasing the probability of hole injection from the anode. The difference in energy between the valence band edges of cuprous sulphide and cadmium sulphide is probably around 1eV which suggests a field dependent injection process, such as, either Schottky emission or quantum mechanical tunnelling. Tunnelling could occur if a high resistivity layer such as copper compensated cadmium sulphide existed at the anode see fig. 5.5.

Holes could also be given sufficient energy to surmount the barrier by energy transfer from energetic electrons falling into the cuprous sulphide anode (see fig. 1.2).

Fig. 5.5

Tunnel injection through copper compensated layer
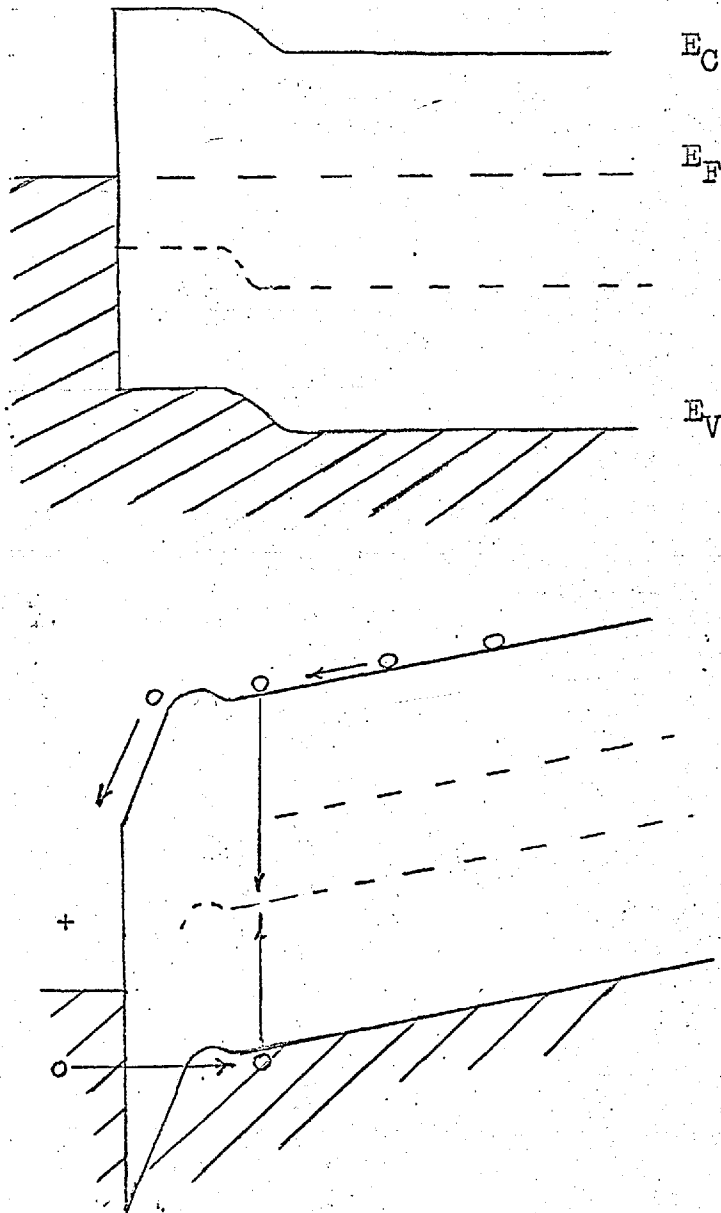
If cuprous sulphide precipitates existed (see 5.1.1) in the anode region they would act as conducting needles in an insulating medium. The field lines would concentrate at the tips of the needles leading to field emission of holes and electrons from opposite ends. The above process has been proposed for electroluminescence observed in zinc sulphide/copper phosphors (FISCHER 1963).

b) Negative resistance region

It is well known that a deep acceptor level exists in cadmium sulphide about 1eV above the valence band and acts as a trapping centre for holes (see for example BUBE 1960). Hence, when holes and electrons are injected into cadmium sulphide a negative resistance occurs (see figs. 4.4, 4.6) for the reasons outlined above.

The nature of the deep level in cadmium sulphide has not yet been elucidated. The level could be due to native defects such as cadmium vacancies or to chemical impurities such as copper. In general more than one energy level is introduced by the defect. Copper for example is known to introduce at least six different levels (BUBE 1960).

From the measurement of optical ionization energies (BUBE and CARDON 1964) and thermal ionization energies (STUPP 1963) it was observed that the deep acceptor level always occurred at the same energy independent of the specific deep acceptor impurities that were present. The above result suggests that addition of acceptor impurities

such as copper leads to the formation of a native defect
such as a cadmium vacancy. Results of ESR measurements
(KASAI et al 1961, SCHNEIDER et al 1963) have indicated
the defect is a complex of a cadmium vacancy surrounded
by three sulphur ions and a donor imperfection. RUSHBY
and WOODS (1966) have observed that switching from a pre-
negative resistance region to a post-negative resistance
region in gold/cadmium sulphide diodes can be caused by
light of quantum energy greater than 1.52eV at 77°K.
This is the energy needed to remove electrons to the con-
duction band from recombination centres about 1eV above
the valence band (equivalent to completely filling the
centres with holes). It was not clear, however, why the
inverse process did not occur when infra-red radiation
of sufficient energy to raise an electron from the valence
band to the deep centre illuminated the device.

The theory of LAMPERT (1962) leads to a value of
hole lifetime τ_p at low injection levels, see equation
5.13, in terms of the threshhold voltage V_B. However,
equation 5.13 cannot be used for accurate calculation of
τ_p because:

1) the voltage drop across the junction is unknown

2) diffusion currents as well as drift currents
are present

3) the effective intercontact distance is not known

Equation 5.13, however, should lead to a value of τ_p

within an order of magnitude of the correct value. For example, device LF/PA (about 30 μ thick) showed a negative resistance threshhold at 24V; hence using a value of $15cm^2/Vsec$ for the hole mobility at room temperature (SPEAR and MORT 1963) a value for $\mathcal{L}_p$ of 1.2×10^{-8} secs. is obtained. SPEAR and MORT (1963) using electron bombardment techniques obtained a value of 3×10^{-7} secs, and MARK (1965) from measurements of the ambipolar diffusion length obtained a value of 5×10^{-8} secs.

The absence of negative resistance at low temperatures (figs. 4.14, 4.15) indicates that hole injection sufficient to fill the hole traps across the crystal did not occur. Hole injection would be reduced if there was an increase in the interfacial surface state density in the junction region. Interfacial surface states are due to interfacial dislocations, dangling bonds and bonding deficiencies at the interface (OLDHAM and MILNES 1964, DONNELLY and MILNES 1966). A lattice misfit between the two components of a heterojunction of 1% will significantly affect the band bending and a misfit of 0.05% will cause significant minority carrier recombination in the interfacial states (OLDHAM and MILNES 1964). Interfacial states will be present in a high density since the lattice misfit between cuprous sulphide is relatively large (see 1.2.4). The interfacial surface state density would increase if the lattice misfit increased with decrease of temperature.

The strain in the cuprous sulphide film would definitely increase since it was evaporated at room temperature.

Reduction of the temperature reduces the concentration of electrons in the conduction band, due to ionized uncompensated shallow donors and, hence the resistivity of region C will approach that of region B of fig. 5.1. Hence hole injection through a layer more highly resistive than the bulk (see fig. 5.4) will be reduced as the applied field is spread more uniformly across the crystal.

The current at 77°K is an electron extraction current from region B to region A complicated by space charge effects in the bulk. For a diffusion-free, space charge limited current a J proportional to V^2 characteristic is expected; for a simple extraction current over a barrier a J proportional to exp $eV/\beta kT$ characteristic is expected (ANDERSON 1962) (where β is in general greater than one). A combination of the two leads to a high power law rise of current with voltage. Power law rises of current up to V^{12} were observed in the present devices at 77°K. The observed characteristics will also be complicated by the presence of diffusion currents in the cadmium sulphide bulk (HILL 1968).

At high currents (greater than 1mA) and voltages (greater than 100V) negative resistance was observed in some devices at 77°K, see fig. 4.16. Sufficient hole injection had now occurred because the extra interfacial

states had been saturated and the modified barrier to hole injection (due to the increase of bulk resistivity in region C) had been surmounted.

Negative resistance did not occur in thin devices (less than 5μ thick), see fig. 4.30, and can be explained by the fact that the hole diffusion length (1 - 5microns) was now of the same order of magnitude as the device length. The current is determined only by the contact barriers and hole traps can be immediately filled across the device. The theory of STAFEEV (1959) is more applicable to thin devices when only the fiffusion terms in equation 5.9 are considered.

Negative resistance did not occur in devices illuminated with visible light (see fig. 4.31) because the hole traps are continuously filled with holes, and the hole lifetime is always approximately equal to the electron lifetime.

c) Post-negative resistance region

The voltage across the devices exhibiting negative resistance decreased to a minimum value following the negative resistance (see fig. 4.6). In some devices the current then increased at almost constant voltage (device LF/A, LF/O, LF/N in fig. 4.6) before changing to a power law variation. The power law variation occurred at high currents and often could only be observed by pulse measurements (device LF/N in fig. 4.6.). Some devices exhibited

a power law variation immediately following the negative resistance (device LF/G in fig. 4.6, device LF/PA in fig. 4.4) generally of the form J proportional to V^3 (see fig. 4.5). LAMPERT (1962) predicted a relationship of this form for space charge limited two carrier current. It would appear that the bulk properties of the devices in the thickness range 20 - 50 μ predominate at high currents. If most of the voltage drop had occurred across the junction an exponential characteristic of the form J proportional exp $eV/\beta kT$ would have occurred. An exponential characteristic occurred for thin devices (fig. 4.30) at high currents.

The increase of current at constant voltage observed in several devices following negative resistance is predicted for double injection along filaments (BARNETT 1966). Evidence for filamentary conduction is the observation of more than one negative resistance region in the device characteristic, see fig. 4.7 corresponding to the formation of more than one filament. The observation that final breakdown occurred at one point on the cuprous sulphide is still further evidence for the filamentary mode of conduction. The conditions for filament formation at one point could be fulfilled by variations in the shallow donor concentration, in the plane containing the c-axis, introduced during growth. Filaments could also be nucleated at the tips of crystallites of cuprous sulphide present at the anode.

5.1.3. OSCILLATIONS AT LOW TEMPERATURE

Space charge limited current devices are characterised by their low noise properties, the noise being suppressed by the space charge. The neutralisation of electronic space charge by hole injection leads to generation-recombination noise (FAZAKAS and FRIEDMAN 1968) which is, of course, not suppressed by space charge. In the present devices the noise increased considerably above the negative resistance region which indicated a transition from a space charge limited to a space charge compensated current regime. The coherent oscillations observed in the present devices below 100°K can be explained by carrier recombination mechanisms.

Several mechanisms involving both types of current carrier have been proposed to account for oscillations in the absence of a negative resistance in semiconductors containing deep impurity levels. Two of these mechanisms are considered here (see 1.6).

a) The formation of recombination waves (KONSTANTINOV and PEREL 1965).

b) Space-charge recombination oscillations (MOORE et al 1967).

a) The mechanism for the formation of recombination waves is as follows:-

1) A random perturbation (increase) of electron concentration occurs.

2) The perturbation is compensated by the corresponding

decrease of negative charge on the deep traps (increase of the fixed positive charge).

3) A perturbation of this sort disappears slowly due to the electron capture rate by the deep level (a fluctuation of the hole concentration would be dissipated in a much shorter time).

4) When a constant electric field is applied polarisation occurs and the negative charge and the compensating positive charge are separated producing a localised field reduction.

5) Assuming the hole capture rate by the deep centre is very rapid then their concentration remains virtually constant. Holes entering the localised field reduction are slowed down which leads to a decrease in the hole current and more holes are retained on traps.

6) The increased positive charge on the traps attracts more electrons into this region and hence the local field is increased.

7) The opposite effect occurs on the other side of the local field reduction and consequently the field reduction moves in the opposite direction to electron drift motion.

The direction of motion of the perturbation may be obtained by the following simplified analysis.

Assuming the current is mainly electronic (this condition is satisfied in the present devices) the electric field perturbation may be obtained by assuming that the current is constant; hence in one dimension:

$$n_0 \, \partial E'/\partial x + E_0 \, \partial n'/\partial x = 0 \quad \ldots\ldots 5.17$$

considering only drift currents.

Where n_0 is the steady state electron concentration, n' the electron perturbation, E' the field perturbation and E_0 the steady field.

The rate of variation of electron concentration in a given volume is equal to the hole trapping rate in that volume, hence:

$$\partial n'/\partial t = -p_0 \mu_p \, \partial E'/\partial x \quad \ldots\ldots 5.18$$

where p_0 is the steady state hole concentration and $_p$ the hole mobility.

Eliminating $\partial E'/\partial x$ from 5.17 and 5.18 leads to –

$$\partial n'/\partial t - p_0 \mu_p E_0/n_0 \, \partial n'/\partial x = 0 \quad \ldots\ldots 5.19$$

Hence the electron perturbation moves against the field with a velocity $p_0 \mu_p/n_0$ per unit field.

A system such as that described above will be unstable if the hole capture rate is finite since the fixed and positive charges in the perturbation region will increase (the hole concentration is not in the steady state).

The problem can be analysed in a simplified form, neglecting the variation with time of τ_n, τ_p and n_0, p_0, using the three equations for one dimensional flow:

1) Current flow equation

$$J_n = (n' + n_0)e\mu_n(E_0+E') + eD_n \, \delta(\overline{n'+n_0})/\delta x$$

$$J_p = (p' + p_0)e\mu_p(E_0+E') - eD_p \, \delta(p'+p_0)/\delta x \quad \ldots 5.20$$

2) Continuity equation

$$\delta n'/\delta t + 1/e(\delta J_n/\delta x) = n'/\tau_n$$

$$\delta p'/\delta t - 1/e(\delta J_p/\delta x) = n'/\tau_p \qquad \ldots 5.21$$

3) Quasi-neutrality condition

$$\text{div } J = 0$$

$$\delta J_n/\delta x + \delta J_p/\delta x = 0 \qquad \ldots 5.22$$

n' and p' were assumed by KONSTANTINOV and PEREL (1965) to vary as $\exp\{-i(\omega t - Kx)\}$, where ω is the frequency and K is the wave constant. The equations are solved for small perturbations to arrive at the wave equation for recombination waves.

Taking into consideration the finite value of electron lifetime for trapping, the diffusion of carriers and the fact that the electron capture rate increases as more holes are trapped, (all factors which oppose instability), several conditions necessary for undamped oscillations to occur can be identified:-

1) The hole lifetime should be less than the electron lifetime $\tau_p > \tau_n$ a condition satisfied in cadmium sulphide containing a deep level.

2) The hole concentration should be sufficiently high so that: $p_0/\tau_p > n_0/\tau_n$ $\qquad \ldots 5.23$

Under double injection conditions in an n-type semiconductor p_o/τ_p is always less than n_o/τ_n and approaches equality at high injection levels as $p_o \to n_o$ and $\tau_p \to \tau_n$ (LAMPERT 1962). However, if the volume generation rate of holes exceeded that of electrons, then the inequality 5.23 may be satisfied. The volume generation rate of holes may be increased by the field enhanced thermal ionization of trapping centres (FISCHLER-HAZONI and WILLIAMS 1967) which is the most probable mechanism at the fields used (10^4V/cm). The temperature should be low so that the electron contribution from uncompensated donor levels is not too high.

3) The electric field should be such that the drift length of holes is much greater than their diffusion length ($\mu_p E > (D_p/\tau_p)^{\frac{1}{2}}$). Since the present devices were operating at average fields of 10^4V/cm before any observable double injection breakdown occurred the above condition is probably satisfied. (For $\mu_p = 10\text{cm}^2/\text{Vsec}$, $E = 10^4$V/cm, $D_p = 10^{-4}$cm, $\tau_p = 10^{-8}$sec, then $\mu_p E/D_p\tau_p = 10$)

4) The electron concentration should be lower than the deep level density. For device LF/3 at 77°K assuming the current was mainly electronic and neglecting contact effects, a free electron concentration of $10^{10}/\text{cm}^3$ is obtained at a current of 1mA (contact area 1mm^2, thickness about 30 microns, τ_n of the order of $2 \times 10^3\text{cm}^2/\text{V sec}$. (MORT and SPEAR 1963)). A deep level density of the order of $10^{16}/\text{cm}^3$ is probable (KEATING 1963).

If the above conditions are satisfied then recombination waves may propagate. Since they are travelling waves observation of the phase change of the oscillation along the crystal would indicate whether or not recombination waves are present. The thinness of the devices used here did not permit such a measurement.

The frequency of such waves is a complex function of the hole concentration which is in general not known. The frequency increases with hole concentration. In the present devices the frequency was observed to increase with applied voltage for the high current type of oscillation (see fig. 4.19) which would be evidence for the field dependence of hole concentration.

Due to the finite size of the specimen the theory predicts that the instability will occur at harmonic frequencies as the field is increased. The high current oscillations exhibited harmonics, see fig. 4.20.

It is suggested that the oscillations observed at high currents (greater than 1mA) in the present devices are due to recombination waves. The unknown value of such parameters as the hole concentration, however, makes it impossible to perform a detailed comparison.

b) The space charge recombination mechanism can be used to explain the oscillations observed in wide band gap semiconductors containing deep impurity levels. The mathematical formalism is complicated and has as yet not been completed (BARDEEN 1968).

The following simple sequence of events can lead to instability.

1) Simultaneous injection of electrons through the cathode and holes through the anode.

2) Some electrons are trapped on deep centres near the cathode, causing a fixed space charge barrier to electron injection, whilst others proceed to the anode where they interact with injected holes.

3) After the excess free electrons have recombined at the anode any remaining excess holes can neutralise the trapped electrons near the cathode and the process can be repeated.

The transit time for electrons at 77°K (of the order of 10^{-10} secs.) is less than both the lifetime and the dielectric relaxation time for cadmium sulphide.

Assuming a small perturbation $\delta n = \delta p$ on the LAMPERT (1962) theory the mobility of the perturbation is approximately:

$$\text{mobility} = (\mu_p\mu_n/\mu_p+\mu_n)(\overline{n-p}/n) \quad \ldots\ldots 5.24$$

(MOORE et al 1967a)

Hence the velocity $\bar{v}_p$ of the perturbation is approximately

$$v_p = (\mu_p\mu_n/\mu_p+\mu_n)(\overline{n-p}/n)E \quad \ldots\ldots 5.25$$

Assuming a uniform field.

The frequency of oscillation f is given by velocity of perturbation divided by distance travelled, hence

$$f \simeq (d/\mu_n E)(1/\tau_n)(\mu_p \mu_n/\mu_p + \mu_n)E/d$$

$$\simeq 1/\tau_n (\mu_p/\mu_n + \mu_p) \qquad \ldots\ldots 5.27$$

The result that the frequency of oscillation is $\propto 1/\tau_n$ is expected since the electron lifetime determines the recombination time of electrons and holes (the hole lifetime being much shorter that that of the electrons).

The above analysis is approximate since the LAMPERT (1962) theory ignores contact effects and diffusion currents and also because the effect of changes in the space charge of the traps has been neglected. The analysis is useful in that it gives an order of magnitude value for the expected frequency.

The frequency observed in the present devices at 77°K was of the order of 5kHz. Assuming a value of 20 for μ_n/μ_p (MORT and SPEAR 1963) leads to an electron lifetime of 10^{-5}sec. which is a reasonable value.

The amplitude of the oscillations should increase with field as more carriers are injected. The amplitude of the low current oscillations in the present devices die increase with applied field (see fig. 4.24).

The linear decrease of the oscillation frequency with applied field for the low current oscillations (see fig.4.23) agrees with results of MOORE et al (1967a) on gold doped silicon p-i-n devices.

The electron lifetime would in general be proportional to the density of filled deep levels. Since the deep level

density in the present devices is unknown and probably uncontrollable the variation of oscillation frequency with deep level density cannot be assessed from the present results.

The low current oscillations in the present devices appear to be of the space charge-recombination type inasmuch as the frequency is of the right order of magnitude and oscillations have an exponential character indicating a domain build up and decay mechanism rather than a domain transit mechanism.

Copper appears to be an essential ingredient and could be responsible for the deep level as only devices with a cuprous sulphide contact exhibited the above positive resistance oscillations (see 4.8).

Summarizing, it is considered that the high current oscillations at low temperature can be accounted for in terms of a domain transit mechanism, whilst those at low current are more probably due to space-charge-recombination instability.

5.2. OTHER DEVICES

A layer of a silicon monoxide deposited between the cuprous sulphide electrode and the cadmium sulphide crystal did not appear to block the extraction of electrons. It is necessary to use an insulator of low work function to block electron extraction but it is difficult to measure the work

functions of insulators since any practical method requires the passage of current. It would appear, however, that the work function of silicon monoxide is greater than that of cadmium sulphide.

The use of a silicon monoxide layer eliminated the current decay previously observed at low currents (see 4.6.3). It is possible, therefore, that the current decay was associated with interfacial surface states between the cuprous sulphide and cadmium sulphide.

The use of a silicon monoxide layer caused relaxation oscillations at room temperature at the negative resistance threshhold (see fig. 4.34) because the silicon monoxide layer was acting as a capacitor in series with a negative resistance.

Tunnel injection of holes could occur through the narrow (order of 100A$^{\circ}$) layer of silicon monoxide leading to the observed negative resistance by a double injection mechanism.

Diffusion of copper into the cadmium sulphide appeared to be prevented by the silicon monoxide layer since the low temperature positive resistance oscillations did not occur.

The constant rise of current with voltage beyond the negative resistance region and the subsequent power law variation (see fig. 4.32) are consistent with filamentary conduction (BARNETT 1966). A lower power law variation was observed ($V^{1.5}$ to V^{2}), than that observed in devices with-

out the silicon monoxide layer, and this was more in agreement with the BARNETT theory.

The voltage drop across the silicon monoxide layer appeared to be of the order of 1 Volt more than that across the cuprous sulphide layer. This was determined by comparing the characteristics of a gold/silicon monoxide and a gold/cuprous sulphide contact on one device (see fig.4.38). The electroluminescence observed at 77°K when a voltage was applied between the above two non-ohmic contacts on one face of the crystal was isolated at spots which suggested it was due to impact ionization at localized field concentrations.

The ohmic nature of the forward characteristic observed in devices with a cuprous iodide anode (see fig. 4.35) indicated hole injection did not occur. Cuprous iodide being a I - VII compound is an ionic solid (see 1.2.3) the p-type conductivity observed (see 3.3) was probably due to the motion of the Cu^{+} ion and not due to hole motion.

5.3. LONG TERM EFFECTS

It was observed in the present devices, that the device characteristics and oscillation parameters could be altered by the application of voltage over a long period of time. It is well known that cadmium sulphide exhibits such long term effects. Recently GERSHUN and TIMAN (1968) have shown that these long term voltage dependent effects are due to the field dependent motion of vacancies and that in cadmium

sulphide they are mainly due to cadmium vacancy movement.

5.5. CONCLUSIONS

The difficulty of obtaining p-type cadmium sulphide, due to the phenomenon of auto-compensation, necessitates the use of heterojunctions in order to obtain hole injection through electrical contacts.

The observation of negative resistance at 300°K and oscillations below 100°K in devices with a cuprous sulphide anode indicated the presence of injected holes in the cadmium sulphide bulk. Although cuprous sulphide exists in many modifications, devices prepared by evaporation and chemical deposition exhibit similar properties. The properties of such devices appear to be governed by a barrier layer of complex nature containing cadmium, copper and sulphur. Hole injection is aided by the formation of a high resistivity layer of copper doped cadmium sulphide and precipitated cuprous sulphide. The injection of holes is not uniform but occurs preferentially along filaments because of impurity fluctuations in the CdS bulk.

Cuprous sulphide forms an inherently poor hole injecting contact (due to electron extraction) because it has a smaller band gap than cadmium sulphide. P-type semiconductors with band gaps greater than cadmium sulphide (viz. cuprous iodide) are generally ionic and do not act as a source of holes when used as anodes. Silicon monoxide inserted as a thin insulating layer between cuprous sulphide and cadmium sulphide

does not appear to increase the barrier for electron extraction relative to that for hole injection.

The tendency for filamentary conduction and the long term variations in the device characteristics suggests that cadmium sulphide in the form used is not technologically suitable for device fabrication.

Addendum

Fig 4.15 shows an apparently anomalous behaviour of the current voltage characteristic between 175°K and 140°K. The resistivity at 140°K is less than that at 175°K for currents around 10^{-5} A whilst the reverse is true at 5×10^{-4} amps. This cross-over is difficult to understand. The effect will obviously depend on two factors:-

a) The carrier mobility which increases with decreasing temperature

b) The free carrier concentration which decreases with decreasing temperature if a trapping mechanism is operative.

It would appear, therefore, that between 175°K and 140°K there is a redistribution of trapped charge as another trapping level comes into operation. The system will be complicated by the fact that the barrier to injection is also changing with temperature.

Careful investigation of trapping levels involving such methods as thermally stimulated current analysis may be necessary to resolve this difficulty.

REFERENCES

ABDULLAEV, G.B. et al (1968) Phys.Stat.Sol.   26, 65

ALLEN, E.J. and J.L.CRENSHAW (1912) Am.J.Sci.   34, 310

ANDERSON, R.L. (1962) Sol.Sta.Electron.   5, 341

ASHLEY, K.L. and A.G.MILNES (1964) Phys.Rev.   35, A369

AUTH, J, (1961) Z.Phys.Chem.   217, 159

AVEN, M. and H.H.WOODBURY (1962) Scient.Rep.No.2. AFCRL contract. No.AF, 19, 604, 8512

AVEN, M. and W.GAWACKI (1963) J.Electrochem.Soc.   110, 401

AVEN, M. and D.A.CUSANO (1964) J.App.Phys.   33, 606

BARBER, H.D. (1965) Ph.D. Thesis Imperial College

BARDEEN, J. (1968) Private communication

BARRAUD, A. (1963) Compt.Rend.   256, 3632

BASOV, N.G. et al (1964)D.A.N.S.S.S.R.   155, 783

BASOV, N.G. et al (1966) Sov.Phys.Sol.Sta.   7, 2932

BEUN, J.A. et al (1962) Physica   28, 184

BIJVOET, J.M. and K.LONSDALE (1953) Phil.Mag.   44, 204

BINGGELI, B. and H.KIESS (1967) J.App.Phys.   38, 4984

BÖER, R.W. and W.E.WILHELM (1964) Phy.Sta.Sol.   4, 237

BÖER, R.W. and R.B.HALL (1966) J.App.Phys.   37, 4739

BRAÜNLICH, P. (1967) Phys.Sta.Sol.   21, 383

BUBE, R.H. (1960) Sol.Sta.Phys.   11, 223

BUBE, R.H. et al (1962) Phys.Rev.   128, A532

BUBE, R.H. (1964) J.App.Phys.   35, 586

BUBE, R.H. and F.CARDON (1964) J.App.Phys.   35, 2712

BÜGET, U. and G.T.WRIGHT (1965) Brit.J.App.Phys.   16, 1449

BUJATTI, M. (1967) Proc. I.E.E.E.   55, 1634

BUJATTI, M. (1968) Brit.J.App.Phys.   1, 581

BUTTLER, W.M. and W.MUSCHEID (1954)   15, 82

CHERNOW, F. et al (1966) App.Phys.Lett.   9, 145

CHIKAWA, J. and T.NAKAYAMA J.App.Phys.   35, 2493

CLARKE, R.L. (1959) J.App.Phys.   30, 957

COURTENS, E. and F.CHERNOW (1966) App.Phys.Lett.   8, 3

CUSANO, D.A. (1963) Sol.Sta.Electron.   6, 217

CZYZAK, S.J. (1952) J.App.Phys.   23, 932

DREBEEN, A. (1964) J.Electrochem.Soc.   111, 174

DONNELLY, J.P. and A.G.MILNES (1964)App.Phys.Lett.   5, 186

DONNELLY, J.P. and A.G.MILNES (1966)I.E.E.E.

                                    Trans. ED -   14, 63

DUMKE, W.D. (1964)Physics of Semiconductors, Paris, p.487

ELLIS, S.E. (1967) J.App.Phys.   38, 2906

FASSBENDER, J. (1956) Z. Physik.   145, 301

FAZAKAS, A.B. and A.FRIEDMAN (1968) Phys.Stat.Sol.   28, 385

FISCHER, A.G. (1961) Sol.Sta.Electron.   6, 217

FISCHER, A.G. (1963) J.Electrochem.Soc.   110, 733

FISCHER, A.G. and H.I.MOSS (1963) J.App.Phys.   34, 2112

FISCHER, A.G. (1964) Electrochem.Soc.Meet.Toronto Abstract 36

FISCHLER-HAZONI, C. and F.WILLIAMS (1965)Phys.Rev. 139, A583

FOCHS, P.D. (1960) J.App.Phys.   31, 1733

FOCHS, P.D. and B.LUNN (1963) J.App.Phys.   34, 1762

FRERICHS, R. (1947) Phys.Rev.   72, A594

FULLER, C.S. and K.B.WOLFSTEIN(1965)J.Phys.Chem.Sol. 26, 1463
GERSHUN, A.S. and B.L.TIMAN(1968)Sov.Phys.Sol.Sta.   10, 1258
GOLDFINGER, P. and M.JEUNEHOMME(1963)Tran.Farad.Soc. 59, 2851

GOODMAN, A. (1963) J.App.Phys.   35, 573

GREINER, R.A. et al (1958) J.App.Phys.   28, 1538

HAYDL, W.H. (1967) Ph.D. Thesis Stanford University

HILL, R.M. (1968) Private communication

HIPPEL VON, A. (1952) Z. Physik.   133, 158

HOLONYAK, N. and S.F.BEVACQUA (1963)App.Phys.Lett.   2, 71

HOLT, D.B. (1968) Private Communication

HOPFIELD, J.J. and D.G.THOMAS (1961) Phys.Rev.   122, A35

HSIAO, C.M. and A.W.SCHLECTEN (1952) J.Metals.   4, 65

HURWITZ, C.E. (1966) App.Phys.Lett.   9, 422

HUTSON, A.R. et al (1961) Phys.Rev.Lett.   7, 237

IBUKI, S. (1959) J.Phys.Soc.Jap.   14, 1181

JACLEVIC, R.C. et al (1963) App.Phys.Lett.   2, 7

JUNOD, P. (1959) Helv.Phys.Act.   32, 567

KABALKINA, S.S. and Z.W.TROITSKAYA (1964)Sov.Phys.Dok. 8,800

KASAI, P.H. et al (1961) Phys.Rev.Lett.   7, 17

KEATING, P.N. (1963) J.Phys.Chem.Sol.   24, 1101

KEATING, P.N. (1964) Phys.Rev.   135, A1407

KEATING, P.N. (1965) J.App.Phys.   36, 2

KOMIYA, et al (1962)Luminescence of organic and inorganic
                                          solids p. 532

KONSTANTINOV, O.V. and V.I.PEREL (1965) Sov.Phys.

Sol.Sta.   6, 2691

KORSUNSKAYA, N.E. (1968) Sov.Phys.Sol.Sta.   10, 409

KREMHELLER, A. (1955) Sylv.Technol.   8, 11

KRÖGER, F.A. et al (1954) Z.Phys.Chem.Leipzig.   203, 1

KRÖGER, F.A. et al (1956) Phys.Rev.   103, A279

KRÖGER, F.A. and H.J.VINK (1956) Sol.Sta.Phys.   3, 301

KULP, B.A. and R.H.KELLEY (1960) J.App.Phys.   31, 1057

LAIDER, K.J. (1951) J.Phys.Coll.Chem.   55, 1067

LAMPERT, M.A. (1956) Phys.Rev.   103, A1648

LAMPERT, M.A. (1962) Phys.Rev.   125, A26

LEBEDEV, A.A. et al (1957) Sov.Phys.Tech.Phys.   1, 2071

LITTON, C.W. and D.C.REYNOLDS (1964) Phys.Rev.   133, A536

LORENZ, R. (1891) Ber.Deutsch.Chem.Ges.Zu Berlin.   24, 1501

LOTOTSKII, B. and L.K.CHIRKIN (1966)Sov.Phys.Sol.

Sta.   8, 1564

MANDEL et al (1964) II-VI Laser Materials Study Final Report

MARK, P. (1965) Phys.Rev.   137, A203

MARLOR, G.A. and J.WOODS (1963)Proc.Phys.Soc.   81, 1073

MARLOR, G.A. and J.WOODS (1965)Brit.J.App.Phys.   16, 1449

MARSHAL, R. and S.S.MITRA (1965)J.App.Phys.   36, 3882

MEDCALFE, W.E. and R.H.FAHRIG (1958)J.Electrochem.

Soc. 105, 719

MILLIGAN, W.O. (1934) J.Phys.Chem.   38, 797

MOORE, J.S. (1967) Ph.D. Thesis University of Illinois

MOORE, J.S. et al (1967) App.Phys.Lett.   10, 58

MOORE, J.S. et al (1967a) Sol.Sta.Electron.   10, 823

MOTT, N.F. and R.W.GURNEY (1940) Electronic processes
                              in ionic crystals.

MYTTON, R.J. (1968) Brit.J.App.Phys.   1, 721

NIELSEN, J.W. and E.D.KOLB (1963) Unpublished work.

NICOLL, F.H. (1967) App.Phys.Lett.   10, 69

NITSCHE, R. (1960) J.Phys.Chem.Sol.   17, 163

NITSCHE, R. and D.RICHMAN (1960) Z.Electrochem.   62, 33

OLDHAM, W.G. and A.G.MILNES (1964)App.Phys.Lett.   5, 186

O'SULLIVAN, D. and E.MALARKEY (1965)App.Phys.Lett.   6, 5

PAULING, L. (1960) Nature of the chemical bond.

PIPER, W.W. and J.J.POLICH(1961) J.App.Phys.   32, 1278

PIPER, W.W. and R.E.HALSTED (1961) Physics of Semi-
                              conductors, Prague.   p.1046

POGORELYI, A.D. (1948) Zhur.Fiz.Khim.   22, 731

READ, (1968) Private communication

REYNOLDS, D.C. et al (1955) Bull.Am.Phys.Soc.   1, 111

REYNOLDS, D.C. et al (1956) J.Chem.Phys.   25, 1177

RIDLEY, B.K. and T.B.WATKINS (1961)Proc.Phys.Soc.   78, 293

RIDLEY, B.K. (1963) Proc.Phys.Soc.   82, 954

RIDLEY, B.K. and R.G.PRATT (1964) Physics of Semi-
                              conductors. Paris.   p. 487

ROSE, A. (1955) Phys.Rev.   97, A1538

ROSE, A. (1964) Phys.Rev.   35, A2664

RUPPEL, W. (1958) Helv.Phys.Act.   31, 311

RUSHBY, A.N. and J.WOODS (1966) Brit.J.App.Phys.   17, 1187

SASAKI, K. (1968) Jap.J.App.Phys.   7, 584

SCHNEIDER, J. et al (1963) Phys.Lett.   5, 312

SCHOSSBERGER, F. (1955) J.Electrochem.Soc.   108, 150

SEITZ, F. (1940) Modern Theory of Solids

SHERMAN, J. (1932) Chem.Revs.   11, 92

SHITAYA, T. and H.SATO (1968) Jap.J.App.Phys.   7, 1348

SHOCKLEY, W. (1948) U.S. Pat.   2, 569, 347

SHOHNO, K. (1955) Jap.J.App.Phys.   3, 114

SIHVONEN, I.T. and D.R.BOYD (1958) J.App.Phys.   28, 1538

SIMHONY, M. et al (1967) J.App.Phys.   39, 152

SINGER, J. and P.FAETH (1967) App.Phys.Lett.   11, 130

SINGER, J. (1968) Private communication.

SMITH, R.W. and A.ROSE (1953) Phys.Rev.   92, A857

SMITH, R.W. (1955) Phys.Rev.   97, A1525

SMITH, R.W. and A.ROSE (1955) Phys.Rev.   97, A1531

SMITH, R.W. (1957) Phys.Rev.   105, 900

SMITH R.W. (1959) R.C.A. Rev.   20, 69

SPAKOWSKI, A.E. (1965)Proc.5th.Photovoltaic Conf. Maryland.

SPEAR, W.E. and J.MORT (1963) Proc.Phys.Soc.   81, 130

STAFEEV, V. (1959) Sov.Phys.Sol.Sta.   1, 763

STANLEY, J.M. (1956) J.Chem.Phys.   24, 1279

STEELE, M.C. et al (1962) J.Phys.Soc.Jap.   17, 1729

STUPP, E.H. (1963) J.App.Phys.   34, 163

STURNER, H.W. and G.E.BLEIL (1964) App.Opt. 3, 1015

SWANSON, J.G. (1967) Ph.D. Thesis Imperial College

SZETO, W. and G.A.SOMORJAI (1966) J.Chem.Phys. 9, 3490

THOMAS, D.G. and J.J.HOPFIELD (1959) Phys.Rev. 116, A573

THOMAS, D.G. et al (1960) Phys.Rev. 119, A570

TRODDEN, G.W. (1967) Brit.J.App.Phys. 18, 401

TUBOTA, H. (1963) Jap.J.App.Phys. 2, 259

TURNER, A.F. and F.K.TRUBY (1951) BAUSCH and LOMB Tech.Rep.

TYLER, W.W. (1954) Phys.Rev. 96, 226

VESELOVSKII, B.K. (1942) Zhur.Priklad.Khim. 15, 422

VITRIKHOVSKII, N.I. and M.V.KURIK (1966) Sov.Phys.
Sol.Sta. 7, 2969

VOHL, P. et al (1967) I.E.E.E. Trans.Electron.
Dev. ED-14, 26

WAGENER, J.L. and A.G.MILNES(1964) App.Phys.Lett. 5, 186

WAGENER, J.L. and A.G.MILNES(1965)Sol.Sta.Electron. 8, 495

WAREKOIS, E.P. et al (1962) J.App.Phys. 33, 6901

WEBER, K. (1961) Ph.D. Thesis Technical High School Munich

WILLCOCKS, J.D. (1968) Ph.D. Thesis Imperial College

WOODS, J. and J.A.CHAMPION(1959)J.Electron.and Cont. 7, 243

WOODBURY, H.H. (1965) J.App.Phys. 36, 228

WRIGHT, G.T. (1958) Nature. 182, 1296

WRIGHT, G.T. (1959) Proc. I.E.E. 106BS, 915

WRIGHT, G.T. (1960) Sol.Sta.Electron. 2, 165

WRIGHT, H.C. and G.A.ALLEN(1965)Mullard Res.Rep. 554

YEE, J.H. and G.A.CONDAS (1968)Sol.Sta.Electron. 11, 419